EFFECT OF FEEDBACK CONTROL WITH LINEAR AND NON-LINEAR TEMPERATURE GRADIENTS TO SOME CONVECTION PROBLEMS

ADIBAH BINTI NAZARUDIN

FACULTY OF SCIENCE
UNIVERSITY OF MALAYA
KUALA LUMPUR

2019

EFFECT OF FEEDBACK CONTROL WITH LINEAR AND NON-LINEAR TEMPERATURE GRADIENTS TO SOME CONVECTION PROBLEMS

ADIBAH BINTI NAZARUDIN

DISSERTATION SUBMITTED IN FULFILMENT OF THE REQUIREMENTS FOR THE DEGREE OF MASTER OF SCIENCE

INSTITUTE OF MATHEMATICAL SCIENCES
FACULTY OF SCIENCE
UNIVERSITY OF MALAYA
KUALA LUMPUR

2019

UNIVERSITY OF MALAYA

ORIGINAL LITERARY WORK DECLARATION

Name of Candidate: **ADIBAH BINTI NAZARUDIN**

Matric No: **SGP150001**

Name of Degree: **MASTER OF SCIENCE (APPLIED MATHEMATICS)**

Title of Project Paper/Research Report/Dissertation/Thesis ("this Work"): **EFFECT OF FEEDBACK CONTROL WITH LINEAR AND NON-LINEAR TEMPERATURE GRADIENTS TO SOME CONVECTION PROBLEMS**

Field of Study: **APPLIED MATHEMATICS**

I do solemnly and sincerely declare that:

(1) I am the sole author/writer of this Work;
(2) This Work is original;
(3) Any use of any work in which copyright exists was done by way of fair dealing and for permitted purposes and any excerpt or extract from, or reference to or reproduction of any copyright work has been disclosed expressly and sufficiently and the title of the Work and its authorship have been acknowledged in this Work;
(4) I do not have any actual knowledge nor do I ought reasonably to know that the making of this work constitutes an infringement of any copyright work;
(5) I hereby assign all and every rights in the copyright to this Work to the University of Malaya ("UM"), who henceforth shall be owner of the copyright in this Work and that any reproduction or use in any form or by any means whatsoever is prohibited without the written consent of UM having been first had and obtained;
(6) I am fully aware that if in the course of making this Work I have infringed any copyright whether intentionally or otherwise, I may be subject to legal action or any other action as may be determined by UM.

Candidate's Signature Date:

Subscribed and solemnly declared before,

Witness's Signature Date:

Name:

Designation:

EFFECT OF FEEDBACK CONTROL WITH LINEAR AND NON-LINEAR TEMPERATURE GRADIENTS TO SOME CONVECTION PROBLEMS

ABSTRACT

In many engineering and industrial applications such as crystallization growth process industries, nuclear reactors, solar heating devices and welding of steels, the onset of instability of convection plays a major role in resulting the satisfactory end-products. The linear stability analysis regarding the non-Newtonian convective flow in electro convection and ferrofluids convection in the presence of feedback control strategy is studied by using single-term Galerkin technique. In the case of Bénard–Marangoni electro convection, the presence of feedback control is analysed using the classical linear stability analysis. Linear, parabolic and inverted parabolic temperature profiles are chosen to investigate in this study. For the case of Rayleigh–Bénard–Marangoni ferrofluids convection, the presence of feedback control is analysed and the influence of various parameters on onset is discussed. In the both non-Newtonian fluid, various value of feedback control and other parameters on onset are tested to examine the presence of feedback control on the onset of convection. The results obtained under the limiting conditions compare well with the previous studied. The numerical results obtained are presented graphically and the influences of various parameters are discussed in detail. The results indicate that the value of critical Marangoni number and other parameters affected in the presence of feedback control which delaying the onset of instabilities.

Keyword: Linear stability analysis; Feedback control strategy; Galerkin technique; Bénard–Marangoni electro convection; Rayleigh–Bénard–Marangoni ferrofluids.

KESAN KEHADIRAN KAWALAN SUAPBALIK BESERTA KESAN KECERUNAN PROFIL SUHU LINEAR DAN PROFIL SUHU BUKAN LINEAR TERHADAP BEBERAPA MASALAH OLAKAN

ABSTRAK

Dalam pelbagai aplikasi kejuruteraan dan industri seperti industri proses pertumbuhan kristal, reaktor nuklear, pembuatan alat pemanasan solar dan pengimpalan besi, permulaan ketakstabilan olakan memainkan peranan yang penting untuk memberikan kualiti hasil yang memuaskan. Analisis kestabilan linear berkenaan aliran olakan bukan Newtonian dalam olakan elekro dan olakan bendalir ferro dengan kehadiran kawalan suapbalik dikaji dengan menggunakan teknik sebutan tunggal Galerkin. Dalam kes bagi olakan elekro Bénard–Marangoni, kehadiran kawalan suapbalik dianalisis menggunakan analisis kestabilan linear klasik. Profil suhu linear, parabola dan parabola berbalik digunakan dalam kajian ini. Bagi kes olakan bendalir ferro Rayleigh–Bénard–Marangoni, kehadiran kawalan suapbalik dianalisis dan pengaruh semua parameter ke atas tercetusnya olakan dibincangkan. Dalam kedua-dua bendalir bukan Newtonian, pelbagai nilai kawalan suapbalik dan parameter lain telah diuji untuk mengkaji kesan kehadiran kawalan suapbalik terhadap tercetusnya olakan. Keputusan kajian yang diperolehi di bawah syarat terhad dibandingkan dengan hasil kerja penyelidik sebelum ini. Keputusan berangka yang terhasil dipersembahkan secara grafik dan pengaruh pelbagai parameter dibincangkan secara terperinci. Hasil kajian menunjukkan bahawa perubahan nombor Marangoni genting dan begitu juga pelbagai parameter lain telah dipengaruhi dengan adanya kawalan suapbalik iaitu kawalan suapbalik memperlahankan permulaan olakan yang tidak stabil.

Kata kunci: Analisis kestabilan linear; Kawalan suapbalik; Teknik sebutan tunggal Galerkin; Olakan elekro Bénard–Marangoni; Bendalir ferro Rayleigh–Bénard–Marangoni.

ACKNOWLEDGEMENTS

Bismillahirrahmanirrahim. Thanks giving and praise to Allah the Almighty for being my guiding light. Peace and blessings to His Messenger, Nabi Muhammad S.A.W., friends and all members of His family. In the deep inside my heart, I feel really thankful that with the help of Allah and encouragement from others, I finally done this thesis even it gets a lot of weaknesses that will be amended in the future.

First and foremost, I would like to express my greatest gratitude and respect to my supervisor, Dr. Zailan bin Siri for his excellent guidance, valuable comments and endless support throughout my research project. I am very thankful by giving me various ideas and suggestions to increase my knowledge about my research topic.

I also would like to thank my beloved parents, brothers and sisters, for their continuous supports and prayers. Special thanks to my lovely husband, Mohamad Izzuddin Sofian for supporting and encouraging me all this while. Without their sacrifices, understanding and encouragement, it would have been impossible for me to complete this work. May Allah reward all of your kindness.

I gratefully acknowledge Institute of Mathematical Sciences and University of Malaya for accepting me to pursue my higher education and provided me excellent facilities and work environment. Greatest appreciation is expressed to the Ministry of Higher Education of Malaysia supporting my learning fees throughout MyMaster Programme.

Last but not least, I would like to thank all the people who involved directly or indirectly in the accomplishing of this master thesis that has taught me a great patient to give out a great outcome. Alhamdulillah, May Allah bless.

TABLE OF CONTENTS

LIST OF FIGURES

LIST OF TABLES

LIST OF ABBREVIATIONS

et al.	:	(et alii): and others, and co-workers
i.e.	:	(id est): that is, in other words
MATLAB	:	Matrix Laboratory
PID	:	proportional-integral differential

NOMENCLATURE

a	overall horizontal wavenumber
$\vec{B}$	magnetic induction
C_v	specific heat
d	thermal depth of the liquid layer
D	differential operator
$\vec{E}$	electric field
$f(z)$	non-uniform basic temperature gradients
g	gravity acceleration
G	perturbation rotation
$\vec{H}$	magnetic field
K	feedback control
L	Electric number
M	Marangoni number
$\vec{M}$	magnetization
N_1	coupling parameter
N_3	couple stress parameter
N_5	micropolar heat conduction parameter
P	hydrodynamic pressure
$\vec{P}$	dielectric polarization
$\vec{q}$	velocity field
r	calibration of the control
R	Rayleigh number
t	time

T	temperature
W	perturbation velocity
x, y, z	Cartesian coordinate space
Z	plane boundary

Greek symbols

α	coefficient of thermal expansion
ε_0	electric permeability of free space
ε_r	dielectric constant
ζ	vortex viscosity
$\vec{I}$	moment of inertia
κ	thermal conductivity
κ_e	thermal susceptibility
η	shear kinematic viscosity
η'	shear spin viscosity
λ'	bulk spin viscosity
θ	perturbation temperature
ρ	fluid density
μ_0	magnetic permeability
N	kinematic viscosity
χ	thermal conductivity
ω	growth rate
$\vec{\omega}$	spin
∇	Laplace operator
∇_1^2	two dimensional Laplace operator

ϕ	electrostatic potential
σ	surface tension

Subscript

$_o$	reference quantity
$_c$	critical
$_b$	basic state value
$_\theta$	changes in temperature
$_D$	differential gain
$_I$	integral gain
$_P$	proportional gain
x, y, z, t	derivative with respect to variables

CHAPTER 1:

INTRODUCTION

1.1 Preliminary

Heat transfer (or heat) can be defined as trade of thermal energy by dissipating heat, between two systems or part of two systems depending on a spatial temperature difference (Incropera et al., 2007). Whenever there exists changing of mechanical energy, heat flows from hot objects to cold objects, just like how water flows, it goes from high surface to low surface. When heat is transferred, it is pulled from hotter objects into colder objects.

Heat transfer has broad applications in numerous manufacturing activities such as, in packaging materials, pasteurization of food, integrated generator engines, air pollution mitigation, biology processes, biomass and biofuel. In these activities, heat transfer efficiency increases which takes place via several heat transfer devices. These devices such as heat sinks, hydro coolers, blast chillers and refrigeration evaporators are desirable to minimize the volume.

Conduction or diffusion, convection, and radiation are mainly classified as modes of heat transfer. When the hot dishes stirred with a metal utensil, instantaneously, the end of the utensil become very warm and a pot holder is needed. The heat energy from the end of the utensil in the hot dishes passes through to the end of human hand. This energy is known as conduction. Meanwhile, convection is the phenomenon of successive motion of electrons, atoms and molecules in fluids called a current. For example, the convection cycle continued from the bottom of the dishes, diffuses and becomes less dense and then, the denser, warm part dishes go upward. The upper surface of the dishes continued denser, spreads out and less warm. After that, the heat cycle continues where the cooler, high dense dishes go down to the below part and begin to float after received the heat. Oppositely during radiation, the energy is transferred by electromagnetic radiation where indirect contact between an item and heat source. Radiation means the energy is passes through vacuum medium or empty space. Basically, we can easily illustrate the mode of heat transfer in boiling water, melting ice and drying of clothes. But then, in this thesis, we will be discussed briefly only on convection in a layer of fluid.

1.2 Convective Heat Transfer

The heated fluid (liquid or gas) is transfer from one medium to another is called convection. The movement of heated fluid occurs because the change of the heat.

Generally, convection also known as convective heat transfer means the process of heat transfer that arises from fluid flow either over or through cold or hot surfaces and the fluid flow acts as an energy carrier.

The heat transfer devices of working fluid is to minimize the associated energy consumption which take place through a vertical, horizontal and inclined cylinder. But then, for this thesis, we only focus on convection in a horizontal plane heated from below which are steady Bénard–Marangoni convection.

1.2.1 Types of Convection

The story begins when Bénard demonstrated a definitive and systematic manner of convection in a thin fluid layer in his earliest experiments, 1900 (Chandrasekhar, 1961).

However, he made false conclusion by saying that the results of the hexagonal shaped is due to buoyancy force.

Rayleigh (1916) tried to explain the phenomenon seen by Bénard through mathematical theory. In 1956, Block has made systematically experiment and finally succeeded to explain that the real force in fluid that caused convection was surface tension force. This result confirmed by theory of mathematics for the first time proposed by Pearson (1958). Since then, many researchers repaired and extended experiments and the classical theory to understand the phenomenon of convection in more complex and realistic situations.

Convection due to buoyancy force is called Bénard convection proposed by Bénard, (1900). Meanwhile, convection due to surface tension force is known as Marangoni convection. Whereas some other researchers studied the convective instabilities due to combined buoyancy force and surface tension force called on Bénard–Marangoni convection.

1.2.2 Applications of Convection

Convection is a great deal factor in mixing of water masses for sea water. On the other side, for weather, convection is main influence for prediction of the weather at small interval scales and a great deal factor of climate prediction at substantial length scales. Application of convection also involving in industries that are crystallization growth process, nuclear reactors, solar heating devices and welding steels.

As stated by Koschmieder (1993), before 1900 means before Bénard get interest on thermal convection in fluid, convection in shallow fluid layers have been recognized and described by several observers. Early observations are kind of historical interest as there are no scientific investigations made under controlled condition. In 1897, Guebhard made an observation, namely as observation of polygonal vortex motions in an abandon bath of film developer. This observation then accidentally observed by Bénard and induced Bénard's spirit to take a thorough look at convection himself. He demonstrated first systematic and definitive investigation of convection warm up from below in a shallow layer of fluid. The outcomes of his doctoral thesis are from these studies which the published article namely "Les tourbillons cellulaires dans une nappe liquid - Méthodes optiques d'observation et d'enregistrement" (Bénard, 1900) and a subsequent paper in 1901.

The first person to give a conclusive experimental demonstration on the role of surface tension in the formation of hexagonal cells is by Block (1956). Then, Pearson (1958) is the pioneer theoretical investigation of convection caused by surface tension gradients using linear stability analysis. The hydrodynamic instability in a freely flow substance is caused by surface gradient force. There given also many factors to cause the instability include the adequate magnitude of proper sense or temperature and concentration tension across the fluid surface. However, the most significant limitation of Pearson's (1958) work is consideration of only the free surface with non- deformable form of study which heated from below corresponding to strong limit of the gradient. On the other hand, if the fluid surface deformed, it will lead to the change of the boundary conditions on top of the layer.

But then, this thesis only focuses on a steady Rayleigh–Bénard–Marangoni convection in the horizontal plane which is heated downside.

1.3 Types of Fluid

Do we really know what fluid is it? Blood flowing in our body or the air we inhaled or exhaled daily is a fluid. Fluid can be state in the form of liquids, gases, plasmas or plastic solids which is essential in our life. There are widely number of engineering applications in fluids such as turbines, engines, windmills, airplanes, jets and sprinklers. To provide great improvement for wide theoretical and experimental work, it is important to study the fluid flow. The prediction of the fluid flow processes help engineers to study practical applications and producing advanced materials, hence produce high quality of the products and in the same time will reduces the conduction of costly works.

In physics, fluid known as a substance that continuously flow as long as the shear stress applied. Mathematically, Amer–Nordin (1995) defined fluid as continuum substances. In other words, the fluid said to be flows and deforms continuously with resulting of shear stress. When in states of no shear stress, the fluid said to be at rest.

Basically, fluids can be grouped into a few classes known as ideal fluid, Newtonian fluid, non-Newtonian fluid and real fluid. A kind of liquid which has zero viscosity property with no stress element, τ and cannot be compressed falls in the category of ideal fluid. Ideal fluid cannot be found in reality or actual practice and can be said as imaginary fluid due to assumptions that all existing fluid in the environment has some viscosity property. Most of real fluid is viscous, means that the viscosity property cannot be ignored at all such as water, oil and air (White, 2008).

Generally, the shear strain is directly proportional to the gradient of velocity known as the Newton's law of viscosity. The real fluid said to be Newtonian fluid which obeys the relation, with linearly proportional to the local strain rate. In experimental calculations, water, air and most types of liquids and gases, can be said as Newtonian. Meanwhile, a kind of fluid which did not obey this constitutive law called non-Newtonian fluid. Many salt solutions, molten polymers and most commonly form substances like jam, yogurt, corn starch, paint and mayonnaise are examples of non-Newtonian fluids.

1.4 Micropolar Fluid

Eringen (1966, 1972) studied the theory of micropolar fluid which plays its role whenever the behavior of fluid flow cannot be explained in the basis of Newtonian fluid. These micropolar fluid described by Eringen consist of suspended particles in a viscous medium and move regularly with a definite volume. Diverse applications of micropolar fluid can be found in industrial colloidal fluids, polymeric suspension and liquid subtances.

According to Eringen (2001), magnetic fluids, dielectric fluids, muddy fluids and biological fluids are some other possible substances that can be modelled by applying the theory of micropolar fluid. Besides, another application in our daily life that using these modeled of micropolar fluid dynamic include blood flow in arteries and capillaries and the presence of dust in the air. Hence, the importance to study the behavior of fluid flows increasing especially involving the theory of micropolar fluid.

Electro convection is an example of natural convection involving the movements of fluid in an electric field. Some of the effects of electric fields are control the motion in fluids, lower values of conductivity and directly converted into the kinetic energy.

The analysis of convection in magnetic fluids called ferroconvection has a temperature that depends on magnetic moment. In a non-electrically conducting carrier fluid like water, kerosene, hydrocarbon and so on, ferrofluids are electrically non-conducting colloidal suspensions of tiny particles of solid ferromagnetic material. Ferrofluids also called the magnetic fluid due to the factor of the fluid magnetization.

Ferrofluids are artificially synthesized and has many important applications in cool down the rate of cooling in loudspeakers, with motors in space and others equipment to enhance convective cooling although not naturally exist. In the electrically conducting nanofluid, continuous strips and filaments are drawn so that the rate of cooling is controlled (Rosmila et al., 2012). In the conventional base fluids, some other compounds containing iron, Magnetite, Hematite, or Cobalt Ferrite are such type of electrically colloidal suspensions in which nanoparticles are suspended known as ferrofluid.

1.5 Control Strategy

What we want to control actually in this study? The control strategy is needed for the system whether it can suppress or augment the onset of convection. Generally, the naturally convective flow patterns may not be able to optimize the process. So, it is important in many technological sciences area to control the complex flow.

Here, are several physical mechanism we can applied for to control the convective instabilities effectively such as by applying electric field, by using controller gain parameter, or by maintaining temperature profile, or by applying magnetic field or using rotation.

Importantly, control the complex convective patterns needed to make sure the process going to be the optimal ones. For example in material processing, it helps produce good ends products and to attain significant savings. But what will happen if the convective instabilities become uncontrolled? Will resulting the poor quality in the production of crystals and poor quality in the penetration welding steels.

1.6 Problem Statements

The lists of the problem statements are:

1. Analysing the onset in the presence of feedback control on Bénard–Marangoni electro convection in a micropolar fluid with parabolic temperature profile.
2. Analysing the presence of feedback control strategy on Rayleigh–Bénard–Marangoni ferrofluids convection. The stability of the onset which is influenced by using linear temperature profile and some various parameters will be studied.
3. Analysing the effects of feedback control with non-uniform temperature profiles for Rayleigh–Bénard–Marangoni ferrofluids. Parabolic and inverted parabolic temperature profiles are chosen to investigate in this problem.

1.7 Research Questions

The some of the research questions are:

1. How the mathematical model of linear stability is derived and analysed and what the boundary conditions applied for both cases of dielectric micropolar layer and ferrofluids layer?
2. What are the effects of feedback control on Bénard–Marangoni electro convection in a micropolar fluid and the effect of feedback control to other parameters such as critical Marangoni number, M_c, Rayleigh number, R, coupling parameter, N_1, couple stress parameter, N_3 and parameter of micropolar heat conduction, N_5 with the basic state temperature profiles?

3. What are the effects of feedback control on Rayleigh–Bénard–Marangoni ferrofluids convection and the effect of feedback control to other parameters such as critical Marangoni number, M_c, Rayleigh number, *R*, and magnetic Rayleigh number, *N* with the basic state temperature profiles?

1.8 Research Objectives and Scopes

The aims of this research are:

1. to develop and extend the mathematical model of electro convection for micropolar fluid investigated by Azmi and Idris (2014) and the mathematical model of ferrofluids convection reported by Shivakumara et al. (2002) by including feedback control in the boundary condition.
2. to develop a numerical code to predict the onset of convection for objective 1.
3. to analyse the numerical results of the problem statements.
4. to compare the output with previous study and make a conclusion / suggestion for the present study.

The scope of this work is to analyse the onset of non-Newtonian flow patterns in electro convection and ferrofluids convection in the presence of feedback control strategy. Basic temperature gradients and also with the effect of others parameters are investigated on the onset. Linear, parabolic and inverted parabolic temperature profile are chosen to study. Hence, the numerical code developed is to predict whether the parameter involved in our study will suppress or augment the onset of convection.

1.9 Thesis Organization

Basically this thesis consists of seven chapters. The first chapter presents the introductory chapter that includes some background about convective heat transfer in fluid and types of fluid. Basic mechanism for convection and applications related the current study will be described accordingly. Then, follow by the research objectives and the scopes of the current work.

The next, Chapter 2 presented the literature review about earlier studied. The literature review survey from the previous study in well-known journal, past thesis, book and also conference proceeding. The related aspects to current investigation also stated in this chapter.

Furthermore, in Chapter 3 described the mathematical formulation and derivation of the governing equations of the model problem. In addition, the method on the problem solution for case of non-Newtonian fluid which is include linear stability analysis and single-term Galerkin method will be discussed here. Thus, in Chapter 4, consists of the completion of the mathematical formulation by the concept of boundary conditions and feedback control strategies applied for both cases of dielectric micropolar layer and ferrofluids layer.

All the verification of the accuracy of numerical finding on effects of the presence of feedback control in micropolar fluid and ferrofluids convection with non-uniform temperature gradients will be presented in Chapter 5. Then, in Chapter 6, the numerical results of the effects of parameters on the onset of Rayleigh–Bénard–Marangoni convection in electroconvection and ferrofluids will be presented graphically. Besides, the solutions of eigenvalues subject to each boundary condition will be discussed as well.

The final chapter, Chapter 7 summarizes and concludes all the results from the previous chapters. Also this last chapter presented the proposed on advanced research which can be extended from existing work and some recommendations will be suggest.

CHAPTER 2:

LITERATURE REVIEW

This section provides some literature survey on related current work in various aspects. Particularly, there are a few sections consists of general discussion on convective instabilities, non-Newtonian fluid which are dielectric micropolar fluid and ferrofluids and the discussion topic on various control strategies used in convective instabilities.

2.1 Convective Instabilities

Convection is found all over the earth. That is how when the sea and land breezes are form (see Figure 2.1) and also causes the plates to move in earth mantle. Besides, in geophysics, convection is a great deal influence in occurring of oceanic and atmospheric structure. On the other side, convective instabilities are the main factor for the formation of the continental surfaces. Application of convection also involving in industries that are crystallization growth process, nuclear reactors, solar heating devices and welding steels. In other context of types of convection, the first one is heat transfer, the other two are known as conduction and radiation. Convection has freely movement of molecules as example in the liquid medium form like fluid and also in the medium of gases. Besides, convection can be formed when material with different densities interacted. Means that, when the less dense material was rising and more dense material was sinking. For example in our environment, warm air were rises because of less dense than cold air. Such movement is referred to Rayleigh–Bénard convection when there is heated downside on a horizontal fluid layer.

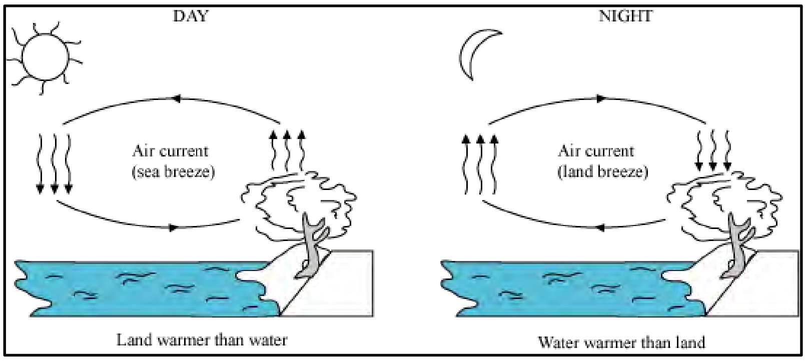

Figure 2.1: Convection currents cause sea breeze and land breeze
Source: https://thattheoreticalphysicist.files.wordpress.com/2014/09/wind_draft1.jpg

A natural type of convection; Rayleigh–Bénard convection which is heated downside in a plane of horizontal fluid layer. The popular commonly studied of convective instabilities by Getling (1998) on Rayleigh–Bénard convection. In 1900, an experiment on convection cells in a thin liquid layer performed by Henri Bénard observed that there existed spontaneous pattern formation. In other words, the convection was seen to organize itself into hexagonal cells throughout the entire domain, as shown in Figure 2.2. The appearance of convection cells is due to the effect of buoyancy. Hence, the initial movement gravity causes the higher fluid density go upside to the upper layer. The cells of convection which is Bénard cells had a regular pattern form (Chandrasekhar, 1961). The false conclusion made by Bénard saying that the formation of hexagonal pattern because of buoyancy force existed.

Figure 2.2: Bénard cells convection under free surface
Source:https://upload.wikimedia.org/wikipedia/ Bénard _cells_convection.jpg

The transfer of thermal energy by the fluid flow either over or through cold or hot surfaces is called convection state by Koschmieder (1993) and Mohammed et al. (2013). Mohammed et al. (2013) has studied a research on natural type of heat transfer include the flows from the top and the bottom of inclined cylinder including the cross sections with different parts of vented enclosure at steady state. But then, for this research work we only focus on steady Rayleigh–Bénard–Marangoni convection heated downside in a plane of horizontal layer. Convection has the most commonly researched of higher attention because of the mathematics and analytical accessibility. Convection may be produced either by buoyancy forces (Bénard convection) studied by Bénard in year 1900 and Rayleigh (1916) or surface tension forces (Marangoni convection) by Pearson (1958) or both buoyancy and surface tension gradient (Bénard–Marangoni convection) by Nield (1964). The Bénard–Marangoni instability problem has received higher attention of research works of Davis and Homsy (1980), Perez-Garcia and Carneiro (1991), Medale and Cerisier (2002) and Giangi et al. (2002). Recently, the convective instabilities problems have studied by many researchers such as Shivakumara et al. (2015) and Arratia et al. (2018). For micropolar fluid convection, Idris et al. (2009) conducted a research on the onset of Bénard–Marangoni about the influence of feedback control.

2.2 Dielectric Micropolar Fluid

The theory of micropolar fluid described by Eringen (1966, 1972) has diverse applications in industrial fluids. That theory described the presence of particles by taking into account particle motions and thermal effects in the fluid (Pranesh and Kiran, 2010). In industrially fluids, the theory and the applications of micropolar fluid have become great field of study by Eringen (1966), and Lukaszewicz (1999). We indicated several possible applications of the theory to suspensions which are liquid crystals, polymeric fluids, certain anisotropic fluids, animal blood, and turbulence (Eringen, 1966, 1972). The problem of the convective instabilities of a micropolar fluid has been studied in the area of heat conducting by Rama Rao (1974), geophysics by Walzer (1976), rotation by Sastry and Ramamohan (1983) and by Qin and Kaloni (1992) and in the factor of electric field by Char and Chiang (1994), Douiebe et al. (2002), El-Sayed (2008), and also Rudraiah and Gayathri (2009). Electroconvection is involving the movements of fluid in an electric field and is an example of convection in natural phenomenon. Some of the effects of electric fields are control the motion in fluids, lower values of conductivity and directly converted into the kinetic energy stated by Roberts (1969), Pranesh and Baby (2012) and also Azmi and Idris (2014). In addition, the presence of various numbers of controllers will suppress or augment the onset of convection had been done (Idris and Hashim, 2010; Mahmud et al., 2010).

2.3 Ferrofluids

The analysis of ferroconvection has many important applications in cool down the rate of cooling in loudspeakers and others equipment to enhance convective cooling. Ferrofluids has a temperature that depends on magnetic moment also called the magnetic fluid and artificially synthesized. In a conducting carrier fluid and non-electrically fluid like hydrocarbon, kerosene and water, the tiny particles of solid ferromagnetic material of electrically non-conducting colloidal suspensions also called as 'ferrofluids'. The reviews by Rosensweig (1985), Bashtovoy et al. (1988) and Berkovsky et al. (1993) in the aspect of the body couple and the force of polarization on different ordinary fluid. A body force distribution can change depend on any variation of magnetic field, temperature and density aspect in the fluid. In the presence of a gradient magnetic field in pure fluids, the rise to ferroconvection analogous to Rayleigh–Bénard convection obtained from Chandrasekhar (1961).

Many researchers focusing on theory of linear stability on Rayleigh–Bénard ferroconvection such as Finlayson (1970), Das Gupta and Gupta (1979), Gotoh and Yamada (1982), Rudraiah and Sekhar (1991), Venkatasubramanian and Kaloni (1994) Meanwhile, Lalas and Carmi (1971) and Straughan (1991) applied the perturbation theory to studied the non-linear stability of ferroconvection. Marangoni ferroconvection has offers new deals for application in microgravity environment studied by Rudraiah et al. (2002), Nanjundappa et al. (2010), Gireesha (2016) and Azmi and Idris (2015). Many researchers such as Qin and Kaloni (1994), Weilepp and Brand (1996), Hennenberg (2005) and Nanjundappa et al. (2013) are attracted to the instability of ferroconvection on the onset in the factor of combined buoyancy forces and surface tension (Rayleigh–Bénard–Marangoni ferroconvection).

2.4 Control Strategies in Convective Instabilities

The control strategy is needed for the industrial process whether it can enhance or delay the convective instability. Generally, the naturally convective flow patterns may not be able to optimize the process. So, it is important in many technological processes had ability to control the complex flow. In spite of that, a lot of researches have be done controlled the flow patterns by applying feedback control strategies. Having a simple way of stabilize non-stable states in Rayleigh–Bénard–Marangoni convection, would be desirable to the critical stage. Controlling the onset of instability and to reduce drag, the characteristics have been analyzed by Gad-el Hak (1994), Choi et al. (1994) and also Bewley and Moin (1994) by applying turbulent channel flow. The experiment of using the neural network and linear control in water tunnel, Jacobson and Reynolds (1995) studied intentionally to induce vorticities. In boundary data, the experiment effected small perturbations to delay the onset of Marangoni convection by Pearson (1958) and Takashima (1970), extended by Bau (1999) who included a feedback control strategy.

Singer and Bau (1991), Yuen and Bau (1996, 1998) and Bau (1999) have been investigated in all kinds of characteristics using of linear and nonlinear control strategies to manageable the chaos. Eventually, with the help of controller proposed by Howle (1997a, 1997b, 2000) the flow showed significantly delay. The research on Rayleigh–Bénard–Marangoni problem, Or and Kelly (2001) reported the basic state stabilization can be achieved by using linear feedback control. In spite of that, nonlinear proportional feedback control can altered the weakly nonlinear flow properties. The application of large controller lead to suppress oscillatory Rayleigh–Bénard convection showed by Or et al. (2001). In the application of proportional feedback control, Tang and Bau (1998) placed the sensors at the heated of the bottom surface which is known as the thermal actuators. Regardless from its conductive, the purpose is to recognize any changes of the temperature at the surface of the fluid. Therefore, the temperature between upper and lower thermal boundaries will be modified using a proportional relationship. Hence, at the heated of the bottom surface, the actuators will directly to make a progressed regardless the unwanted disturbances. Besides that, the instabilities of Marangoni–Bénard convection has been proved by Or et al. (1999) that by the aid of feedback control, the long wavelength shown stabilized motion. Further research by Bau (1999) investigated on a linear basis with no-slip conditions at the bottom boundary theoretically showed with helped of feedback control suppressed the convective instabilities of Marangoni–Bénard convection. Due to this great important of controlled the flow patterns, a lot of researches have be done using feedback control such as by Siri and Hashim (2008, 2009a, 2009b), Kechil and Hashim (2008), Siri et al. (2009), Idris and Hashim (2010), Hashim et al. (2010), Loodts et al. (2014) and also Budroni et al. (2017).

In spite of the feedback control strategies used, Morton (1957), Lick (1965) and Foster (1965) proposed non-uniform temperature gradient on the ferroconvection pertains to buoyancy force. Ultimately, the presence of temperature gradient effectively delaying or enhance the onset of convection studied by Rudraiah and Chandna (1986) and Currie (1967). Rudraiah et. al (1986) performed the similar research using a suitable temperature gradient pertains to Bénard–Marangoni ferroconvection. The problem of combined buoyancy and surface tension forces of ferroconvection has been studied by Shivakumara et al. (2002) by adding the effect of basic temperature profiles and studied by Ravisha et al. (2017). However, magnetic field is the other factors that are added up by Hennenberg et al. (2005) on the problem of Rayleigh–Bénard–Marangoni ferroconvection to view the effect on the onset while acted normal to the boundaries. Further research on the onset of Marangoni ferroconvection, with the aim of understanding control of convection, Shivakumara and Nanjundappa (2006) and Shivakumara et al. (2014, 2015) applied various initial temperature profiles. Due to its important in space studies, Siddheshwar and Pranesh (1998) performed the non-uniform temperature profiles with the aid of internal heat source.

CHAPTER 3:

MATHEMATICAL FORMULATION AND METHOD OF SOLUTIONS

In this chapter, the derivation on the mathematical models of linear stability will be explained. Then, follow by the concept of Boussinesq approximation and classical linear stability theory. In the next section, the derivation on the mathematical formulation specifically for each fluid case, basic condition for that fluid at the rest state and also the analysis for linear stability theory to solve the problem will be discussed. Then, follow by the discussions on the boundary conditions for both cases of dielectric micropolar layer and ferrofluids layer. Finally, the completion of the chapter by the concept of feedback control strategies applied to the system.

3.1 General Model Linear Stability Convection

Generally, a fluid layer of infinite horizontal length in the direction of x and y, heated from below and bounded with two horizontal plane boundaries at $z = 0$ and $z = d$ in Figure 3.1 is considered. Temperature at the rigid surface represents by T_1 and temperature at the free surface represents by T_2. This research study based on non-Newtonian fluid, and will be focused on dielectric micropolar fluid and ferrofluid layer.

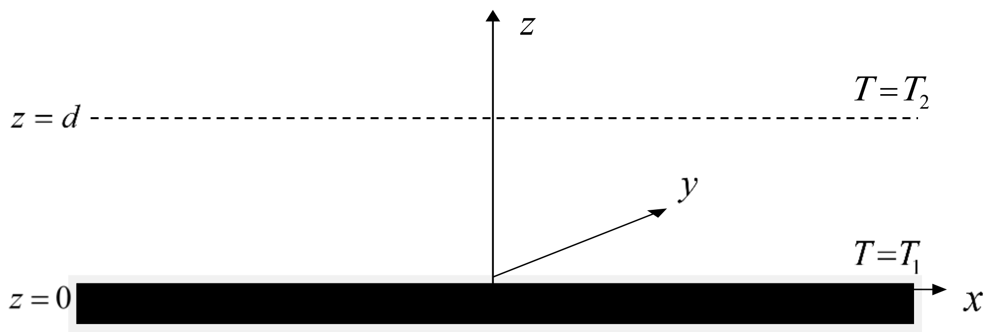

Figure 3.1: Schematic general physical model of the problem

The boundary conditions for each type of fluid were selected from these models. The set of hydrodynamic equations basically derived from the statement of Bénard–Marangoni convection problem using the Boussinesq approximations. Based on Chandrasekhar (1961), a fluid density, ρ from Boussinesq approximation has been proven linearly dependent with reference temperature, T_0 also known as equation of state, as equation below:

$$\rho = \rho_0\left[1-\alpha\left(T-T_0\right)\right], \tag{3.1.1}$$

where the coefficient of thermal expansion as α and assumed to be small. Also, assuming small influence of the material characteristics in the considered problem of the fluid, such as kinematic viscosity, ν, thermal conductivity, k and coefficient α itself. Hence, the density and these characteristics will assume to be constant on all terms in momentum equations. But for the density variation which has been multiplied by gravity acceleration term, g, the relating term on convection's phenomenon must be retained in terms of buoyancy force. In spite of that, we can negligible the heat release found from the loss of viscosity.

The Boussinesq equations can be written as follow based on stated assumption;

Continuity formulation:

$$\nabla \cdot \vec{q} = 0, \tag{3.1.2}$$

Conservation of energy:

$$\frac{\partial T}{\partial t} + \vec{q} \cdot \nabla T = \kappa \nabla^2 T, \tag{3.1.3}$$

Momentum equation:

$$\rho_0\left[\frac{\partial \vec{q}}{\partial t} + \left(\vec{q} \cdot \nabla\right)\vec{q}\right] = -\nabla p + \rho\vec{g} + \nu\nabla^2\vec{q}, \tag{3.1.4}$$

where $\nabla = \left(\frac{\partial^2}{\partial x^2} + \frac{\partial^2}{\partial y^2} + \frac{\partial^2}{\partial z^2} \right)$ is the Laplace operator, the velocity as $\vec{q} = (\vec{u}, \vec{v}, \vec{w})$, the pressure as *p*, the fluid density at reference temperature as ρ_0, the density as ρ, $\vec{g} = (0,0,-g)$ is the gravity acceleration, the time as t, T is the temperature, and κ is the thermal conductivity.

Generally, the governing equations for Newtonian fluids are also known as in equations (3.1.2) to (3.1.4). Whereas, these Boussinesq equations (3.1.3) and (3.1.4) for non-Newtonian fluids are slightly different expressions depends on considered type of fluids.

Therefore, in this thesis, we consider non-Newtonian fluids that are dielectric micropolar fluid and ferrofluid convection. Discussion on governing equations for momentum and energy will be given separately based on the research problem.

Before we start discussing in details about mathematical formulation for the model problem, here will be discussed a basic about the theory of linear stability (Chandrasekhar, 1961) that given to solve the linear convective problem. By assuming that the initial flow is in steady state, then based on classical linear stability theory, some physical variables that explaining on the flow are assumed to increase in very small quantities (infinitesimal). So, it is important to get the governing equations for these increments. To get these equations (increment equations) from relevant motion equations, all multiplication and power higher than the first will be ignored for the increments. So, only linear terms will be considered. The linear stability theory is the theory derived on the basis of such linearised equations. In contrast, finite amplitudes of the perturbations are used for non-linear theories. Stability that defined here is stability with respect to all possible disturbances (infinitesimal). To complete the investigation on stability, we must examine the reaction of the system to all possible disturbances. The details on linear stability theory can be found in Appendix.

3.2 Mathematical Formulation for Electroconvection in a Micropolar fluid

We noted that the Boussinesq fluid in a layer of infinite horizontal with depth d which has electrically conducting fluid. The layer is subject to a uniform electric field act normal to it and parallel to gravity $\vec{g}$. We let the origin with a system of Cartesian coordinate (x, y, z) at the bottom of the boundaries with the direction of vertical z-axis goes upwards and subject to a temperature drop ΔT. We assume the micro-rotation is vanished at the surfaces.

The relevant governing expressions for Rayleigh–Bénard–Marangoni electroconvection consist of the conservation equation of linear momentum, angular momentum conservation equation, energy conservation equation, dielectric constant equation, Faraday's law and polarization field equation following Baby and Pranesh (2012) and Azmi and Idris (2014), are as follow:

Conservation of linear momentum:

$$\rho_0\left[\frac{\partial \vec{q}}{\partial t}+(\vec{q}\cdot\nabla)\vec{q}\right]=-\nabla p-\rho\vec{g}\hat{k}+(2\zeta+\eta)\nabla^2\vec{q}+\zeta(\nabla\times\vec{\omega})+(\vec{p}\cdot\nabla)\vec{E}, \tag{3.2.1}$$

Angular momentum conservation equation:

$$\rho_0\vec{I}\left[\left(\frac{\partial \vec{\omega}}{\partial t}+(\vec{q}\cdot\nabla)\vec{\omega}\right)\right]=(\lambda'+\eta')\nabla(\nabla\cdot\vec{\omega})+\left(\eta'\nabla^2\vec{\omega}\right)+\zeta(\nabla\times\vec{q}-2\vec{\omega}), \tag{3.2.2}$$

Energy conservation equation:

$$\frac{\partial T}{\partial t}+\left(\vec{q}-\frac{\beta}{\rho_0 C_v}\nabla\times\vec{\omega}\right)\cdot\nabla T=\kappa\nabla^2 T, \tag{3.2.3}$$

Dielectric constant equation:

$$\varepsilon_r = (1+\kappa_e) - e(T - T_0), \tag{3.2.4}$$

Faraday's law:

$$\begin{aligned} \nabla \times \vec{E} &= 0, \\ \vec{E} &= -\nabla \phi, \end{aligned} \tag{3.2.5}$$

Polarization field equation:

$$\begin{aligned} \nabla \cdot \left(\varepsilon_0 \vec{E} + \vec{P}\right) &= 0, \\ \vec{P} &= \varepsilon_0 (\varepsilon_r - 1)\vec{E}, \end{aligned} \tag{3.2.6}$$

where the density of the fluid as ρ_0 at reference temperature, the velocity as $\vec{q} = (\vec{u}, \vec{v}, \vec{w})$, *t* is the time, the temperature as T, $\nabla = \left(\frac{\partial^2}{\partial x^2} + \frac{\partial^2}{\partial y^2} + \frac{\partial^2}{\partial z^2}\right)$ is the Laplace operator, the pressure as p, the density as ρ, $\vec{g}$ is the gravity acceleration, the unit vector in the direction of z as $\hat{k}$, ζ is the coefficient of coupling viscosity or vortex viscosity, the coefficient of shear kinematic viscosity as η, the spin as $\vec{\omega}$, the inertia moment as $\vec{I}$, the coefficient of bulk spin viscosity as λ', the coefficient of shear spin viscosity as η',the specific heat as C_v, the thermal conductivity as κ, the thermal susceptibility as κ_e, the electric field as $\vec{E}$, the electrostatic potential as ϕ, the free state of electric permeability as ε_0, the dielectric polarization as $\vec{P}$, and the dielectric constant as ε_r.

At rest, the electrically conducting Boussinesq fluid with depth d which the uniform electrical field acting normal to the infinite horizontal layer with non-deformable free surface, the expression of the basic state given by Azmi and Idris (2014):

$$\vec{q}_b = 0, \qquad \vec{\omega}_b = 0,$$

$$p = p_b(z), \qquad \rho = \rho_b(z),$$

$$\vec{E} = \vec{E}_b(z), \qquad \vec{P} = \vec{P}_b(z), \tag{3.2.7}$$

$$T = T_b(z), \qquad \frac{-d}{\Delta T}\frac{dT_b}{dz} = f(z).$$

The basic temperature gradients, $f(z)$, non-dimensional and monotonic satisfies the condition $\int_0^1 f(z)dz = 1$ which is non-negative,.

For basic state, equations (3.1.1), (3.1.2) and (3.2.1)–(3.2.6) specified by equation (3.2.7) and can be written in the form:

$$\rho_b = \rho_0\left[1 - \alpha\left(T_b - T_0\right)\right], \qquad \vec{q}_b = 0,$$

$$\frac{dp_b}{dz} = -\rho_b g + \vec{P}_b \frac{\partial \vec{E}_b}{\partial z}, \qquad \frac{d^2 T_b}{dz^2} = 0,$$

$$\varepsilon_r = \left(1 + \kappa_e\right) - e\left(T_b - T_0\right), \tag{3.2.8}$$

$$E_b = \left[\frac{\left(1 + \kappa_e\right)E_0}{\left(1 + \kappa_e\right) + \dfrac{e\Delta T_z}{h}}\right],$$

$$P_b = \varepsilon_0 E_0 \left(1 + \kappa_e\right)\left[1 - \frac{1}{\left(1 + \kappa_e\right) + \dfrac{e\Delta T_z}{h}}\right].$$

The stability of considered fluid will be analyzed by performing the linear stability theory. The instability and the superposed of infinitesimal perturbations on the quiescent basic state is analyzed. Hence, the following perturbations will be introduced:

$$\vec{q} = \vec{q}_b + \vec{q}', \qquad \vec{\omega} = \vec{\omega}_b + \vec{\omega}', \tag{3.2.9}$$
$$p = p_b + p', \qquad \rho = \rho_b + \rho',$$
$$\vec{E} = \vec{E}_b + \left(\vec{E}_1' + \vec{E}_3'\right), \qquad \vec{P} = \vec{P}_b + \left(\vec{P}_1' + \vec{P}_3'\right),$$
$$T = T_b + T',$$

where we assumed the small and perturbed ones as the primed quantities while the basic state value represented by subscripts 'b'.

By linearized equation (3.2.6), we get:

$$P_i' = \varepsilon_0 \kappa_e E_i', \qquad \text{for } i = 1, 2. \tag{3.2.10}$$
$$P_3' = \varepsilon_0 \kappa_e E_3' - e\varepsilon_0 E_0 T'.$$

Linear terms are only taken from linearization equations governing the perturbed ones by using linear stability theory. Substituting equation (3.2.9) into equations (3.1.1), (3.1.2) and (3.2.1)–(3.2.6) and by using equation (3.2.8), the derivation as follows:

From equation (3.1.1): Perturbed,

$$\rho_b + \rho' = \rho_0\left[1 - \alpha\left(T_b + T' - T_0\right)\right],$$
$$\rho_0\left[1 - \alpha\left(T_b - T_0\right)\right] + \rho' = \rho_0\left[1 - \alpha\left(T_b - T_0 + T'\right)\right],$$
$$\rho_0\left[1 - \alpha\left(T_b - T_0\right)\right] + \rho' = \rho_0\left[1 - \alpha\left(T_b - T_0\right) - \alpha T'\right],$$
$$\rho_0\left[1 - \alpha\left(T_b - T_0\right)\right] + \rho' = \rho_0\left[1 - \alpha\left(T_b - T_0\right)\right] - \rho_0 \alpha T',$$

Then, we get:

$$\rho' = -\rho_0 \alpha T'. \tag{3.2.11}$$

From equation (3.1.2): Perturbed,

$$\nabla \cdot \left(\vec{q}_b + \vec{q}'\right) = 0,$$
$$\nabla \cdot \vec{q}_b + \nabla \cdot \vec{q}' = 0,$$
$$\vec{q}_b = \left(\vec{u}_b, \vec{v}_b, \vec{w}_b\right) = (0,0,0),$$

Then, we get:

$$\nabla \cdot \vec{q}' = 0. \tag{3.2.12}$$

From equation (3.2.1): Perturbed,

$$\begin{aligned}
\rho_0\left[\frac{(\partial\vec{q}_b + \partial\vec{q}')}{\partial t} + ((\vec{q}_b + \vec{q}')\cdot\nabla)(\vec{q}_b + \vec{q}')\right] &= -\nabla(p_b + p') - (\rho_b + \rho')\vec{g}\hat{k} \\
&\quad + (2\zeta + \eta)\nabla^2(\vec{q}_b + \vec{q}') + \zeta(\nabla \times (\vec{\omega}_b + \vec{\omega}')) \\
&\quad + ((\vec{P}_b + \vec{P}')\cdot\nabla)(\vec{E}_b + \vec{E}'), \\
&= -\nabla(p_b + p') - (\rho_b + \rho')\vec{g}\hat{k} \\
&\quad + (2\zeta + \eta)\nabla^2(\vec{q}_b + \vec{q}') + \zeta(\nabla \times (\vec{\omega}_b + \vec{\omega}')) \\
&\quad + (\vec{P}_b \cdot \nabla + \vec{P}' \cdot \nabla)(\vec{E}' + \vec{E}_b),
\end{aligned}$$

Then, we get:

$$\rho_0\left[\frac{\partial\vec{q}'}{\partial t}\right] = -\nabla p' - \rho'\vec{g}\hat{k} + (2\zeta + \eta)\nabla^2\vec{q}' + \zeta(\nabla \times \vec{\omega}') + (\vec{P}_b \cdot \nabla)\vec{E}' + (\vec{P}' \cdot \nabla)\vec{E}_b. \tag{3.2.13}$$

From equation (3.2.2): Perturbed,

$$\begin{aligned}
\rho_0\vec{I}\left[\frac{\partial(\vec{\omega}_b + \vec{\omega}')}{\partial t} + ((\vec{q}_b + \vec{q}')\cdot\nabla)(\vec{\omega}_b + \vec{\omega}')\right] &= (\lambda' + \eta')\nabla(\nabla \cdot (\vec{\omega}_b + \vec{\omega}')) + (\eta'\nabla^2(\vec{\omega}_b + \vec{\omega}')) \\
&\quad + \zeta(\nabla \times (\vec{q}_b + \vec{q}') - 2(\vec{\omega}_b + \vec{\omega}')),
\end{aligned}$$

Then, we get:

$$\rho_0\vec{I}\left[\frac{\partial\vec{\omega}'}{\partial t}\right] = (\lambda' + \eta')\nabla(\nabla \cdot \vec{\omega}') + \eta'\nabla^2\vec{\omega}' + \zeta(\nabla \times \vec{q}' - 2\vec{\omega}'). \tag{3.2.14}$$

From equation (3.2.3): Perturbed,

$$\frac{\partial(T_b + T')}{\partial t} + \left((\vec{q}_b + \vec{q}') - \frac{\beta}{\rho_0 C_v}\nabla \times (\vec{\omega}_b + \vec{\omega}')\right)\cdot\nabla(T_b + T') = \kappa\nabla^2(T_b + T'),$$

Then, we get:

$$\frac{\partial(T_b + T')}{\partial t} + \left(\vec{q}' - \frac{\beta}{\rho_0 C_v} \nabla \times \vec{\omega}'\right) \cdot \nabla(T_b + T') = \kappa \nabla^2 (T_b + T'). \tag{3.2.15}$$

From equation (3.2.4): Perturbed,

$$\begin{aligned} &(1+\kappa_e) - e(T_b - T_0) = (1+\kappa_e) - e(T_b - T' - T_0), \\ &-e(T_b - T_0) = -e((T_b - T_0) - T'), \\ &0 = -eT', \end{aligned}$$

Assume $\frac{\varepsilon'}{\varepsilon_0} = 0$,

Then, $\frac{\varepsilon'}{\varepsilon_0} = -eT'$,

Hence, we get:

$$\varepsilon' = -\varepsilon_0 e T'. \tag{3.2.16}$$

From equation (3.2.5): can be implied as:

$$\vec{E} = -\nabla \phi', \tag{3.2.17}$$

where ϕ' is the perturbed electric scalar potential.

From equation (3.2.6): Perturbed,

$$\nabla \cdot \left(\varepsilon_0 (\vec{E}_b + \vec{E}') + (\vec{P}_b + \vec{P}')\right) = 0,$$

Then, we get:

$$\nabla \cdot \left(\varepsilon_0 \vec{E}' + \vec{P}'\right) = 0. \tag{3.2.18}$$

The following definition used by non-dimensional equations (3.2.11)–(3.2.18):

$$\left(x^*, y^*, z^*\right) = \left(\frac{x}{d}, \frac{y}{d}, \frac{z}{d}\right), \qquad W^* = \frac{W'}{\left(\frac{\kappa}{d}\right)},$$

$$\vec{\omega}^* = \frac{\vec{\omega}'}{\left(\frac{\kappa}{d}\right)}, \qquad t^* = \frac{t}{\left(\frac{d^2}{\kappa}\right)}, \tag{3.2.19}$$

$$T^* = \frac{T'}{\Delta T}, \qquad \phi^* = \frac{\phi'}{\left(\frac{eE_0 \Delta T d}{(1+\kappa_e)}\right)},$$

$$\Omega^* = \nabla \times \frac{w}{\left(\frac{\kappa}{d^3}\right)},$$

The equation (3.2.11) substitute into equation (3.2.13) and taking the resulting equation curl twice by using the definition (3.2.19):

$$\rho_0\left[\frac{\partial \vec{q}'}{\partial t} + (\vec{q}' \cdot \nabla)\vec{q}'\right] = -\nabla p' + \rho_0 \alpha T' \vec{g}\hat{k} + (2\zeta + \eta)\nabla^2 \vec{q}' + \zeta(\nabla \times \vec{\omega}') + \left(\vec{P}_b \cdot \nabla\right)\vec{E}' + \left(\vec{P}' \cdot \nabla\right)\vec{E}_b, \tag{3.2.20}$$

Taking curl once to eliminate the pressure:

$$\rho_0\left[\frac{\partial \nabla \times \vec{q}'}{\partial t} + \nabla \times [(\vec{q}' \cdot \nabla)\vec{q}']\right] = -\nabla \times \nabla p' + \rho_0 \alpha \vec{g}\hat{k}(\nabla \times T') + (2\zeta + \eta)\left(\nabla \times \nabla^2 \vec{q}'\right) + \zeta(\nabla \times \nabla \times \vec{\omega}') + \nabla \times \left(\vec{P}_b \cdot \nabla\right)\vec{E}' + \nabla \times \left(\vec{P}' \cdot \nabla\right)\vec{E}_b,$$

$$\rho_0\left[\frac{\partial(\nabla \times \vec{q}')}{\partial t}\right] = \rho_0 \alpha \vec{g}\hat{k}(\nabla \times T') + (2\zeta + \eta)\left(\nabla \times \nabla^2 \vec{q}'\right) + \zeta(\nabla \times \nabla \times \vec{\omega}') + \nabla \times \left(\vec{P}_b \cdot \nabla\right)\vec{E}' + \nabla \times \left(\vec{P}' \cdot \nabla\right)\vec{E}_b,$$

Taking curl once again:

$$\rho_0\left[\frac{\partial\nabla\times\nabla\times\vec{q}'}{\partial t}\right]=\rho_0\alpha\vec{g}\hat{k}\left(\nabla\times\nabla\times T'\right)+\left(2\zeta+\eta\right)\left(\nabla\times\nabla\times\nabla^2\vec{q}'\right)+\zeta\left(\nabla\times\nabla\times\nabla\times\vec{\omega}'\right)$$

$$+\nabla\times\nabla\times\left(\vec{P}_b\cdot\nabla\right)\vec{E}'+\nabla\times\nabla\times\left(\vec{P}'\cdot\nabla\right)\vec{E}_b,$$

$$\rho_0\left[\frac{\partial\left[\nabla\left(\nabla\cdot\vec{q}\right)-\nabla^2\cdot\vec{q}'\right]}{\partial t}\right]=\rho_0\alpha\vec{g}\left[\nabla\left(\nabla\cdot T'\right)-\nabla^2\cdot T'\right]\hat{k}+\left(2\zeta+\eta\right)\left[\nabla\left(\nabla^2\cdot\vec{q}\right)-\nabla^4\cdot\vec{q}'\right]$$

$$+\zeta\left[\nabla\left(\nabla\cdot\vec{\omega}'\right)-\nabla^2\cdot\vec{\omega}'\right]+\left(\vec{P}_b\cdot\nabla\right)\left[\nabla\left(\nabla\cdot\vec{E}'\right)-\nabla^2\cdot\vec{E}'\right]$$

$$+\left[\nabla\left(\vec{P}'\cdot\nabla\right)-\nabla^2\cdot\left(\vec{P}'\cdot\nabla\right)\right]\vec{E}_b,$$

Hence, we get:

$$\rho_0\left[\frac{\partial\left(\nabla^2\cdot\vec{q}'\right)}{\partial t}\right]=\alpha\rho_0\vec{g}\nabla^2\cdot T'\hat{k}+\left(2\zeta+\eta\right)\nabla^4\vec{q}'+\zeta\nabla^2\cdot\left(\nabla\times\vec{\omega}'\right)+\nabla^2\vec{E}'\left(\vec{P}_b\cdot\nabla\right) \tag{3.2.21}$$

$$+\nabla^2\left(\vec{P}'\cdot\nabla\right)\vec{E}_b,$$

The equation (3.2.21) will become as follow, after considering the steady convection:

$$\alpha\rho_0\vec{g}\nabla^2\cdot T'\hat{k}+\left(2\zeta+\eta\right)\nabla^4\vec{q}'+\zeta\nabla^2\cdot\left(\nabla\times\vec{\omega}'\right)+\nabla^2\vec{E}'\left(\vec{P}_b\cdot\nabla\right)+\nabla^2\left(\vec{P}'\cdot\nabla\right)\vec{E}_b=0, \tag{3.2.22}$$

Then, by using definition from equation (3.2.19), the equation (3.2.22) reduced into non-dimensional equations:

$$\frac{\alpha\rho_0\vec{g}\Delta T}{d^2}\left[\frac{\partial^2T^*}{\partial x^{*2}}+\frac{\partial^2T^*}{\partial y^{*2}}\right]+\left(2\zeta+\eta\right)\frac{\kappa}{d^5}\left[\frac{\partial^4u^*}{\partial x^{*4}}+\frac{\partial^4v^*}{\partial y^{*4}}+\frac{\partial^4w^*}{\partial z^{*4}}\right]+\zeta\,\frac{\kappa}{d^5}\nabla^2\Omega^*$$

$$-\frac{\varepsilon_0e^2E_0^2\Delta T^2d^2}{\left(1+\kappa_e\right)\left(\zeta+\eta\right)\kappa}\nabla_1^2Tf(z)-\frac{\varepsilon_0e^2E_0^2\Delta T^2d^2}{\left(1+\kappa_e\right)\left(\zeta+\eta\right)\kappa}\frac{\partial}{\partial z}\left(\nabla_1^2\phi\right)f(z)=0,$$

$$\frac{\alpha\rho_0\vec{g}\Delta Td^3}{\kappa}\left[\frac{\partial^2T^*}{\partial x^{*2}}+\frac{\partial^2T^*}{\partial y^{*2}}\right]+\zeta\nabla^4W^*+\left(\zeta+\eta\right)\nabla^4W^*+\zeta\nabla^2W^*+\zeta\nabla^2\Omega^*$$

$$-\frac{\varepsilon_0e^2E_0^2\Delta T^2d^2}{\left(1+\kappa_e\right)\left(\zeta+\eta\right)\kappa}\nabla_1^2Tf(z)-\frac{\varepsilon_0e^2E_0^2\Delta T^2d^2}{\left(1+\kappa_e\right)\left(\zeta+\eta\right)\kappa}\frac{\partial}{\partial z}\left(\nabla_1^2\phi\right)f(z)=0,$$

$$\frac{\alpha\rho_0\vec{g}\Delta Td^3}{\left(\zeta+\eta\right)\kappa}\left[\frac{\partial^2T^*}{\partial x^{*2}}+\frac{\partial^2T^*}{\partial y^{*2}}\right]+\frac{\zeta}{\left(\zeta+\eta\right)}\nabla^4W^*+\nabla^4W^*+\frac{\zeta}{\left(\zeta+\eta\right)}\nabla^2W^*+\frac{\zeta}{\left(\zeta+\eta\right)}\nabla^2\Omega^*$$

$$-\frac{\varepsilon_0e^2E_0^2\Delta T^2d^2}{\left(1+\kappa_e\right)\left(\zeta+\eta\right)\kappa}\nabla_1^2Tf(z)-\frac{\varepsilon_0e^2E_0^2\Delta T^2d^2}{\left(1+\kappa_e\right)\left(\zeta+\eta\right)\kappa}\frac{\partial}{\partial z}\left(\nabla_1^2\phi\right)f(z)=0,$$

Dropped out the asterisk:

$$R\nabla_1^2 T + (1+N_1)\nabla^4 W + N_1\nabla^2 W + N_1\nabla^2\Omega_z + L\nabla_1^2 T f(z) + L\frac{\partial}{\partial z}\left(\nabla_1^2\phi\right) f(z) = 0, \qquad (3.2.23)$$

For equation (3.2.14), taking curl once and by using definition from equation (3.2.19), the resulting equation reduced into non-dimensional equation:

$$\rho_0\vec{I}\left[\frac{\partial\nabla\times\vec{\omega}'}{\partial t} + \nabla\times(\vec{q}'\cdot\nabla)\vec{\omega}'\right] = (\lambda'+\eta')\nabla\times(\nabla(\nabla\cdot\vec{\omega}')) + \eta'\nabla\times(\nabla^2\vec{\omega}')$$
$$+\nabla\times(\zeta(\nabla\times\vec{q}' - 2\vec{\omega}')),$$
$$\eta'\nabla^2(\nabla\times\vec{\omega}') - \zeta\nabla^2\vec{q}' - 2\zeta(\nabla\cdot\vec{\omega}') = 0,$$
$$\eta'\left[\nabla^2(\nabla\times\vec{\omega}')\right] - \zeta\nabla^2 W' - 2\zeta(\nabla\cdot\vec{\omega}') = 0,$$
$$\eta'\left[\nabla^2\left(\Omega^*\left(\frac{\kappa}{d^3}\right)\right)\right] - \zeta\nabla^2 W^*\left(\frac{\kappa}{d}\right) - 2\zeta\Omega^*\left(\frac{\kappa}{d^3}\right) = 0,$$
$$\left[\frac{\eta'\nabla^2\Omega^*}{d^2} - \zeta\nabla^2 W^* - 2\zeta\Omega^*\right]\left[\frac{1}{(\zeta+\eta)}\right] = 0,$$

Dropped out the asterisk:

$$N_3\nabla^2\Omega_z - N_1\nabla^2 W - 2N_1\Omega_z = 0, \qquad (3.2.24)$$

Next, by using definition from equation (3.2.19), the equation (3.2.15) reduced into non-dimensional equations:

$$(\vec{q}'\cdot\nabla)(T_b + T') = \frac{\beta}{\rho_0 C_v}\left[(\nabla\times\vec{\omega}')\cdot\nabla(T_b+T')\right] + \kappa\nabla^2(T_b+T'),$$

$$(W'\cdot\nabla)(T_b+T') = \frac{\beta}{\rho_0 C_v}\left[(\nabla\times\vec{\omega}')\cdot\left(\frac{d}{dx}(T_b+T')\hat{i} + \frac{d}{dy}(T_b+T')\hat{j} + \frac{d}{dz}(T_b+T')\hat{k}\right)\right]$$
$$+\kappa\nabla^2(T_b+T'),$$

$$-W'\frac{\Delta T}{d}f(z) = \frac{\beta}{\rho_0 C_v}\left[(\nabla\times\vec{\omega}')\cdot\left(\frac{\Delta}{d}f(z)\right)\hat{k}\right] + \kappa\nabla^2 T',$$

$$-W^*\frac{\kappa\Delta T}{d^2}f(z) = \frac{\beta}{\rho_0 C_v}\left[\frac{\kappa}{d^3}\Omega^*\left(\frac{-\Delta}{d}f(z)\right)\hat{k}\right] + \frac{\kappa}{d^2}\nabla^2 T^*,$$

$$\nabla^2 T^* - f(z)\left[W^* - \frac{\beta}{\rho_0 C_v d^2}\Omega^*\hat{k}\right] = 0,$$

Dropped out the asterisk:

$$\nabla^2 T - \left[W - N_5\Omega\right] f(z) = 0, \tag{3.2.25}$$

For equation (3.2.18), by using equations (3.2.10), (3.2.17) and definition from equation (3.2.23), substitute the resulting equation with equation (3.2.8) and reduced into non-dimensional equation:

$$\begin{aligned}
&\left\{\nabla \cdot \left(\varepsilon_0 E' + \varepsilon_0 \kappa_e - e\varepsilon_0 E_0 T'\right) = 0\right\} \times \frac{1}{\varepsilon_0}, \\
&\nabla \cdot \left[(1+\kappa_e)(E - E_b)\right] - \nabla\left(eE_0 T'\right) = 0, \\
&\nabla \cdot \left[(1+\kappa_e)(-\nabla\phi' - E_b)\right] - \nabla\left(eE_0 T'\right) = 0, \\
&\nabla \cdot \left[(1+\kappa_e)\left(-\nabla\phi' - \frac{(1+\kappa_e)E_0}{(1+\kappa_e) + \frac{e\Delta T_z}{h}}\right)\right] - \nabla\left(eE_0 T'\right) = 0, \\
&\nabla \cdot \left[(1+\kappa_e)\left(-\nabla\phi^* \frac{eE_0\Delta Td}{(1+\kappa_e)} - \frac{(1+\kappa_e)E_0}{(1+\kappa_e) + e\Delta T}\right)\right] - \nabla\left(eE_0 T^* \Delta T\right) = 0, \\
&\left\{\nabla^2\left(\phi^* eE_0 \Delta Td\right) - \nabla\left(eE_0 T^* \Delta Td\right) = 0\right\} \times \frac{1}{eE_0\Delta Td}, \\
&\nabla^2\phi^* - \nabla T^* = 0,
\end{aligned}$$

Dropped out the asterisk:

$$\nabla^2\phi - \frac{\partial T}{\partial z} = 0, \tag{3.2.26}$$

where, $\nabla_1^2 = \frac{\partial^2}{\partial x^2} + \frac{\partial^2}{\partial y^2}$ is the two-dimensional Laplace operator.

After neglecting the asterisks, the non-dimensional parameter defined as in Table 3.1:

Table 3.1: Non-Dimensional Parameter of Dielectric Micropolar Convection

Symbol	Definition	Parameter
N_1	$\dfrac{\zeta}{\zeta+\eta},\ 0 \le N_1 \le 1$	Coupling
N_3	$\dfrac{\eta}{(\zeta+\eta)d^2},\ 0 \le N_3 \le m$	Couple stress
N_5	$\dfrac{\beta}{\rho_0 C_v d^2},\ 0 \le N_5 \le n$	Micropolar heat conduction
R	$\dfrac{\rho_0 \alpha \bar{g} \Delta T d^3}{\chi(\zeta+\eta)}$	Rayleigh number
M	$\dfrac{\sigma_T \Delta T d}{\mu \kappa}$	Marangoni number
L	$\dfrac{\varepsilon_0 e^2 E_0^2 \Delta T^2 d^2}{(1+\chi_e)(\zeta+\eta)\chi}$	Electric number

Performing the dependent variables of the normal mode expansion (Chandrasekhar, 1961) in the form:

$$\begin{bmatrix} w \\ \Omega_z \\ T \\ \phi \end{bmatrix} = \begin{bmatrix} W(z) \\ G(z) \\ \theta(z) \\ \phi(z) \end{bmatrix} e^{i(lx+ny)}, \tag{3.2.27}$$

where $W(z), G(z), \theta(z), \phi(z)$, are respectively, the amplitude of perturbation velocity of z-component, perturbation rotation, perturbation temperature, perturbation electrostatic potential with l and n, wave number $\vec{a}$, in the directions of x and y respectively.

The equation (3.2.27) substitute into equations (3.2.23)–(3.2.26), we obtain:

$$(1+N_1)(D^2-a^2)^2 W - a^2 R\theta + N_1(D^2-a^2)G - a^2 L\theta f(z) + a^2 LD\phi f(z) = 0, \tag{3.2.28}$$

$$N_3(D^2-a^2)G - N_1(D^2-a^2)W - 2N_1 G = 0, \tag{3.2.29}$$

$$(D^2-a^2)\theta + (W - N_5 G)f(z) = 0, \tag{3.2.30}$$

$$(D^2-a^2)\phi - D\theta = 0, \tag{3.2.31}$$

where the differential operator as $D = \frac{d}{dz}$ and the overall horizontal wavenumber as $a = \sqrt{l^2 + m^2}$.

The non-dimensional and perturbed variables had the boundary conditions that take the form as follow:

$$W = DW = \theta = \frac{\partial \phi}{\partial z} = 0 \text{ at } \mathrm{z} = 0, \tag{3.2.32}$$

and

$$W = D^2W + M\,a^2\theta = D\phi = D\theta = 0 \text{ at } z = 1, \tag{3.2.33}$$

and

$$\theta(0) + K\theta(1) = 0, \tag{3.2.34}$$

where the Marangoni number as $M = \frac{\sigma_T \Delta T d}{\mu\kappa}$ and the feedback control as *K*.

3.3 Mathematical Formulation for Ferrofluids Convection

Consider a Boussinesq ferromagnetic fluid which has electrically non-conducting fluid in a layer of infinite horizontal with depth *d*. The layer is subject to a uniform magnetic field $\vec{H}_0$ act normal to it and parallel to gravity $\vec{g}$. The lower rigid boundary $z = 0$ is at rigid surface condition, while the upper non-deformable layer $z = d$ assumed to be free. The vertically direction of z-axis goes upwards and the system of Cartesian co-ordinate (x, y, z) is taken with the origin at the bottom boundaries. Then, the boundaries subject to a temperature drop ΔT and assume the surface tension σ linearly dependent with temperature as $\sigma = \sigma_0 - \sigma_T \Delta T$, where the unperturbed denoted as σ_0, value and the rate of change of surface tension with the temperature as $-\sigma_T$.

The relevant governing expressions of Rayleigh–Bénard–Marangoni ferroconvection, following Rosenswig (1985) and Shivakumara et al. (2002) are as follow:

Equation of state and continuity equation is the same as equation (3.1.1) and (3.1.2).

Linear momentum conservation equation:

$$\rho_0\left[\frac{\partial \vec{q}}{\partial t}+(\vec{q}\cdot\nabla)\vec{q}\right]=-\nabla p+\rho\vec{g}+\mu_0\left(\vec{M}\cdot\nabla\right)\vec{H}+\mu\nabla^2\vec{q}, \tag{3.3.1}$$

$$\left[\rho_0 C_{V,H}-\mu_0\vec{H}\cdot\left(\frac{\partial \vec{M}}{\partial T}\right)_{V,H}\right]\frac{DT}{Dt}+\mu_0 T\left(\frac{\partial \vec{M}}{\partial T}\right)_{V,H}\frac{D\vec{H}}{Dt}=\kappa\nabla^2 T, \tag{3.3.2}$$

$$\vec{B}=\mu_0\left(\vec{M}+\vec{H}\right), \tag{3.3.3}$$

$$\vec{M}=\frac{\vec{H}}{H}M(H,T), \tag{3.3.4}$$

$$M=M_0+\chi(H-H_0)-K(T-T_a), \tag{3.3.5}$$

$$\nabla\cdot\vec{B}=0, \tag{3.3.6a}$$

$$\nabla\times\vec{H}=0, \tag{3.3.6b}$$

where $\nabla=\left(\frac{\partial^2}{\partial x^2}+\frac{\partial^2}{\partial y^2}+\frac{\partial^2}{\partial z^2}\right)$ is the Laplace operator, the velocity as $\vec{q}=(\vec{u},\vec{v},\vec{w})$, the density of the fluid at reference temperature as ρ_0, the time as t, p is the pressure, the density as ρ, the acceleration due to gravity as $\vec{g}$, the magnetic permeability as μ_0, the magnetization as $\vec{M}$, the coefficient of thermal expansion as α, the magnetic field as $\vec{H}$, the temperature as T, the average temperature as T_a, the specific heat at constant volume and magnetic field as $C_{V,H}$, the thermal conductivity as κ, the magnetic induction as $\vec{B}$, the magnetic susceptibility as $\chi = \left(\frac{\partial M}{\partial H}\right)_{H_0,T_a}$, the pyromagnetic coefficient as $K = \left(\frac{\partial M}{\partial T}\right)_{H_0,T_a}$, and $M_0 = M(H_0, T_a)$.

At rest, ferromagnetic fluid layer with depth, *d* that has electrically non-conducting fluid with non-deformable free surface is subject to a uniform magnetic field act normal to the layer, basic state of the fluid followed as Shivakumara et al. (2002):

$$\vec{q} = \vec{q}_b = 0, \qquad p = p_b(z), \qquad -\frac{dT_b}{dz} = f(z), \tag{3.3.7}$$
$$\vec{H}_b = \left[H_0 + \frac{K(T_b - T_a)}{1+\chi}\right]\hat{k}, \qquad \vec{M}_b = \left[M_0 - \frac{K(T_b - T_a)}{1+\chi}\right]\hat{k},$$

where the unit vector $\hat{k}$ in the z-direction and non-dimensional, monotonic basic temperature gradients *f*(z) satisfies the condition $\int_0^d f(z)dz = \frac{\Delta T}{d}$.

The following perturbations had been analyzed from the basic state stability are as follow:

$$\vec{q} = \vec{q}_b + \vec{q}\,', \qquad p = p_b(z) + p', \tag{3.3.8}$$
$$T = T_b(z) + T', \qquad \vec{H} = \vec{H}_b(z) + \vec{H}',$$
$$\vec{M} = \vec{M}_b(z) + \vec{M}'.$$

The primes (′) represents the quantities are infinitesimal thermal perturbations and they are predicted to be small while the subscript ‘*b*’ represents the value at the basic state.

By using equation (3.3.3), substituting equation (3.3.8) into equations (3.3.4) and (3.3.5) yields:

$$H_i' + M_i' = \left(1 + \frac{M_0}{H_0}\right)H_i', \qquad i = 1, 2, \tag{3.3.9}$$

$$H_3' + M_3' = (1+\chi)H_3' - KT', \tag{3.3.10}$$

where assumed $K(T_b - T_a)$ « $(1+\chi)H_0$,

From equation (3.3.6b) can be implied as:

$$H' = \nabla\phi', \tag{3.3.11}$$

where the perturbed magnetic potential as ϕ'.

Substituting the principle of linear stability equations (3.3.7) and (3.3.8) into equations (3.3.1) till (3.3.3), the derivation as follows:

From equation (3.1.2): Perturbed,

$$\begin{aligned}
&\nabla \cdot (\vec{q}_b + \vec{q}') = 0, \\
&\nabla \cdot \vec{q}_b + \nabla \cdot \vec{q}' = 0, \\
&\vec{q}_b = (\vec{u}_b, \vec{v}_b, \vec{w}_b) = (0,0,0),
\end{aligned}$$

Then, we get:

$$\nabla \cdot \vec{q}' = 0, \tag{3.3.12}$$

From equation (3.1.1): Perturbed,

$$\begin{aligned}
&\rho_b + \rho' = \rho_0[1-\alpha(T_b + T' - T_0)], \\
&\rho_0[1-\alpha(T_b - T_0)] + \rho' = \rho_0[1-\alpha(T_b - T_0 + T')], \\
&\rho_0[1-\alpha(T_b - T_0)] + \rho' = \rho_0[1-\alpha(T_b - T_0) - \alpha T'], \\
&\rho_0[1-\alpha(T_b - T_0)] + \rho' = \rho_0[1-\alpha(T_b - T_0)] - \rho_0\alpha T',
\end{aligned}$$

Then, we get:

$$\rho' = -\rho_0\alpha T', \tag{3.3.13}$$

From equation (3.3.3): Perturbed,

$$\begin{aligned}\vec{B} &= \mu_0\left(\vec{M}_b + \vec{M}' + \vec{H}_b + \vec{H}'\right),\\ &= \mu_0\left(\vec{M}_b + \vec{H}_b + \vec{M}' + \vec{H}'\right),\\ &= \mu_0\left(\left[M_0 - \frac{K(T_b - T_a)}{1+\chi}\right]\hat{k} + \left[H_0 + \frac{K(T_b - T_a)}{1+\chi}\right]\hat{k} + \vec{M}' + \vec{H}'\right),\end{aligned}$$

Then, we get:

$$\vec{B} = \mu_0\left((M_0 + H_0)\hat{k} + \vec{M}' + \vec{H}'\right), \tag{3.3.14}$$

From equation (3.3.1): Perturbed,

$$\begin{aligned}\rho_0\left[\frac{(\partial\vec{q}_b + \partial\vec{q}')}{\partial t} + ((\vec{q}_b + \vec{q}')\cdot\nabla)(\vec{q}_b + \vec{q}')\right] &= -\nabla(p_b + p') + (\rho_b + \rho')\vec{g} + \mu\nabla^2(\vec{q}_b + \vec{q}')\\ &\quad + \mu_0\left((\vec{M}_b + \vec{M}')\cdot\nabla\right)(\vec{H}_b + \vec{H}'),\\ &= -\nabla(p_b + p') + (\rho_b + \rho')\vec{g} + \mu\nabla^2(\vec{q}_b + \vec{q}')\\ &\quad + \mu_0\left(\vec{M}_b\cdot\nabla + \vec{M}'\cdot\nabla\right)(\vec{H}_b + \vec{H}'),\end{aligned}$$

Then, we get:

$$\rho_0\left[\frac{\partial\vec{q}'}{\partial t}\right] = -\nabla p' + \rho'\vec{g} + \mu\nabla^2\vec{q}' + (\vec{M}_b\cdot\nabla)\vec{H}' + (\vec{M}'\cdot\nabla)\vec{H}_b, \tag{3.3.15}$$

Taking the resulting equation curl twice after substituting equation (3.3.13) into equation (3.3.15):

$$\rho_0\left[\frac{\partial\vec{q}'}{\partial t} + (\vec{q}'\cdot\nabla)\vec{q}'\right] = -\nabla p' + \rho_0\alpha T'\vec{g} + \mu\nabla^2\vec{q}' + (\vec{M}_b\cdot\nabla)\vec{H}' + (\vec{M}'\cdot\nabla)\vec{H}_b,$$

Taking curl once to eliminate the pressure:

$$\begin{aligned}\rho_0\left[\frac{\partial\nabla\times\vec{q}'}{\partial t} + \nabla\times[(\vec{q}'\cdot\nabla)\vec{q}']\right] &= -\nabla\times\nabla p' + \rho_0\alpha\vec{g}(\nabla\times T') + \mu(\nabla\times\nabla^2\vec{q}')\\ &\quad + \nabla\times(\vec{M}_b\cdot\nabla)\vec{H}' + \nabla\times(\vec{M}'\cdot\nabla)\vec{H}_b,\end{aligned}$$

$$\rho_0\left[\frac{\partial(\nabla\times\vec{q}')}{\partial t}\right] = \rho_0\alpha\vec{g}\hat{k}(\nabla\times T') + \mu(\nabla\times\nabla^2\vec{q}') + \nabla\times(\vec{M}_b\cdot\nabla)\vec{H}' + \nabla\times(\vec{M}'\cdot\nabla)\vec{H}_b,$$

Taking curl once again:

$$\rho_0\left[\frac{\partial\nabla\times\nabla\times\vec{q}'}{\partial t}\right]=\rho_0\alpha\vec{g}\hat{k}(\nabla\times\nabla\times T')+\mu\left(\nabla\times\nabla\times\nabla^2\vec{q}'\right)$$

$$+\nabla\times\nabla\times\left(\vec{M}_b\cdot\nabla\right)\vec{H}'+\nabla\times\nabla\times\left(\vec{M}'\cdot\nabla\right)\vec{H}_b,$$

$$\rho_0\left[\frac{\partial\left[\nabla(\nabla\cdot\vec{q})-\nabla^2\cdot\vec{q}'\right]}{\partial t}\right]=\rho_0\alpha\vec{g}\left[\nabla(\nabla\cdot T')-\nabla^2\cdot T'\right]+\mu\left[\nabla\left(\nabla^2\cdot\vec{q}\right)-\nabla^4\cdot\vec{q}'\right]$$

$$+\left(\vec{M}_b\cdot\nabla\right)\left[\nabla\left(\nabla\cdot\vec{H}'\right)-\nabla^2\cdot\vec{H}'\right]$$

$$+\left[\nabla\left(\vec{M}'\cdot\nabla\right)-\nabla^2\cdot\left(\vec{M}'\cdot\nabla\right)\right]\vec{H}_b,$$

$$\rho_0\left[\frac{\partial\left(\nabla^2\cdot\vec{q}'\right)}{\partial t}\right]-\mu\left(\nabla^4\cdot\vec{q}'\right)=\rho_0\alpha\vec{g}\left[\nabla(\nabla\cdot T')-\nabla^2\cdot T'\right]$$

$$+\left(\vec{M}_b\cdot\nabla\right)\left[\nabla\left(\nabla\cdot\vec{H}'\right)-\nabla^2\cdot\vec{H}'\right]$$

$$+\left[\nabla\left(\vec{M}'\cdot\nabla\right)-\nabla^2\cdot\left(\vec{M}'\cdot\nabla\right)\right]\vec{H}_b\ ,$$

$$\rho_0\frac{\partial}{\partial t}\left(\nabla^2\cdot\vec{q}'\right)-\left(\mu\nabla^2\right)\left(\nabla^2\cdot\vec{q}'\right)=\rho_0\alpha\vec{g}\left[\nabla(\nabla\cdot T')-\nabla^2\cdot T'\right]+\left(\vec{M}_b\cdot\nabla\right)\nabla^2\vec{H}'$$

$$+\nabla^2\left(\vec{M}'\cdot\nabla\right)\vec{H}_b,$$

After considering the steady convection and neglecting the primes for simplicity, we obtained:

$$\left(\rho_0\frac{\partial}{\partial t}-\mu\nabla^2\right)\nabla^2 w=\rho_0\alpha g\nabla_1^2 T-\mu_0 Kf(z)\frac{\partial}{\partial z}\left(\nabla_1^2\phi\right)+\frac{\mu_0 K^2 f(z)}{1+\chi}\nabla_1^2 T. \tag{3.3.16}$$

With the notation of the standard linear stability analysis, computing equation (3.3.2) by using equations (3.3.7) and (3.3.8), we obtained:

$$\left[\rho_0 C_{V,H} - \mu_0\left(\vec{H}_b + \vec{H}'\right)\cdot\left(\frac{\partial\left(\vec{M}_b + \vec{M}'\right)}{\partial T}\right)_{V,H}\right]\frac{D(T_b + T')}{Dt}$$

$$+ \mu_0(T_b + T')\left(\frac{\partial\left(\vec{M}_b + \vec{M}'\right)}{\partial T}\right)_{V,H}\frac{D\left(\vec{H}_b + \vec{H}'\right)}{Dt} = \kappa\nabla^2(T_b + T'),$$

$$\rho_0 C_{V,H}\frac{D(T_b + T')}{Dt} - \mu_0\left(\vec{H}_b + \vec{H}'\right)\cdot K\frac{D(T_b + T')}{Dt}$$

$$+ \mu_0(T_b + T')\left(\frac{\partial\vec{M}_b + \vec{M}'}{\partial T}\right)_{V,H}\frac{D\left(\vec{H}_b + \vec{H}'\right)}{Dt} = \kappa\nabla^2(T_b + T'),$$

$$\rho_0 C_0\frac{\partial(T_b + T')}{\partial t} - \mu_0 K\frac{\partial(T_b + T')}{\partial t}\frac{\partial}{\partial t}\left(\vec{H}_b + \vec{H}'\right)$$

$$+\left(\frac{\mu_0 T_0 K^2}{1+\chi}wf(z) - \rho_0 C_0 wf(z)\right) = \kappa\nabla^2(T_b + T').$$

After considering the steady convection and neglecting the primes for simplicity, we get:

$$\rho_0 C_0\frac{\partial T}{\partial t} - \kappa\nabla^2 T - \mu_0 K T_0\frac{\partial}{\partial t}\left(\frac{\partial\phi}{\partial z}\right) = \left(\rho_0 C_0 - \frac{\mu_0 K^2 T_0}{1+\chi}\right)wf(z), \tag{3.3.17}$$

Next, for equation (3.3.10), with the notation of the standard linear stability analysis, by substituting equations (3.3.7) and (3.3.8):

$$\left(1 + \frac{M_0}{H_0}\right)H' + (1+\chi)H_3' - KT' = 0, \tag{3.3.18}$$

After neglecting the primes for simplicity, we considered the steady convection as follows:

$$\left(1+\frac{M_0}{H_0}\right)\nabla_1^2\phi+(1+\chi)\left(\frac{\partial^2\phi}{\partial z^2}\right)-K\frac{\partial T}{\partial z}=0, \tag{3.3.19}$$

where,

$$\rho_0 C_0=\rho_0 C_{V,H}+\mu_0 K H_0\,,$$

$$\nabla=\frac{\partial^2}{\partial z^2},$$

$$\nabla_1^2\equiv\frac{\partial^2}{\partial x^2}+\frac{\partial^2}{\partial y^2},$$

and $\nabla^2\equiv\nabla_1^2+\dfrac{\partial^2}{\partial z^2}.$

A normal mode solution is permitted in the form:

$$\begin{bmatrix} w \\ T \\ \phi \end{bmatrix}=\begin{bmatrix} W(z) \\ \theta(z) \\ \phi(z) \end{bmatrix}e^{i(lx+ny)+\omega t}, \tag{3.3.20}$$

where the amplitude of perturbation velocity of z-component as $W(z)$, the perturbation temperature as $\theta(z)$, the perturbation magnetization as $\phi(z)$ while the growth rate as ω, and the horizontal components of the wave number $\vec{a}$, are *l* and *n* respectively.

By replacing equation (3.3.20) into the equation (3.3.16):

$$\left[\rho_0 \frac{\partial}{\partial t} - \mu\left(\frac{\partial^2}{\partial x^2} + \frac{\partial^2}{\partial y^2} + \frac{\partial^2}{\partial z^2}\right)\right]\left[\frac{\partial^2}{\partial x^2} + \frac{\partial^2}{\partial y^2} + \frac{\partial^2}{\partial z^2}\right] W(z) e^{i(lx+ny)+\omega t}$$

$$= \rho_0 \alpha g \left(\frac{\partial^2}{\partial x^2} + \frac{\partial^2}{\partial y^2}\right) \theta(z) e^{i(lx+ny)+\omega t}$$

$$- \mu_0 K f(z) \frac{\partial}{\partial z}\left[\left(\frac{\partial^2}{\partial x^2} + \frac{\partial^2}{\partial y^2}\right) \phi(z) e^{i(lx+ny)+\omega t}\right]$$

$$+ \frac{\mu_0 K^2 f(z)}{1+\chi}\left(\frac{\partial^2}{\partial x^2} + \frac{\partial^2}{\partial y^2}\right) \theta(z) e^{i(lx+ny)+\omega t},$$

$$\left(\rho_0 \frac{\partial}{\partial t}\right) W(z) e^{i(lx+ny)+\omega t}\left(-a^2 + D^2\right)$$

$$- \mu\left(-a^2 + D^2\right)\left(-a^2 + D^2\right) W(z) e^{i(lx+ny)+\omega t}$$

$$= \rho_0 \alpha g\left(-a^2\right)\theta(z) e^{i(lx+ny)+\omega t} - \mu_0 K f(z) \frac{\partial}{\partial z}\left[\left(-a^2\right)\phi(z) e^{i(lx+ny)+\omega t}\right]$$

$$+ \frac{\mu_0 K^2 f(z)}{1+\chi}\left(-a^2\right)\theta(z) e^{i(lx+ny)+\omega t},$$

$$(\rho_0 \omega) W(z)\left(D^2 - a^2\right) - \mu\left(D^2 - a^{2^2}\right)\left(D^2 - a^2\right) W(z)$$

$$= \left(-a^2\right)\rho_0 \alpha g \theta(z) - \mu_0 K f(z) \frac{\partial}{\partial z}\left[\left(-a^2\right)\phi(z)\right] + \frac{\mu_0 K^2 f(z)}{1+\chi}\left(-a^2\right)\theta(z),$$

We simplified the resulting equation as follow:

$$\left[\rho_0 \omega - \mu\left(D^2 - a^2\right)\right]\left(D^2 - a^2\right) W = -a^2 \alpha g \theta + a^2 \mu_0 K f(z) D\phi - \frac{a^2 \mu_0 K^2 f(z)}{1+\chi}\theta, \qquad (3.3.21)$$

By substituting equation (3.3.20) into equations (3.3.17):

$$\rho_0 C_0 \frac{\partial}{\partial t}\theta(z)e^{i(lx+ny)+\omega t} - \kappa\left[\frac{\partial^2}{\partial x^2}+\frac{\partial^2}{\partial y^2}+\frac{\partial^2}{\partial z^2}\right]\theta(z)e^{i(lx+ny)+\omega t}$$

$$-\mu_0 K T_0 \frac{\partial}{\partial t}\left(\frac{\partial}{\partial z}\phi(z)e^{i(lx+ny)+\omega t}\right)$$

$$=\left(\rho_0 C_0 - \frac{\mu_0 K^2 T_0}{1+\chi}\right)\left(W(z)e^{i(lx+ny)+\omega t}\right)f(z),$$

$$\rho_0 C_0 \omega\theta(z) - \kappa\left(-a^2 + D^2\right)\theta(z) - \mu_0 K T_0 \omega\left(D\phi(z)\right) = \left(\rho_0 C_0 - \frac{\mu_0 K^2 T_0}{1+\chi}\right)W(z)f(z),$$

We simplified the resulting equation as follow:

$$\omega\theta - \kappa\left(D^2 - a^2\right)\theta - \frac{\mu_0 K T_0}{\rho_0 C_0}\omega D\phi = \left(1 - \frac{\mu_0 K^2 T_0}{(1+\chi)\rho_0 C_0}\right)Wf(z), \tag{3.3.22}$$

By substituting equation (3.3.20) into equations (3.3.18):

$$\left(1+\frac{M_0}{H_0}\right)\left(\frac{\partial^2}{\partial x^2}+\frac{\partial^2}{\partial y^2}\right)\phi(z)e^{i(lx+ny)+\omega t} + (1+\chi)\left(\frac{\partial^2}{\partial z^2}\phi(z)e^{i(lx+ny)+\omega t}\right)$$

$$-K\frac{\partial}{\partial z}\theta(z)e^{i(lx+ny)+\omega t} = 0,$$

$$\left(1+\frac{M_0}{H_0}\right)\left(-a^2\right)\phi(z) + (1+\chi)\left(D^2\phi(z)\right) - KD\theta(z) = 0,$$

We simplified the resulting equation as follow:

$$(1+\chi)D^2\phi - \left(1+\frac{M_0}{H_0}\right)a^2\phi - KD\theta = 0, \tag{3.3.23}$$

where,

$D = \dfrac{d}{dz}$ is the differential operator,

$$\frac{\partial^2}{\partial x^2}\left(W(z)e^{i(lx+ny)+\omega t}\right) = -W(z)l^2 e^{i(lx+ny)+\omega t},$$

$$\frac{\partial^2}{\partial y^2}\left(W(z)e^{i(lx+ny)+\omega t}\right)=-W(z)n^2e^{i(lx+ny)+\omega t},$$

$$\left(\frac{\partial^2}{\partial x^2}+\frac{\partial^2}{\partial y^2}\right)\left(W(z)e^{i(lx+ny)+\omega t}\right)=-W(z)\left(l^2+n^2\right)e^{i(lx+ny)+\omega t},$$

$$\frac{\partial^2}{\partial x^2}\left(\theta(z)e^{i(lx+ny)+\omega t}\right)=-\theta(z)l^2e^{i(lx+ny)+\omega t},$$

$$\frac{\partial^2}{\partial y^2}\left(\theta(z)e^{i(lx+ny)+\omega t}\right)=-\theta(z)n^2e^{i(lx+ny)+\omega t},$$

$$\left(\frac{\partial^2}{\partial x^2}+\frac{\partial^2}{\partial y^2}\right)\left(\theta(z)e^{i(lx+ny)+\omega t}\right)=-\theta(z)\left(l^2+n^2\right)e^{i(lx+ny)+\omega t},$$

$$\frac{\partial^2}{\partial x^2}\left(\phi(z)e^{i(lx+ny)+\omega t}\right)=-\phi(z)l^2e^{i(lx+ny)+\omega t},$$

$$\frac{\partial^2}{\partial y^2}\left(\phi(z)e^{i(lx+ny)+\omega t}\right)=-\phi(z)n^2e^{i(lx+ny)+\omega t},$$

$$\left(\frac{\partial^2}{\partial x^2}+\frac{\partial^2}{\partial y^2}\right)\left(\phi(z)e^{i(lx+ny)+\omega t}\right)=-\phi(z)\left(l^2+n^2\right)e^{i(lx+ny)+\omega t},$$

and the overall horizontal wavenumber as $a=\sqrt{l^2+n^2}$.

Next, non-dimensional equation definition is setting as follow:

$$\begin{aligned} &(x^*,y^*,z^*)=\left(\frac{x}{d},\frac{y}{d},\frac{z}{d}\right), && W^*=\frac{d}{v}W, \\ &a^*=ad, && D^*=dD, \\ &\theta^*=\frac{\kappa}{\beta v d}\theta, && \phi^*=\frac{(1+\chi)\kappa}{K\beta v d^2}\phi, \\ &f(z)^*=\frac{1}{\beta}f(z)\ \text{ where } \left(\beta=-\frac{\Delta T}{d}\right). \end{aligned} \tag{3.3.24}$$

Considering the exchange principle of the stability is true and the equations (3.3.21) rendered to non-dimensional form by using definition from equation (3.3.24):

$$\left[\rho_0\left(\frac{v\sigma}{d^2}\right)-\mu\left(\left(\frac{D^*}{d}\right)^2-\left(\frac{a^*}{d}\right)^2\right)\right]\left(\left(\frac{D^*}{d}\right)^2-\left(\frac{a^*}{d}\right)^2\right)\left(\frac{W^*v}{d}\right)$$

$$=-\left(\frac{a^*}{d}\right)^2\alpha g\left(\frac{\theta^*\beta v d}{\kappa}\right)+\left(\frac{a^*}{d}\right)^2\mu_0 K\left(\beta f(z)^*\right)\left(\frac{D^*}{d}\right)\left(\frac{\phi^* K\beta v d^2}{(1+\chi)\kappa}\right)$$

$$-\frac{\left(\frac{a^*}{d}\right)^2\mu_0 K^2\left(\beta f(z)^*\right)}{1+\chi}\left(\frac{\theta^*\beta v d}{\kappa}\right),$$

$$\rho_0\left(\frac{v\sigma}{d^2}\right)\left[\left(\left(\frac{D^*}{d}\right)^2-\left(\frac{a^*}{d}\right)^2\right)\left(\frac{W^*v}{d}\right)\right]-\mu\left(\left(\frac{D^*}{d}\right)^2-\left(\frac{a^*}{d}\right)^2\right)\left[\left(\left(\frac{D^*}{d}\right)^2-\left(\frac{a^*}{d}\right)^2\right)\left(\frac{W^*v}{d}\right)\right]$$

$$=-\left(\frac{a^*}{d}\right)^2\alpha g\left(\frac{\theta^*\beta v d}{\kappa}\right)+\left(\frac{a^*}{d}\right)^2\mu_0 K\left(\beta f(z)^*\right)\left(\frac{D^*}{d}\right)\left(\frac{\phi^* K\beta v d^2}{(1+\chi)\kappa}\right)$$

$$-\frac{\left(\frac{a^*}{d}\right)^2\mu_0 K^2\left(\beta f(z)^*\right)}{1+\chi}\left(\frac{\theta^*\beta v d}{\kappa}\right),$$

$$-\frac{\mu v}{d^5}\left((D^*)^2-(a^*)^2\right)\left[(W^*)\left((D^*)^2-(a^*)^2\right)\right]$$

$$=-\left(\frac{v}{d}\right)\frac{\alpha\beta}{\kappa}(a^*)^2(\theta^*)+\left(\frac{v}{d}\right)(a^*)^2 f(z)^* D^*\phi^*\left(\frac{\mu_0 K^2\beta^2}{(1+\chi)\kappa}\right)$$

$$-\left(\frac{v}{d}\right)(a^*)^2 f(z)^*\theta^*\left(\frac{\mu_0 K^2\beta^2}{(1+\chi)\kappa}\right),$$

Then, the asterisk is dropped out, to get the non-dimensional equation:

$$\left(D^2-a^2\right)^2 W = Ra^2\theta - Na^2 f(z)D\phi + Na^2 f(z)\theta, \tag{3.3.25}$$

Next, by operating the equations (3.3.22) to non-dimensional form by using definition from equation (3.3.24):

$$\frac{\nu\sigma}{d^2}\left(\frac{\theta^*\beta\nu d}{\kappa}\right)-\kappa\left(\left(\frac{D^*}{d}\right)^2-\left(\frac{a^*}{d}\right)^2\right)\left(\frac{\theta^*\beta\nu d}{\kappa}\right)-\frac{\mu_0 K T_0}{\rho_0 C_0}\omega\left(\frac{D^*}{d}\right)^2\left(\frac{\phi^* K\beta\nu d^2}{(1+\chi)\kappa}\right)$$

$$=\left(1-\frac{\mu_0 K^2 T_0}{(1+\chi)\rho_0 C_0}\right)\left(\frac{W^*\nu}{d}\right)\left(\beta f(z)^*\right),$$

$$\frac{\nu\sigma}{d^2}\left(\frac{\theta^*\beta\nu d}{\kappa}\right)-\left(\left(\frac{D^*}{d}\right)^2-\left(\frac{a^*}{d}\right)^2\right)\left(\theta^*\beta\nu d\right)-\frac{\mu_0 K^2 T_0}{(1+\chi)\rho_0 C_0}\omega\left(D^*\right)^2\left(\frac{\phi^*\beta\nu d}{\kappa}\right)$$

$$=\left(1-\frac{\mu_0 K^2 T_0}{(1+\chi)\rho_0 C_0}\right)\left(\frac{W^*\nu}{d}\right)\left(\beta f(z)^*\right),$$

$$\frac{\nu\sigma}{d^2}\left(\frac{\theta^*\beta\nu d}{\kappa}\right)-\frac{\beta\nu}{d}\left(\left(D^*\right)^2-\left(a^*\right)^2\right)\left(\theta^*\right)-\frac{\mu_0 K^2 T_0}{(1+\chi)\rho_0 C_0}\omega\left(D^*\right)^2\left(\frac{\phi^*\beta\nu d}{\kappa}\right)$$

$$=\left(\frac{\nu\beta}{d}\right)\left(1-\frac{\mu_0 K^2 T_0}{(1+\chi)\rho_0 C_0}\right)W^* f(z)^*,$$

$$-\frac{\beta\nu}{d}\left(\left(D^*\right)^2-\left(a^*\right)^2\right)\left(\theta^*\right)=\left(\frac{\nu\beta}{d}\right)\left(1-\frac{\mu_0 K^2 T_0}{(1+\chi)\rho_0 C_0}\right)W^* f(z)^*,$$

Then, the asterisk is dropped out to get the non-dimensional equation:

$$\left(D^2-a^2\right)\theta=-(1-M_2)Wf(z), \tag{3.3.26}$$

For equation (3.3.23), by substituting definition from equation (3.3.24):

$$(1+\chi)\left(\frac{D^*}{d}\right)^2\left(\frac{\phi^* K\beta\nu d^2}{(1+\chi)\kappa}\right)-\left(\frac{M_0}{H_0}+1\right)\left(\frac{a^*}{d}\right)^2\left(\frac{\phi^* K\beta\nu d^2}{(1+\chi)\kappa}\right)-K\left(\frac{D^*}{d}\right)\left(\frac{\theta^*\beta\nu d}{\kappa}\right)=0,$$

$$D^{*2}\left(\frac{\phi^* K\beta\nu}{\kappa}\right)-a^{*2}\left(\frac{M_0}{H_0}+1\right)\left(\frac{\phi^* K\beta\nu}{(\chi+1)\kappa}\right)-KD^*\left(\frac{\theta^*\beta\nu}{\kappa}\right)=0,$$

$$D^{*2}\phi^*\left(\frac{K\beta\nu}{\kappa}\right)-\frac{1+\frac{M_0}{H_0}}{(1+\chi)}a^{*2}\phi^*\left(\frac{K\beta\nu}{\kappa}\right)-D^*\theta^*\left(\frac{K\beta\nu}{\kappa}\right)=0,$$

$$\left(D^{*2}-\frac{\left(1+\frac{M_0}{H_0}\right)}{(1+\chi)}a^{*2}\right)\phi^*-D^*\theta^*=0,$$

Then, the asterisk is dropped out to reduce into non-dimensional equation:

$$\left(D^2-a^2M_3\right)\phi-D\theta=0, \tag{3.3.27}$$

Thus, for simplicity, we defined the non-dimensional parameter as in Table 3.2:

Table 3.2: Non-Dimensional Parameter of Ferrofluids

Symbol	Definition	Parameter
R	$\frac{\alpha \bar{g} \beta d^4}{\nu\kappa}$	Rayleigh number
N	$\frac{\mu_0 K^2 \beta^2 d^4}{(1+\chi)\kappa\mu}$	Magnetic Rayleigh number
M_2	$\frac{\mu_0 K^2 T_0}{(1+\chi)\rho_0 C_0}$	Negligibly small non-dimensional parameter
M_3	$\frac{\left(1+\frac{M_0}{H_0}\right)}{(1+\chi)}$	Non-linearity of magnetization
M	$\frac{\sigma_T \Delta T d}{\mu\kappa}$	Marangoni number
f(z)	$\int_0^1 f(z)dz=1$	Non-dimensional parameter variables

The perturbed non-dimensional parameter of the boundary conditions in term of:

$$W=DW=\frac{\partial\phi}{\partial z}=\theta=0 \text{ at } z=0, \tag{3.3.28}$$

and

$$W=M\,a^2\theta+D^2W=D\theta=D\phi=0 \text{ at } z=1, \tag{3.3.29}$$

and

$$\theta(0)+K\theta(1)=0, \tag{3.3.30}$$

where the Marangoni number, $M=\frac{\sigma_T\Delta Td}{\mu\kappa}$ and the feedback control as K.

3.4 Boundary Conditions

Let us now assume that both cases of dielectric micropolar layer and ferrofluids layer are subject to the combination of boundary conditions which is bounded by rigid and isothermal boundary condition from below and bounded by adiabatic non-deformable upper free of surface condition (Idris and Hashim, 2010).

Boundary condition on velocity at the free surface given as:

$$w = 0, \qquad \frac{\partial^2 w}{\partial z^2} = M\nabla_1^2\theta, \tag{3.4.1}$$

Boundary condition on velocity at the rigid surface given as:

$$w = \frac{\partial w}{\partial z} = 0, \tag{3.4.2}$$

Isothermal boundary condition given as:

$$\theta = 0, \tag{3.4.3}$$

Adiabatic boundary condition given as:

$$\frac{\partial \theta}{\partial z} = 0, \tag{3.4.4}$$

Boundary condition for electric/ magnetic potential given as:

$$\frac{\partial \phi}{\partial z} = 0, \tag{3.4.5}$$

The perturbed non-dimensional variables of the boundary conditions in the term of:

$$W = \frac{\partial w}{\partial z} = \theta(0) + K\theta(1) = \frac{\partial \phi}{\partial z} = 0, \text{ at } \mathrm{z} = 0, \tag{3.4.6}$$

and

$$W = \frac{\partial^2 w}{\partial z^2} + M\,\nabla_1^2\theta = \frac{\partial \theta}{\partial z} = \frac{\partial \phi}{\partial z} = 0, \text{ at } z = 1, \tag{3.4.7}$$

where, the Marangoni number, $M = \dfrac{\sigma_T \Delta T d}{\mu\kappa}$ and the feedback control as K.

3.5 Feedback Control

The feedback control strategy parameter on convective instabilities first proposed by Bau (1999) stated that by using proportional feedback control will delay or suppress the onset. In spite of that, by using this feedback control mechanism, the actuators are located at the surface heated from below and then the sensors used as a detection of the conductive conditions of the temperature at the surface. Furthermore, the control determination of a $q(t)$ depending on the controller of the proportional-integral differential (PID) as suggested by Bau in the form of:

$$q(t) = K[e(t)] + c, \tag{3.5.1}$$

and

$$e(t) = \hat{n}(t) - n(t), \tag{3.5.2}$$

with

$$K = K_D \frac{d}{dt} + K_I \int_0^t dt + K_P, \tag{3.5.3}$$

where, c is the control calibration, $e(t)$ is the deviation or an error from the state measurement, $\hat{n}(t)$ is the desired value, or $n(t)$, value of the reference, with the integral gain, K_I, the differential gain, K_D and the corresponding gain, K_P.

Besides, the perturbation fields suggested by Bau (1999), the actuator will modified the temperature of the heated surface depending on a corresponding dependent relationship of the upper $\left(z = z_u\right)$ thermal boundaries and lower $\left(z = z_l\right)$ boundaries based on equations (3.5.1) and (3.5.2) in term of:

$$\theta(x, y, z_l, t) - \theta(x, y, z_l) = -K\left[\theta(x, y, z_u, t) - \theta(x, y, z_u)\right], \tag{3.5.4}$$

or equivalently,

$$\hat{\theta}(x, y, z_l, t) = -K\hat{\theta}(x, y, z_u, t) \tag{3.5.5}$$

which $\hat{\theta}$ represented the deviation of the fluid temperature from the conductive value. Hence, we validated the uncontrolled system done by Baby and Pranesh (2012) when the controller gain parameter absence at $K = 0$. For this research, we will be focused for the case when $K > 0$. Thus, the perturbed non-dimensional variables of the boundary conditions in term of:

$$W = DW = \theta(0) + K\theta(1) = D\phi = 0, \text{ at } z = 0. \tag{3.5.6}$$

CHAPTER 4:

PROBLEM FORMULATION AND SOLUTION PROCEDURE

4.1 Introduction

In this chapter, the mathematical formulation and method of solutions for the effects of feedback control on electroconvection in a micropolar fluid and ferrofluids will be presented. The classical analysis of linear stability is used to analyse the influence of feedback control on the onset of the convection and also the effect of various parameters. The critical solution for these problems is obtained by using a single-term Galerkin method.

4.2 The Onset Of Bénard–Marangoni Electroconvection In A Micropolar Fluid With The Presence Of Feedback Control And Non–Linear Temperature Profiles

In this section, the mathematical formulations and the solution procedure for the effects of feedback control on the onset with non-uniform temperature profiles on Bénard–Marangoni electroconvection will be discussed. Parabolic and inverted parabolic temperature profiles are chosen to investigate the problem.

The dimensionless equations given by Azmi and Idris (2014) are as in chapter 3 which are equation (3.2.28) to equation (3.2.34).

In order to find the solution, single term Galerkin expansion procedure is used, which gives reasonable results based on report from Azmi and Idris (2014). By using MAPLE software, 4 by 4 matrix is used to calculate the relevant parameters. Then, follow by the approximated eigenvalue.

Constitute together the equations (3.2.28)–(3.2.31) with the boundary conditions (3.2.32)–(3.2.34) providing the approximated eigenvalue with R or M as an eigenvalue. Accordingly the variables are take the form of trial functions written as:

$$\begin{aligned} &W(z) = AW_1(z), \\ &G(z) = BG_1(z), \\ &\theta(z) = C\theta_1(z), \\ &\text{and } \phi(z) = E\phi_1(z). \end{aligned} \tag{4.2.1}$$

Meanwhile, for the case of rigid isothermal lower boundary and perfectly insulating of non-deformable upper boundary, the selected trial functions written as:

$$W = z^4 - \frac{5z^3}{2} + \frac{3z^2}{2}, \tag{4.2.2}$$

$$G = z(1-z), \tag{4.2.3}$$

$$\theta = z(2-z), \tag{4.2.4}$$

and

$$\phi = z^2(3-2z). \tag{4.2.5}$$

W, G, θ, ϕ are trials functions satisfied all the respective boundary conditions in (3.2.32)–(3.2.34), except the one written as:

$$D^2W + M a^2\theta = 0 \text{ at } z = 1. \tag{4.2.6}$$

However, the residual from the differential equations is added as the residual from this equation while the constants denoted as A, B, C and E.

By substituting equation (3.2.34) into equations (3.2.28)–(3.2.31), the resulting momentum equation multiplied by $W_1(z)$, spin equation by $G_1(z)$, energy equation by $\theta_1(z)$ and the electric scalar equation by $\phi_1(z)$. Next, operating the integration by parts in the respect of z from 0 to 1 and the constants: *A*, *B*, *C* and *E* are all eliminated from the solution equations. After that, by applying the boundary conditions (3.2.32)–(3.2.34) into the operating equations, then, obtained an eigenvalue Marangoni number, *M* as follows:

$$M = \frac{-\left[\left\langle (D\theta)^2 + a^2\theta^2 \right\rangle + K\theta(1) \right]\beta_1 + Ra^2\langle W\theta\rangle\beta_3 + La^2\beta_3\beta_4}{(1+N_1)a^2 DW(1)\theta(1)\beta_3}, \tag{4.2.7}$$

where,

$$\beta_1 = (1+N_1)\left\langle (D^2W)^2 + 2a^2(DW)^2 + a^4W^2 \right\rangle\beta_2 + N_1^2\left\langle W(D^2-a^2)G\right\rangle\left\langle G(D^2-a^2)W\right\rangle,$$
$$\beta_2 = N_3\left\langle (DG)^2 + a^2G^2 \right\rangle - 2N_1\left\langle G_1^2\right\rangle,$$

$$\beta_3 = N_1N_5\left\langle G(D^2-a^2)W\right\rangle\left\langle f(z)G\theta\right\rangle - \beta_2\left\langle f(z)W\theta\right\rangle,$$

and $\quad \beta_4 = \left\langle f(z)W\theta\right\rangle - \dfrac{\langle \phi D\theta\rangle\langle f(z)WD\phi\rangle}{\left\langle (D\phi)^2 + a^2\phi^2\right\rangle}.$

The basic temperature distributions and the nature of boundaries determined the value of *M*. The symbol of angle bracket, $\langle\cdot\rangle$ presenting the integration by parts in the respect of z from $z=0$ to $z=1$. In this research, the rigid isothermal of lower boundary and the perfectly insulating non-deformable upper boundary will be performed with different basic temperature gradients as given in Table 4.1.

Table 4.1: Reference State Basic Temperature Profiles

Model	**Reference State Basic Temperature Profiles**	$f(z)$
1	Linear	$f(z)=1$
2	Parabolic	$f(z)=2z$
3	Inverted Parabolic	$f(z)=2(1-z)$

4.3 Feedback Control Of Linear Temperature Profile On Rayleigh–Bénard–Marangoni Convection In Ferrofluids

In this section, the study of Rayleigh–Bénard–Marangoni convection in ferrofluids will be analyzed using the classical analysis of linear stability with the presence of feedback control. Linear temperature profile is chosen to investigate the problem. The mathematical formulation of the present study based on the equations shown by Shivakumara et al. (2002) together with Bau's feedback control as follows:

$$\left(D^2-a^2\right)^2 W = Ra^2\theta - Na^2 f(z)D\phi + Na^2 f(z)\theta, \tag{4.3.1}$$

$$\left(D^2-a^2\right)\theta = -\left(1-M_2\right)Wf(z), \tag{4.3.2}$$

$$\left(D^2-a^2 M_3\right)\phi - D\theta = 0, \tag{4.3.3}$$

where,

$R=\dfrac{\alpha\bar{g}\beta d^4}{\nu\kappa}$ is Rayleigh number,

$N=\dfrac{\mu_0 K^2\beta^2 d^4}{(1+\chi)\kappa\mu}$ is magnetic Rayleigh number,

$M_2=\dfrac{\mu_0 K^2 T_0}{(1+\chi)\rho_0 C_0}$ is negligibly small non-dimensional parameter,

$M_3 = \dfrac{\left(1+\dfrac{M_0}{H_0}\right)}{(1+\chi)}$ is non-linearity of magnetization,

and $\int_0^1 f(z)dz = 1$ is non-dimensional parameter profile.

The perturbed non-dimensional equations of boundary conditions written in terms of:

$$W = DW = \theta = \frac{\partial \phi}{\partial z} = 0 \text{ at } z = 0, \tag{4.3.4}$$

and

$$W = D^2W + M\,a^2\theta = D\phi = D\theta = 0 \text{ at } z = 1, \tag{4.3.5}$$

together with Bau (1999) feedback control condition:

$$\theta(0) + K\theta(1) = 0, \tag{4.3.6}$$

where the Marangoni number denoted as $M = \dfrac{\sigma_T \Delta T d}{\mu\kappa}$ and the feedback control parameter denoted as K.

In order to find the solution, single term Galerkin expansion procedure is used, which gives reasonable results based on report from Shivakumara et al. (2002). By using a MAPLE software, 3 by 3 matrix is used to calculate the relevant parameters. Then, follow by the approximated eigenvalue.

Since the Galerkin technique is based on the equations of linear system. Constitute together the equations (4.3.1)–(4.3.3) with the boundary conditions (4.3.4)–(4.3.6) providing the approximated eigenvalue with R or M as an eigenvalue. Accordingly the variables are take the form of trial functions written as:

$$W(z) = AW_1(z), \tag{4.3.7}$$
$$\theta(z) = B\theta_1(z),$$
$$\text{and } \phi(z) = C\phi_1(z).$$

Meanwhile, the chosen trial functions for rigid isothermal lower boundary and perfectly insulating of non-deformable upper boundary, written as:

$$W = z^4 - \frac{5z^3}{2} + \frac{3z^2}{2}, \tag{4.3.8}$$

$$\theta = z(2-z), \tag{4.3.9}$$

and

$$\phi = z^2(3-2z). \tag{4.3.10}$$

The chosen trial functions satisfied all the respective boundary conditions in (4.3.4)–(4.3.6), except the one namely as:

$$D^2W + M a^2\theta = 0 \text{ at } z = 1. \tag{4.3.11}$$

However, the residual from the differential equations is added as the residual from this equation while the constants denoted as *A*, *B* and *C*. From equation (4.3.1)–(4.3.3), after substituting equation (4.3.7), the resulting energy equation multiplied by $\theta_1(z)$, momentum equation by $W_1(z)$, and the magnetic potential equation by $\phi_1(z)$. Then, the equations are integrated in the respect of z from z=0 to z=1 and from the resulting equations; all the constants *A*, *B* and *C* are eliminated. Lastly for the resulting equations, by applying the boundary conditions (4.3.4)–(4.3.6) then obtained the Marangoni number, *M* written as follows:

$$M = \frac{1}{a^2 DW(1)\theta(1)}\left[\begin{array}{c}\dfrac{-\left[\left\langle (D\theta)^2 + a^2\theta^2\right\rangle + K\theta(1)\right]\left\langle (D^2W)^2 + 2a^2(DW)^2 + a^4W^2\right\rangle}{\langle f(z)W\theta\rangle} \\ + Ra^2\langle W\theta\rangle + Na^2\langle f(z)W\theta\rangle + \dfrac{Na^2\langle \phi D\theta\rangle\langle f(z)WD\phi\rangle}{\left\langle (D\phi)^2 + a^2\phi^2 M_3\right\rangle}\end{array}\right], \tag{4.3.12}$$

where, the symbol of angle bracket, $\langle\cdot\rangle$ presenting the integration by parts in the respect of z from $z=0$ to $z=1$. The basic temperature distributions and the nature of boundaries determined the value of *M*. From this research, the rigid isothermal of lower boundary and the perfectly insulating non-deformable upper boundary will be considered with linear model of basic temperature gradient of $f(z)=1$.

4.4 Feedback Control Of Non-Linear Temperature Profiles On Rayleigh–Bénard–Marangoni Convection In Ferrofluids

In this section, the effects of feedback control on the onset with non-uniform temperature profiles on Rayleigh–Bénard–Marangoni convection in ferrofluids will be studied. The comparisons on the Marangoni number for the different effects of various physical parameters are analysed using classical analysis of linear stability. Non-linear temperature gradients such are parabolic and inverted parabolic temperature profiles are considered. Then, the mathematical formulation will be formulated.

Consider the mathematical formulations and the solution procedure as equation (4.3.1)–(4.3.3) as stated in Section 4.3. The perturbed non-dimensional equations of boundary conditions written in terms of:

$$W = DW = \theta = \frac{\partial \phi}{\partial z} = 0 \text{ at } z = 0, \tag{4.4.1}$$

and

$$W = D^2W + M a^2\theta = D\phi = D\theta = 0 \text{ at } z = 1, \tag{4.4.2}$$

together with Bau (1999) feedback control condition:

$$\theta(0) + K\theta(1) = 0, \tag{4.4.3}$$

where the Marangoni number denoted as $M = \dfrac{\sigma_T \Delta T d}{\mu\kappa}$ and the feedback control parameter denoted as K.

By using a MAPLE software, 3 by 3 matrix is used to calculate the relevant parameters. Since the Galerkin technique is based on the equations of linear system. Then, the approximated eigenvalue is calculated.

In order to find the solution, single term Galerkin expansion procedure is used, which gives reasonable results based on report from Shivakumara et al. (2002).

Constitute together the equations (4.3.1)–(4.3.3) together with the boundary conditions (4.4.1)–(4.4.3) providing the approximated eigenvalue with R or M as an eigenvalue. Accordingly the variables are take the form of trial functions written as:

$$\begin{aligned} &W(z) = AW_1(z), \\ &\theta(z) = B\theta_1(z), \\ &\text{and } \phi(z) = C\phi_1(z). \end{aligned} \tag{4.4.4}$$

Meanwhile, the chosen trial functions for rigid isothermal lower boundary and perfectly insulating of non-deformable upper boundary, written as:

$$W = z^4 - \frac{5z^3}{2} + \frac{3z^2}{2}, \tag{4.4.5}$$

$$\theta = z(2 - z), \tag{4.4.6}$$

and

$$\phi = z^2(3 - 2z). \tag{4.4.7}$$

The trials function, W, θ, ϕ satisfied all the respective boundary conditions in (4.4.1)–(4.4.3), except the one written as follow:

$$D^2W + M a^2\theta = 0 \text{ at } z = 1. \tag{4.4.8}$$

However, the residual from the differential equations is added as the residual from this equation while the constants denoted as *A*, *B* and *C*. From equation (4.3.1)–(4.3.3), after substituting equation (4.4.4), the resulting energy equation multiplied by $\theta_1(z)$, momentum equation by $W_1(z)$, and the magnetic potential equation by $\phi_1(z)$. Then, the equations are integrated in the respect of z from z=0 to z=1 and from the resulting equations; all the constants *A*, *B* and *C* are eliminated. Lastly for the resulting equations, by applying the boundary conditions (4.4.1)–(4.4.3) then obtained the Marangoni number, *M* written as follows:

$$M = \frac{1}{a^2 DW(1)\theta(1)}\left[\begin{array}{l} \dfrac{-\left[\left\langle (D\theta)^2 + a^2\theta^2\right\rangle + K\theta(1)\right]\left\langle \left(D^2W\right)^2 + 2a^2(DW)^2 + a^4W^2\right\rangle}{\langle f(z)W\theta\rangle} \\ + Ra^2\langle W\theta\rangle + Na^2\langle f(z)W\theta\rangle + \dfrac{Na^2\langle\phi D\theta\rangle\langle f(z)WD\phi\rangle}{\left\langle (D\phi)^2 + a^2\phi^2M_3\right\rangle} \end{array}\right], \tag{4.4.9}$$

where, the symbol of angle bracket, $\langle\cdot\rangle$ presenting the integration by parts in the respect of z from $z = 0$ to $z = 1$. The basic temperature distributions and the nature of boundaries determined the value of *M*. From this research, the rigid isothermal of lower boundary and the perfectly insulating non-deformable upper boundary will be performed with other basic temperature profiles as present in Table 4.2.

Table 4.2: Reference Basic State Temperature Profiles

Model	**Reference Basic State Temperature Profiles**	$f(z)$
1	Parabolic	$f(z) = 2z$
2	Inverted Parabolic	$f(z) = 2(1 - z)$

CHAPTER 5:

CODE VALIDATION

5.1 Introduction

In this chapter, the results of the study on Rayleigh–Bénard–Marangoni convection in electroconvection and ferrofluids will be analyzed and compared well with the previous work. The comparisons on the Marangoni number for the different effects of various physical parameters are analysed.

The objective of the research in Section 5.2 is to extend the work of Azmi and Idris (2014) on influences of the combination of surface tension gradient and buoyancy force (Nield, 1964), the parabolic and inverted parabolic temperature gradients as considered by Rudraiah and Siddheshwar (2000) and an additional of controller gain parameter (Bau, 1999) together with micronsized suspended particles in the micropolar fluid (Eringen, 1972) and electrical forces (Roberts, 1969) on the onset of convection.

However, the main objective of the research in Section 5.3 is to study the presence of controller gain parameter (Bau, 1999) with extending the work of Shivakumara et al. (2002) on the Rayleigh–Bénard–Marangoni instability (Nield, 1964). Linear temperature gradients as considered by Qin and Kaloni (1994), and the magnetic forces (Rudraiah et al., 1986) on onset of convection in ferrofluids will be studied. Then, the critical solution is obtained by using the single-term Galerkin method on the onset of convection.

Furthermore, on the Section 5.4, the analysis on the effect of controller gain parameter (Bau, 1999) in magnetic fluids (Rudraiah et al., 1986) called ferroconvection will be studied on the Rayleigh–Bénard–Marangoni convection (Nield, 1964). The present research by following the work that has been done by Shivakumara et al. (2002) based on the different forms of non-uniform temperature gradients which are parabolic temperature and inverted parabolic temperature profile.

5.2 The Onset Of Bénard–Marangoni Electroconvection In A Micropolar Fluid With The Presence Of Feedback Control And Non–Linear Temperature Profiles

In this section, a verification of the accuracy of the numerical results will be conducted for Bénard–Marangoni electroconvection in the case of an absence of the controller gain parameter (K=0) and no buoyancy case (R=0) for Marangoni electroconvection. Therefore, to make sure the numerical code is predict a good approximations, the problem is tested for steady marginal stability curve reported by Azmi and Idris (2014) for K=0, R=0 and L=100 for linear temperature profile as shown in Figure 6.1 (a). Besides, from the present study, we also recovered the results of Azmi and Idris (2014) as a limiting case when K=0, R=0, $L \neq 0$, N_1=0.1, N_3=2.0, N_5=1.0 as illustrates in Figure 6.4 for linear temperature profile.

5.3 Feedback Control Of Linear Temperature Profile On Rayleigh–Bénard–Marangoni Convection In Ferrofluids

In order to verify the accuracy of the method solution, the present results are compared with the existing work written by Shivakumara et al. (2002). Hence, the data showed an excellent agreement by comparing the values of the critical Marangoni number, M_c for the absence of the controller gain parameter (K=0) and the absence of the magnetic Rayleigh number (N=0) as tabulated in Table 5.1 for linear temperature profile.

Table 5.1: Comparison of Values of M_c For Different Values of R with Results of Shivakumara et al. (2002) When K=0 and N=0

R	**Values of M_c**	
	Present	**Shivakumara et al. (2002)**
0	79.000383	79.00
100	67.571811	67.57
200	56.143240	56.14
300	44.714669	44.71
400	33.286097	33.29
500	21.857526	21.86
600	10.428954	10.43
669	2.543240	2.54
691.25	0.000383	0.00
691.253349	0.000000	N/A

5.4 Feedback Control Of Non-Linear Temperature Profiles On Rayleigh–Bénard–Marangoni Convection In Ferrofluids

The current analysis is compared with the results reported by Shivakumara et al. (2002) for K=0 and N=0 to achieve the outcome of the good results. Therefore, the result showed there has a good agreement between them as tabulated in Table 5.2 for the parabolic temperature profile and Table 5.3 for the inverted parabolic temperature profile.

Table 5.2: Comparison of Values of M_c of Parabolic Temperature Profile For Different Values of R With Results of Shivakumara et al. (2002) When K=0 and N=0

R	**Values of M_c**	
	Present	**Shivakumara et al. (2002)**
0	65.379627	65.379
572.071	0.000084	0.000
572.071737	0.000000	N/A

Table 5.3: Comparison of Values of M_c of Inverted Parabolic Temperature Profile For Different Values of R With Results of Shivakumara et al. (2002) When K=0 and N=0

R	**Values of M_c**	
	Present	**Shivakumara et al. (2002)**
0	99.789957	99.7898
873.161	0.000129	0.0001
873.162126	0.000000	N/A

CHAPTER 6:

RESULT AND DISCUSSIONS

6.1 Introduction

In this chapter, the analysis on the numerical results about the effects of feedback control on the onset on Rayleigh–Bénard–Marangoni convection in electroconvection and ferrofluids will be discussed. The comparisons on the Marangoni number for the different effects of various physical parameters are analysed using classical analysis of linear stability. The numerical results obtained will be discussed and analysed. The numerical results for section 6.2 will be displayed graphically in terms of:

i. Marangoni number, M as a function of wave number, a,
ii. critical Marangoni number, M_c as a function of feedback control, K,
iii. critical Marangoni number, M_c as a function of Rayleigh number, R, and
iv. critical Marangoni number, M_c as a function of coupling parameter, N_1, couple stress parameter, N_3 and micropolar heat conduction parameter, N_5, respectively, for different non-uniform temperature profiles.

Then, the numerical results obtained in section 6.3 will be discussed which will be displayed graphically in terms of:

i. Marangoni number, M as a function of wave number, a,
ii. critical Marangoni number, M_c as a function of feedback control, K,
iii. critical Marangoni number, M_c as a function of Rayleigh number, R.

Meanwhile, the numerical results for section 6.4 will be displayed graphically in terms of:

i. Marangoni number, M as a function of wave number, a for parabolic temperature profile for several values of feedback control, K,

ii. Marangoni number, M as a function of wave number, a for inverted parabolic temperature profile for several values of feedback control, K,

iii. critical Marangoni number, M_c as a function of feedback control, K, for parabolic and inverted parabolic temperature profiles for different cases of magnetic Rayleigh number, N and Rayleigh number, R,

iv. critical Marangoni number, M_c as a function of Rayleigh number, R for parabolic and inverted parabolic temperature profiles with several values of feedback control, K, and different cases of magnetic Rayleigh number, N,

v. critical Marangoni number, M_c as a function of normalize Rayleigh number, $\frac{R}{R_C}$ for parabolic and inverted parabolic temperature profiles with several values of feedback control, K, and different cases of magnetic Rayleigh number, N.

6.2 The Onset Of Bénard–Marangoni Electroconvection In A Micropolar Fluid With The Presence Of Feedback Control And Non–Linear Temperature Profiles

In this section, the effects of the presence of feedback control on the onset with parabolic and inverted parabolic temperature gradients of the Bénard–Marangoni electroconvection will be discussed. The minimum of the global minima of each marginal stability curve is definition of the critical Marangoni number for a given set of parameters on the onset of convection. Noted that, the corresponding critical wave number as a_c, the value of critical Marangoni number as M_c, the Rayleigh number as *R*, the feedback control by *K*, coupling parameter as N_1, couple stress parameter as N_3 and micropolar heat conduction parameter by N_5.

The plot of result obtained by Azmi and Idris (2014) as illustrates in Figure 6.1 (a) for linear temperature profile at *K*=0 means that in the absence of the controller and no buoyancy case, *R*=0. Figure 6.1 represents marginal stability curve for various cases of temperature profiles for several values of *K* and *R*. From the observation, M_c will increases rapidly when *K* increases for all of the chosen basic temperature profiles. The plot showed dramatic increasing of M_c and a_c when *K* is applied to the system. In the observation for the critical wavenumber, a_c the increasing trend for a_c are not so significant when increasing the value of *K*. In spite of that, the critical Marangoni number, M_c showed significantly increases when the value of *K* increased. Consequently, the size of the convection cells is reducing because the effect of increasing in the both value of M_c and a_c .

However, noted that when compared to the linear and parabolic temperature profiles, the inverted parabolic temperature gradient shows more value of M_c and a_c when providing the additional value of *K*. Means that, the onset of the convection will be delay with the presence of feedback control strategy for all of the chosen basic temperature profiles. In spite of that, the system is most unstable for the case of parabolic type of basic temperature profile when gives smaller value of M_c and a_c. This is due to the condition nearer the less restrictive of free surface when changing in the temperature occurs. Oppositely, the system becomes stable for the inverted parabolic type of basic temperature profile. Hence, in the presence of feedback control strategy, the onset of Bénard–Marangoni electroconvection is possibly control effectively in spite of using different forms of basic temperature profiles.

Furthermore, in the case of $R \neq 0$, the value of M_c always less than the M_c value when *R*=0 for all temperature profiles. Hence, increasing the value of *R*, decreases the critical Marangoni number. This is because the presence of *R* will increase the intensity of Bénard–Marangoni electroconvection. Thus, *R* is destabilizing factor of the convection since added the more value of *R* into the system, will resulting unstable to the system. Oppositely, when *K* is applied into the system, M_c will increases as *K* increases. The same phenomenon can be found for a_c. Hence, *K* can delay the onset of the convection for both cases *R*=0 and $R \neq 0$ with all considered temperature profiles.

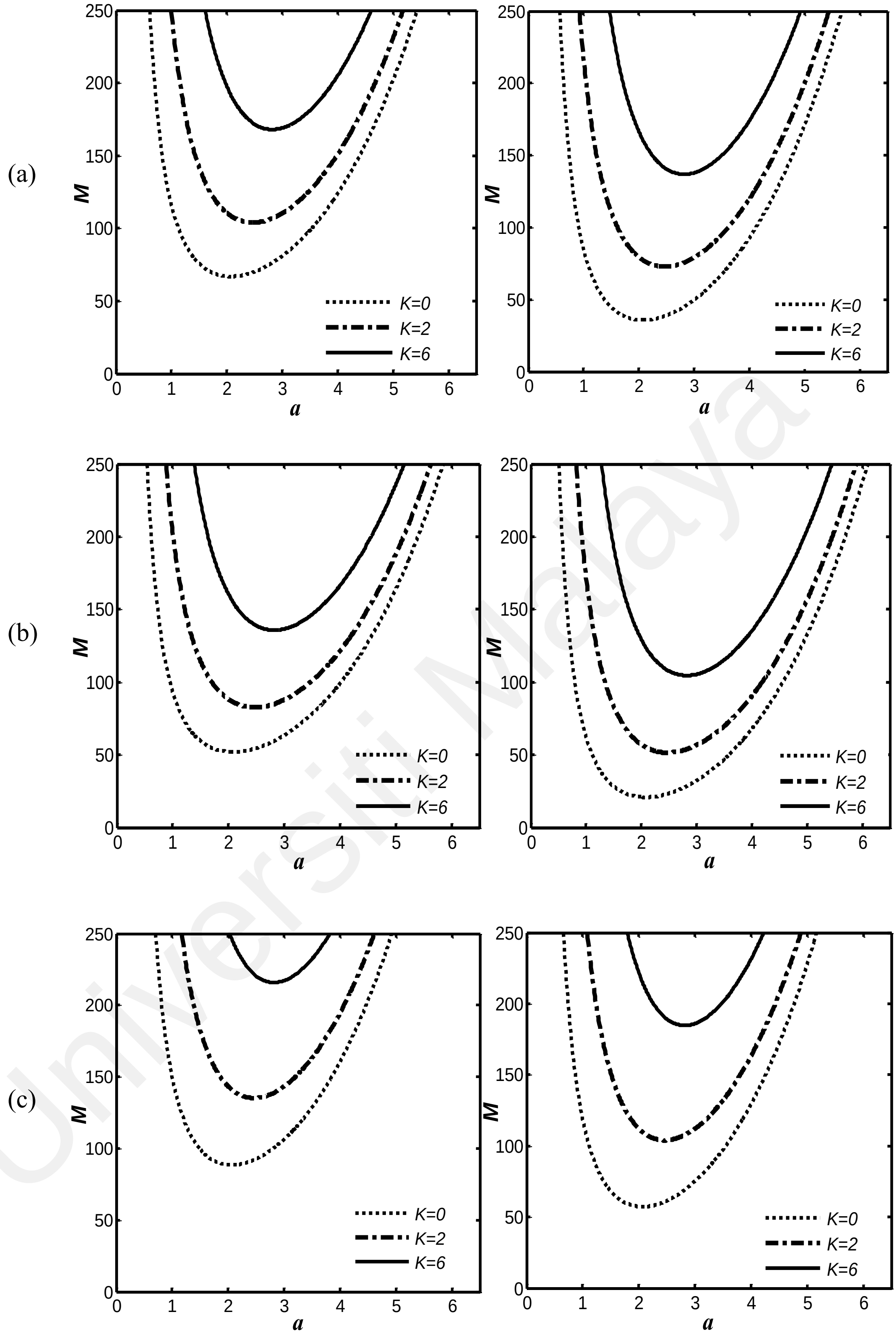

Figure 6.1: M as a function of a for (a) linear temperature (b) parabolic temperature and (c) inverted parabolic temperature profile, for the case of R=0 (left) and R=300 (right) for several values of K

On the other hand, Figure 6.2 depicts the effects of controller gain, K on the critical Marangoni number M_c. Clearly observed that, as the value of K increased, the value of M_c shows gradually increased. As well as when K applied to the system for the cases of R=0 and $R \neq 0$, the value of M_c increased. Thus, the onset of convection will be suppressed as K increased. Additionally, compared to the value of M_c for linear and parabolic temperature gradients, the inverted parabolic temperature gradient always results bigger value of M_c even though when K or R had been applied to the system. The outcome showed the most stabilizing temperature profile that being compared to linear and parabolic temperature profiles is the inverted parabolic temperature gradient. On top of that, clearly observed that the line for different temperature gradients are intersecting each other as depicted in Figure 6.2. This can be seen for the case of R=0 for linear temperature gradient and R=300 due to inverted parabolic temperature gradient. Moreover, noted also there are also the intersection line between parabolic temperature profile for the cases R=0 for and R=300 for linear temperature profile. Hence, at a certain point of the controller at K=2 and at K=6, there are equal value of M_c although different case temperature profiles are performed. Consequently, when performed the feedback control strategy on the Bénard–Marangoni electroconvection, the instabilities of the onset effectively controlled with the presence of various basic temperature gradient.

Meanwhile, Figure 6.3 illustrates the plot of the critical Marangoni number M_c as a function of Rayleigh number, R with different values of feedback control and with different temperature gradients. Clearly observed, as the value of R increased, the value of M_c gradually decreased. On the contrary, when applied the feedback control, K will resulting higher value of M_c on the plot. Thus, there is adverse effect on the value of

M_c by performing the various cases of instability parameter which are *R* and *K*. Means, *R* gives destabilizing effect to the system but *K* gives stabilizing effect to the system.

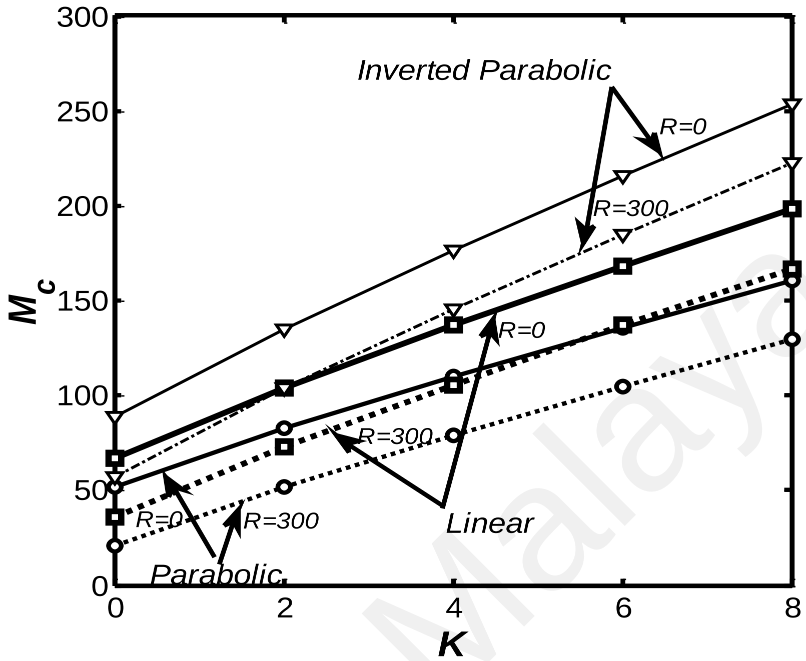

Figure 6.2: M_c as a function of *K* for the case of *R*=0 and *R*=300 for different temperature profiles

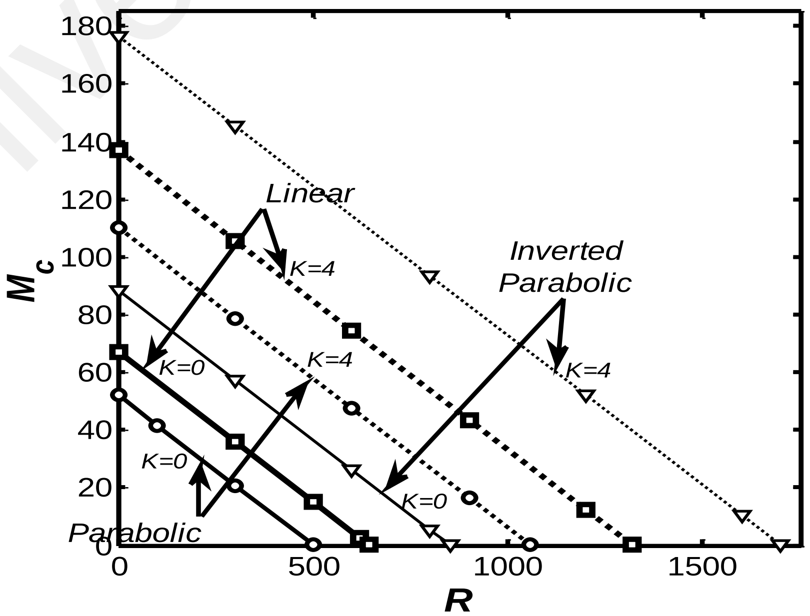

Figure 6.3: M_c as a function of *R* for the case of *K*=0 and *K*=4 for different temperature profiles

Further inspection of Figure 6.3, reveals that R will reached it's critical point as the value of R increased further, which means there exist a critical point of Rayleigh number, R_c. The value of M_c tend to become zero value when reached the point of R_c. Consequently, we can say that as R increase, the value of M_c decrease until the buoyancy is predominant on the system of convection. Hence, the zero value of M_c can be said that there is negligible effect of surface tension and the convection system dominated by buoyancy force. The various case of basic temperature profile affects the decrease of surface tension effect because of R. In addition, Figure 6.3 showed the comparison of the value M_c that is always lower for linear and parabolic temperature gradients than the M_c value of the inverted parabolic temperature gradient which is always greater when R had been applied to the system. As stated before, the most stabilizing profile is the inverted parabolic temperature profile compared to the other considered temperature profiles on the research.

From the present study plotted in Figure 6.4, for linear temperature profile, recovered the following result of Azmi and Idris (2014) as a limiting case of K=0, R=0, $L \neq 0$, N_1=0.1, N_3=2.0, and N_5=1.0. Figure 6.4 shows the variation of the critical Marangoni number M_c as a function of N_1, N_3 and N_5, respectively, for various form non-uniform temperature profiles. Hence, the results indicate that the value M_c is generally show increasing exponential function of coupling parameter, N_1 but oppositely show decreasing exponential function of couple stress parameter, N_3. On top of that, the increasing value of N_1 indicates that the biggest part of the energy is consume by the microelements. Hence, causes the concentration of these microelements of the system increases. However, increasing value of N_3 causes the couple stress dropped. Ultimately, get the Newtonian value when the stress of the fluid levels off.

Hence, results the microrotation decreases. However, from the Figure 6.4 (c), observed that the plot shows a slightly increases of M_c with increasing the parameter of micropolar heat conduction, N_5 for all cases of temperature gradients. This is due to the reducing of the heat transfer from top to bottom boundaries as N_5 increases and the microelements increase. The results of increases the critical Marangoni number, M_c along increasing N_1 and N_5 showing that these elements have the stabilizing effect but are in difference of the Newtonian results of N_3 for different cases of basic temperature profiles. In spite of that, observed that the value of M_c increased as feedback control, K applied to the system for various function of N_1, N_3 and N_5 parameter. Gradually increases in the value of K showing that this control K is responsible for suppressing the onset with different cases of temperature gradients. Moreover, Figure 6.4 reveals that the most destabilizing among these considered cases of non-uniform basic temperature profiles is the parabolic temperature gradient as the value of M_c is the lowest compared than the value of M_c for the inverted parabolic gradient which is the most stabilizing one.

The research in a micropolar fluid on Bénard–Marangoni convection with imposed of the feedback control with non-uniform basic temperature profiles has been analysed theoretically. The influence of vertical electric field with non-uniform basic temperature profiles of Bénard–Marangoni instability has been investigated. In spite of that, as the feedback control, K increases, M_c increases monotonically, shows that for all wave numbers, the feedback control is stabilizing the no-motion state. Meanwhile, the presence of buoyancy force, R promotes the onset of convection. On top of that, R leads to a more unstable system. Ultimately, when adding up the micron-sized suspended particles have been act as stabilizing effect to the system along increasing the value of

N_1 and N_5. Contrary with the Newtonian results of N_3 which act as destabilizing effect for different cases of basic temperature profiles. To sum up, the model of inverted parabolic temperature gradient is showed to be the most stabilizing from those three cases temperature profiles, as shown in the arrangement value of the critical Marangoni number; $M_{c(Parabolic)} < M_{c(Linear)} < M_{c(Inverted\,Parabolic)}$. The above results indicated that there is possibility to delay the convective instability by imposed the basic state temperature profile. Inverted parabolic is the most stabilizing one compared to linear and parabolic temperature profiles. On the other hand, there is no significant changing in the value of a_c for adding any value of *R*. It is showed the value of a_c are not being affecting at all in the presence of parameter *R*. However, the value of a_c is increase drastically as increasing the *K*. Firmly conclude that for the convective instabilities, the feedback control *K*, is a stabilizing factor to suppress the onset.

(a)

(b)

(c)

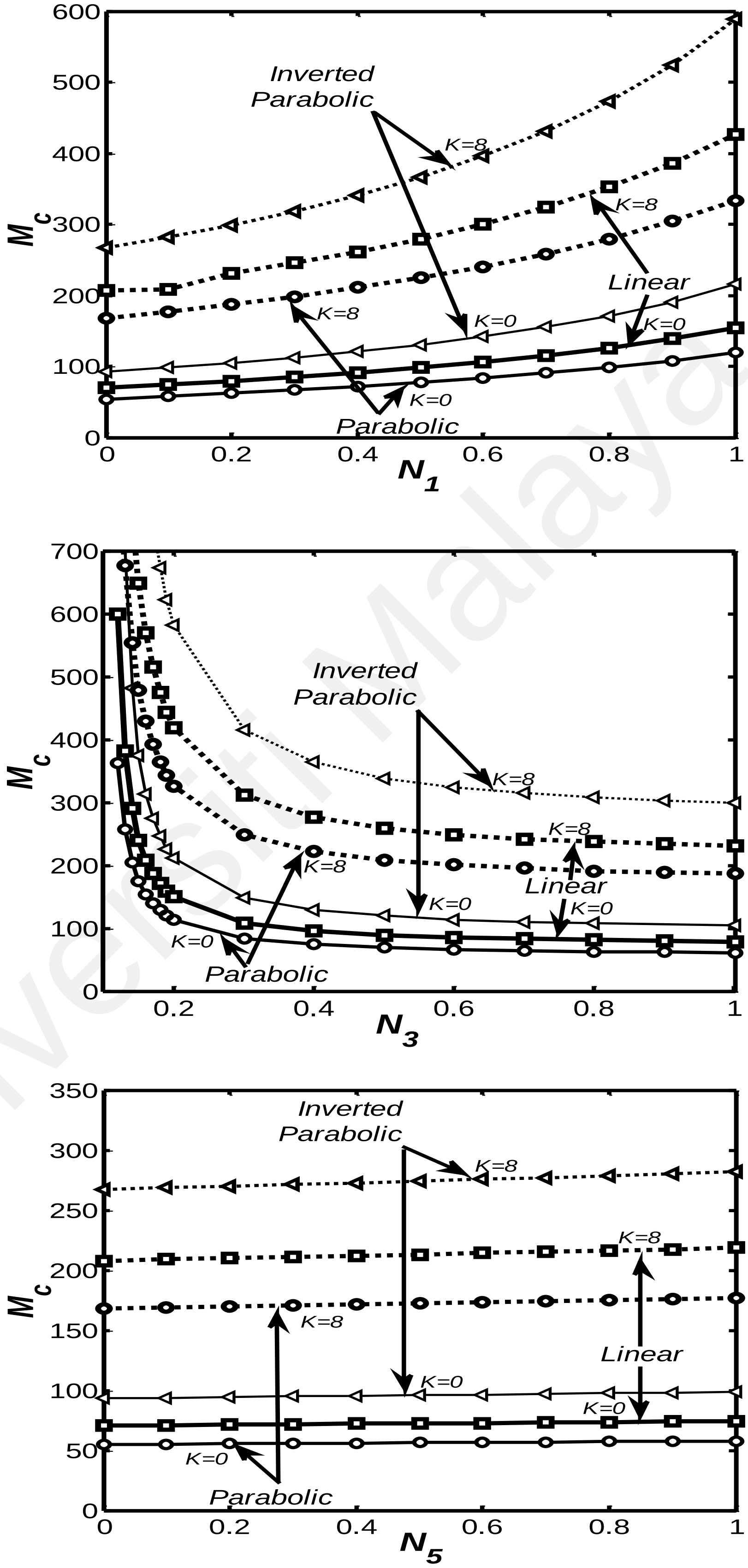

Figure 6.4: M_c as a function of (a) N_1 (b) N_3 (c) N_5 for the case of K=0 and K=8 for different temperature profiles

6.3 Feedback Control Of Linear Temperature Profile On Rayleigh–Bénard–Marangoni Convection In Ferrofluids

In this section, the influences of linear temperature gradient on Rayleigh–Bénard–Marangoni convection together with a feedback control on the onset of ferrofluids convection will be discussed. The effects of various parameters on the convective instabilities such as Rayleigh number *R*, and magnetic Rayleigh number *N*, have been studied using the linear stability analysis.

First and foremost, the effects of the parameters *K*, *R* and *N* on the Marangoni number, *M* with wave number *a* are portrayed in Figure 6.5 for linear temperature profile. The critical Marangoni number, M_c of marginal stability curve as shown in Figure 6.5 is the minimum point of each curve. Then, the validation on the numerical result obtained by Shivakumara et al. (2002) represents graphically in Figure 6.5 (a) in the absence of the controller at *K*=0 when *N*=0 and *R*=0. From observation, when *K* is added up into the system, the graph showed rapidly increased in the value of M_c. This can be proven by looking at the comparison between the value of the *M* number recorded between *K*=4 and *K*=6 and the big difference shown in the *M* number recorded between *K*=0 and *K*=4. Besides, the value of M_c is increasing whenever the value of *K* increase along various cases of *R* and *N*. The cases are as follow; *N*=0 when *R*=300, and *N*=100 when *R*=0 and *R*=300. As a result, the presence of feedback control along the increase in the *K* number gives the increases in the critical Marangoni number with decrease the intensity of Bénard–Marangoni ferrofluids convection. Therefore, for all cases of *R* and *N* with effect of linear temperature profiles on the onset of convection, *K* can be said to be a stabilizing factor which is with the imposed of feedback control strategy will delaying the onset. However, from the observation for the case of *N*=0 as illustrate in Figure 6.5, the value of M_c is higher than the value of M_c for the case of

N=100. Similarly, noted that when R is added up into the system, M_c is decreasing. Hence, R and N promote instability as the value of M_c decreased. Means, the system became unstable when adding more value of R and N.

The graph of critical Marangoni number, M_c as a function of feedback control, K is portrayed in Figure 6.6. Evidently showed that as increased the value of K, the value of M_c increased steadily for both cases of N=0 and N=100. Similarly, for the cases of R=0 and R=300, yield the same phenomenon when increasing M_c, increases K. Therefore, the effect of imposed K to the system is to delay the onset. In spite of that, for the study case of magnetic Rayleigh number, N for linear temperature profile, the value of M_c always shows higher for the case of N=0, compared the value of M_c for the cases of N=100. Meanwhile, imposing the Rayleigh number to the system, for the case of R=300, gives a lower value of M_c compared than R=0. Obviously, we can see the results showed increasing N and R, decreases M_c. Therefore, the instability parameter N and R implying a destabilizing effect due to the changing value of M_c.

Meanwhile, the graph of M_c as a function of Rayleigh number, R is plotted in Figure 6.7. It is clearly observed that when increasing the value of R and the value of N, M_c steadily decreasing. Contrastively, adding up the value of K gives the increases in the M_c. Thus, performing the varying of instability parameter N and K on the system will giving the opposite effect to M_c. Further, we identified that as the value of R increase further, R will reached it's critical point, namely critical point of Rayleigh number, R_c. Consequently, the value of M_c approaches a zero value which is the surface tension effects on the onset of convection has vanished at a point of R_c.

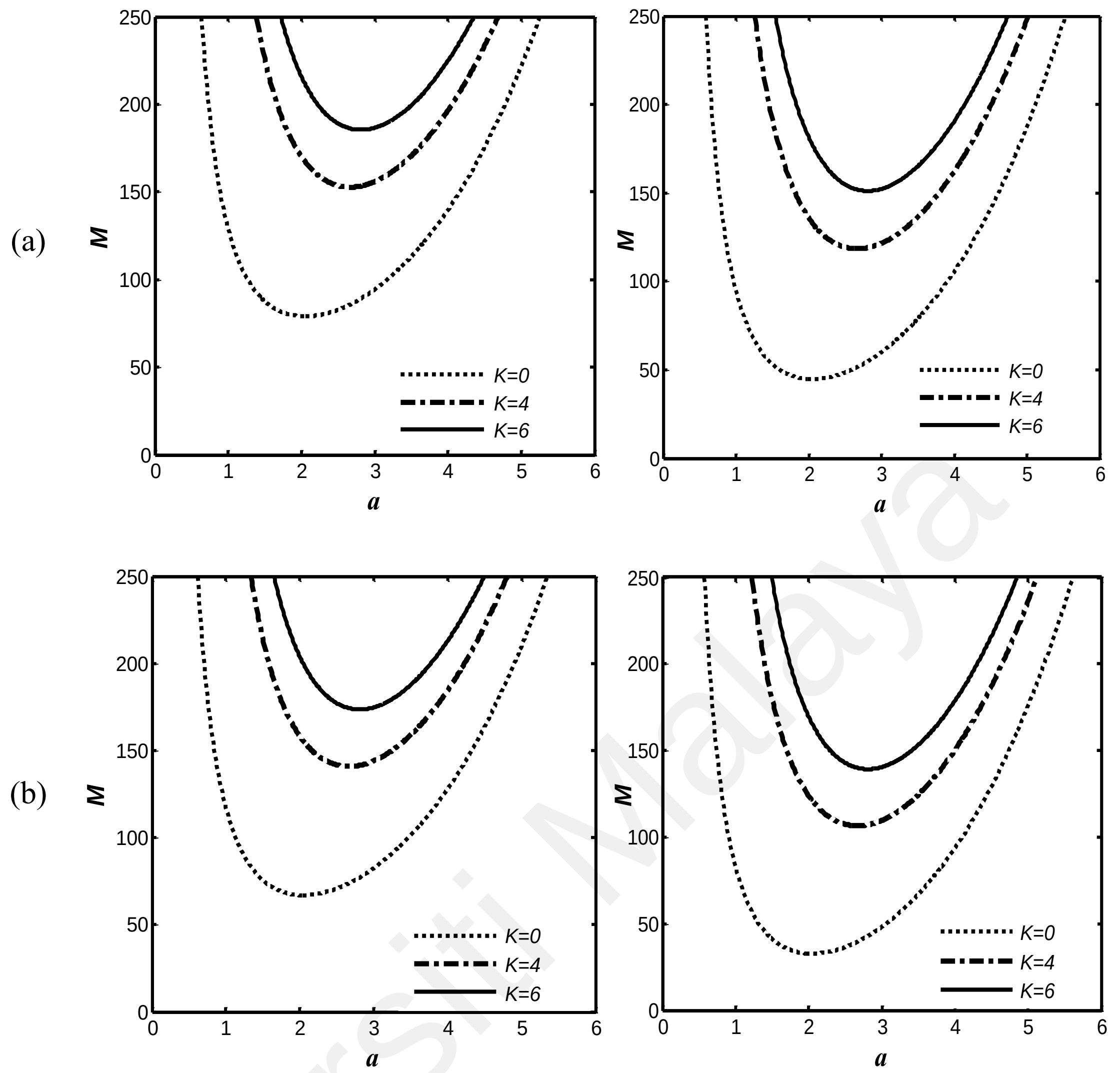

Figure 6.5: M as a function of a (a) when N=0 and (b) when N=100, for the case of R=0 (left) and R=300 (right) for several values of K

Based on the results obtained, some of the conclusions can be briefly drawn. First and foremost, the results published by Shivakumara et al. (2002) for K=0, R=0 and N=0 were recovered for linear temperature profile. When applying the feedback control to the system, the value of M_c increased steadily. It is proved that K is stabilizing factor as discussed in Or and Kelly (2001), Siri and Hashim (2008), Awang–Kechil and Hashim (2008). Means that, the onset of convection can be delay in the presence of K. Oppositely, with the imposed of parameter R or/and N on the system, the value of M_c will decreasing. A glance at the plot in Figure 6.7 reveals the existing of a critical point of Rayleigh number, R_c. Consequently, as *R* increase, the value of M_c decrease until the buoyancy is predominant on the system of convection. Hence, the zero value of M_c can be said that there is negligible effect of surface tension and the convection system dominated by buoyancy force. The various case of magnetic Rayleigh number, *N* affects the decrease of surface tension effect because of *R*. The value of M_c tend to become zero value when reached the point of R_c. Therefore, *R* and *N* is a destabilizing factor to enhance the convective instabilities of Rayleigh–Bénard–Marangoni ferroconvection. For additional information, the value of a_c is increase but only at a small value as *K* increased. Ultimately, the imposed of the feedback control *K*, delay the onset of convective instabilities and thus act as a stabilizing factor to the system. On the other hand, there is no significant changing in the value of critical wavenumber a_c by adding any value of *N* and *R*. Evidently, the value of a_c are not being affecting at all in the presence of parameter *N* and *R*. Hence, the size of the convection cells will not decreases.

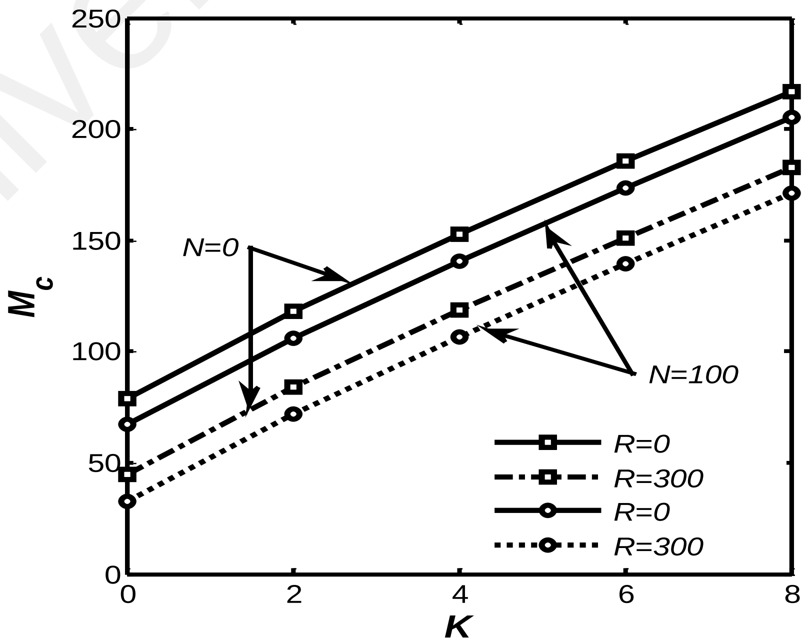

Figure 6.6: M_c as a function of *K* for the case of *N*=0 and *N*=100 when *R*=0 and *R*=300

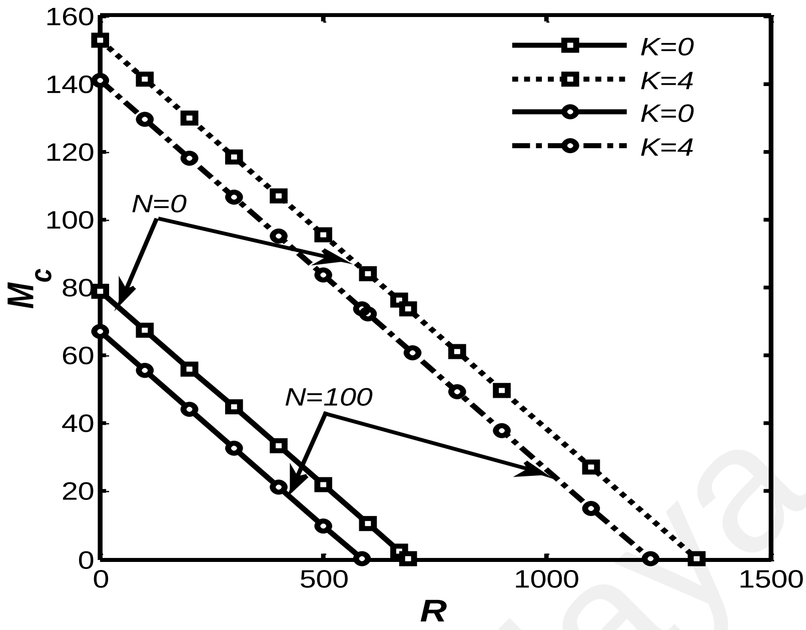

Figure 6.7: M_c as a function of R for for the case of N=0 and N=100 when K=0 and K=4

6.4 Feedback Control Of Non-Linear Temperature Profiles On Rayleigh–Bénard–Marangoni Convection In Ferrofluids

In the remainder of the previous section focussing on the influences of feedback control K, on the onset of Rayleigh–Bénard–Marangoni ferroconvection with linear temperature profile. Meanwhile, in this Section 6.4, non-uniform temperature gradients which are parabolic and inverted parabolic temperature gradients are chosen for the research studied. Other various parameters such as Rayleigh number R, magnetic Rayleigh number N, also have been analysed on the onset using the analysis of linear stability.

The plot of marginal stability curve for parabolic temperature profile for several values of K are represents in Figure 6.8. Meanwhile, the marginal stability curve for inverted parabolic temperature profile plotted as in Figure 6.9. The minimum point of each curve known as the critical Marangoni number, M_c and the critical wave number, a_c. From the observation in Figure 6.8 and Figure 6.9, M_c will increases rapidly when *K* is applied to the system. The graph showed dramatic rising of M_c and a_c when *K* increases. Accordingly, for the critical wavenumber, a_c the increasing trend for a_c are not so significant when added the value of *K*. However, the increasing trend for critical Marangoni number, M_c gives dramatic increases in the presence of *K*. Consequently, the size of the convection cells is reducing because the effect of increasing in the both value of M_c and a_c. However, noted that there are a big difference shown in the *M* number recorded between *K*=0 and *K*=4 compared than the *M* number recorded between *K*=4 and *K*=6. This is because whenever providing the additional value of *K*, the graph showed rapidly increased in the value of M_c. Furthermore, from both temperature gradients can observe the increasing value of M_c whenever increase the value of *K* along the various cases of *R* and *N*. The cases are as follow; *N*=0 when *R*=300, and *N*=100 when *R*=0 and *R*=300. In spite of that, the presence of feedback control along the increase in the *K* number gives the increases in the critical Marangoni number with decrease the intensity of Bénard–Marangoni ferrofluids convection. This can be proved that *K* is a stabilizing factor for the system to become stable as discussed in Section 6.3. Oppositely, in the case of *R*=300 from Figure 6.8 and 6.9, the value of M_c always less than the M_c value when *R*=0 for each temperature profile. Similarly, increasing the value of *N*, decreases the critical Marangoni number. This is because the presence of *R* and *N* will increase the intensity of Bénard–Marangoni ferroconvection because the present of the magnetic field. Thus, *R* and *N* are destabilizing factor of the convection since added the more value of *R* or *N* into the system, will causing unstable system. In addition from Figure 6.8 and 6.9, even though when *K* and other parameter are added up into the system, the graph showed greater increased in the value of M_c and a_c for inverted parabolic temperature profile compared to parabolic temperature profile. Because, at the maximum level of energy and level of momentum, the change in temperature is concentrated near the free surface with low restrictive. Therefore, the effect of the each parameter performed on the critical Marangoni number is greater pronounced on the onset with an inverted parabolic temperature gradient. It means, the most stabilizing temperature profile is the inverted parabolic temperature gradient as performing the feedback control strategy on the system will suppressing the onset compared than parabolic temperature gradient.

On the other hand, in Figure 6.10 portrayed the critical Marangoni number, M_c as a function of feedback control, for different value of magnetic Rayleigh number, *N* which are when *N*=0 and $N \neq 0$ with both temperature profiles. From observation, in the cases of *N*=0, *N*=100; when increases the value of *K*, will steadily rising the value of M_c. Moreover, for each temperature profiles observed that whenever the value of *K* added into the system, M_c rising rapidly. Hence, *K* helping in suppressing the onset and can be said as stabilizing effect on the system. However, the value of M_c oppositely decreasing when adding the *R* from zero Rayleigh number, *R*=0 (no buoyancy effect) to *R*=300 (with buoyancy effect). Means that whenever the buoyancy forces become predominant on the system, the surface tension effect attend to become negligible.

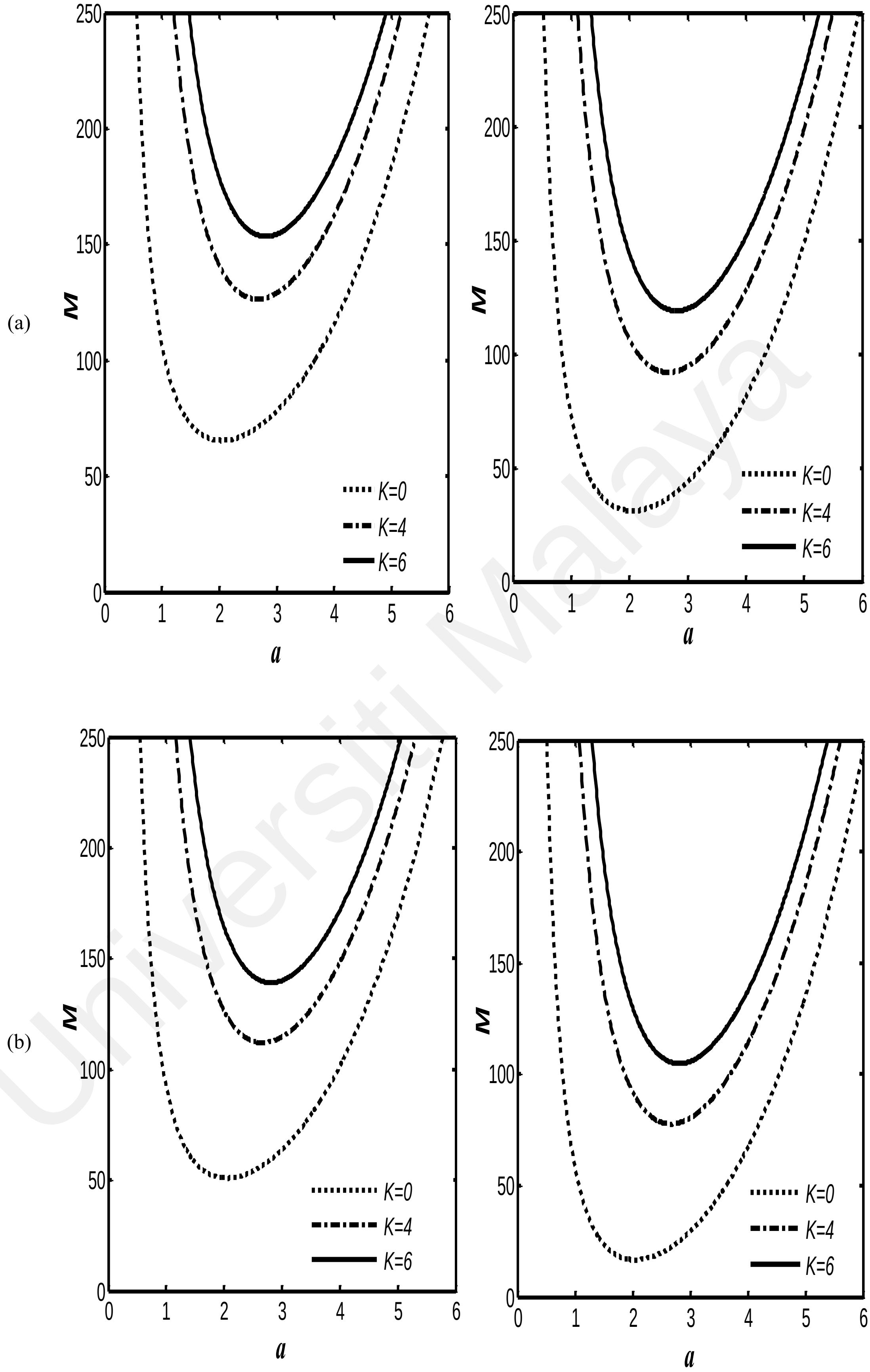

Figure 6.8: M as a function of a for parabolic temperature profile (a) when N=0 and (b) when N=100 for the case of R=0 (left) and R=300 (right) for several values of K

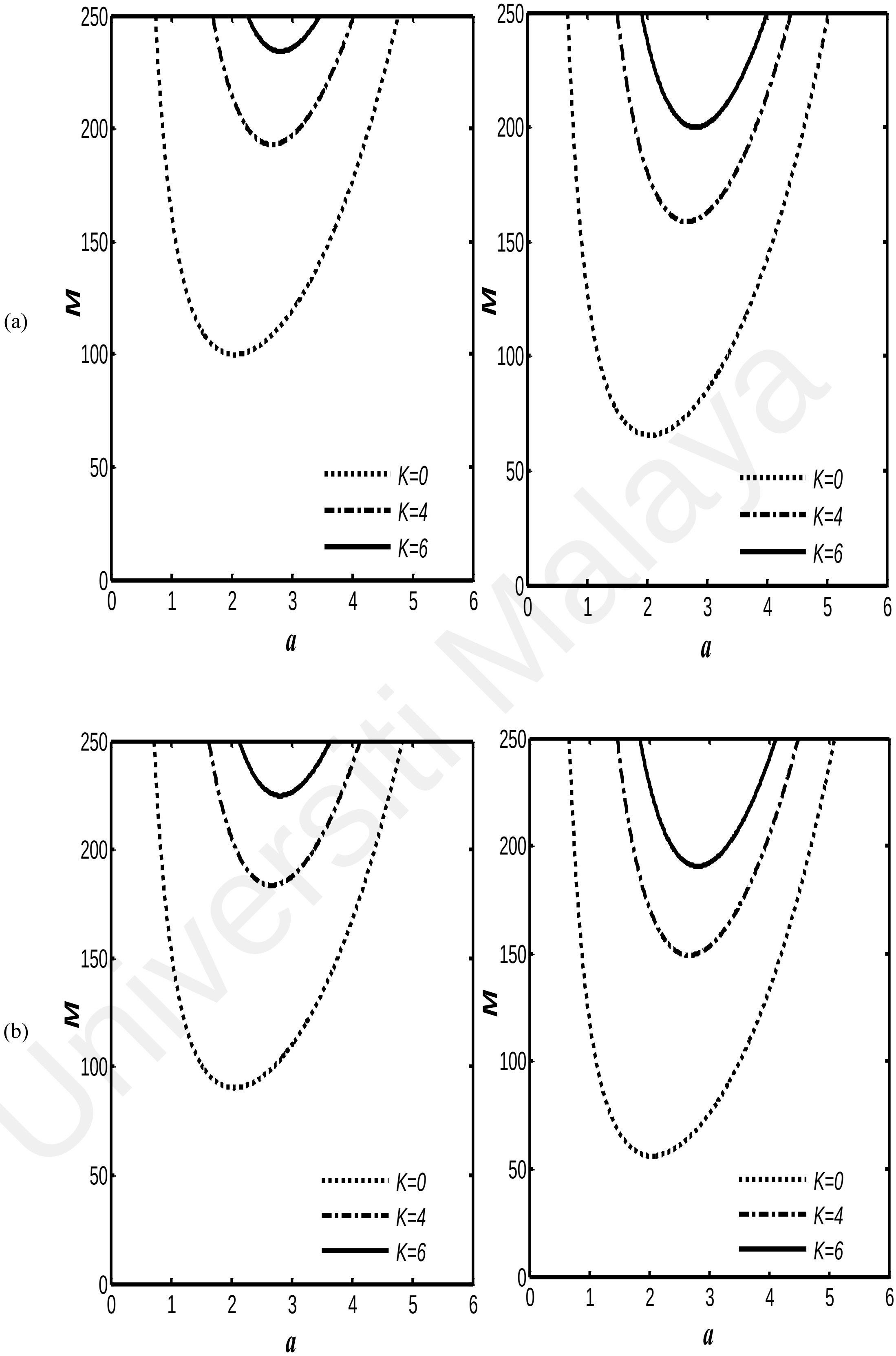

Figure 6.9: M as a function of a for inverted parabolic temperature profile (a) when N=0 and (b) when N=100 for the case of R=0 (left) and R=300 (right) for several values of K

Same phenomenon applied for each temperature gradients with the case of *N*=100, the value of M_c less than M_c when the cases of zero magnetic effect, *N*=0. Consequently, the mechanisms of *N* or *R* can be said to be the effect of destabilizing because of the decreases M_c value whenever added the *N* and *R* value on the system. In other means, the growth rates increases for unstable modes which the layer become not stabilize since the *R* or *N* value increases.

Next, the comparison between M_c value of parabolic temperature profile which is always less than the M_c value of inverted parabolic temperature profile in Figure 6.10. Nevertheless, there exist the intersection line between both temperature gradients which is the line of *R*=300 for inverted parabolic temperature gradient and the line of *R*=0 for parabolic temperature gradient for the case of *N*=0. In spite of this, the result shows that without the controller at *K*=0 and without the magnetic effect at *N*=0, there exist the equal tension forces at the beginning, but oppositely the tension effect change whether increase or decrease as *K* increase or *N* increase. Clearly we can observe the effect from the next plot in Figure 6.11.

Therefore, from Figure 6.11 depicted the plot of M_c as a function of Rayleigh number, *R*. The plot showed dramatic decreasing of M_c when *R* is increase and *N* added to *N*=100. Despite that, the value of M_c keep increases when adding *K* into the system. Whenever increase the value of *K*, the value of M_c increases for both profiles, hence act as a stabilizing effect to the system. Oppositely, whenever increase the value of *R* and *N*, the value of M_c decrease, hence act as destabilizing effect to the system. Further inspection, *R* reached it's critical point of Rayleigh number, R_c as increases its value and at that point the M_c reached the zero value. Consequently, the value of M_c keep decrease as *R* increase till the buoyancy is predominant on the system of convection. Therefore, the zero value of M_c indicate that the negligible effect of surface tension and the convection system dominated by buoyancy force. The both cases of basic temperature profiles affected the decrease of surface tension effect because of *R*. Moreover, when *R* had been applied to the system, observed that the value of M_c always lower for parabolic temperature gradient compared than the M_c value of the inverted parabolic temperature gradient. As stated before, the most stabilizing profile is the inverted parabolic temperature profile compared to the other considered temperature profile on the research.

In addition, the plot of M_c as a function of $\frac{R}{R_c}$ depicted in Figure 6.12 where $\frac{R}{R_c}$ is the normalize Rayleigh number, *R* when the maximum value of *R* is 1. From the observation, when *N* is added up into the system from *N*=0 increase to *N*=100, and increased the value of $\frac{R}{R_c}$, the graph showed steadily decreased in the value of M_c. However, adding the value of *K*=4 for example, will rapidly increase the value of M_c. Consequently, performing the instability mechanisms of *K* and *N* give opposite effect to the system whether delay or hasten the onset of instability for both temperature gradients. Furthermore, inverted parabolic temperature profile shown the most stabilizing effect on the system when the value of M_c is always higher on the plot compared than parabolic temperature gradient for the cases of *N*=0 and *N*=100. Hence, Model 2 which is inverted parabolic temperature profile decreased the intensity of Bénard–Marangoni ferrofluids convection better.

As a summarization, first and foremost, the results published by Shivakumara et al. (2002) for parabolic and inverted parabolic temperature gradients for *K*=0, *R*=0 and *N*=0 provided an excellent agreement with the present study. The influence of feedback control, K, magnetic field, N and Rayleigh number, R with non-uniform basic temperature gradients of Bénard–Marangoni ferroconvection has been studied. The results showed rapidly increased on the value of M_c as K is added onto the system. Therefore, with the presence basic temperature gradients and K, shows that for all wave numbers, the feedback control is stabilizing the no-motion state and delaying the onset of instabilities. K can be said as a factor of stabilizing. Nevertheless, the instabilities mechanisms of R or/and N decreased the M_c. In other words, R and N can be acted as a factor of destabilizing. The influence of increasing the value of R and N are to hasten and reinforce together the instabilities of ferroconvection. Moreover, from observation, M_c value of inverted parabolic temperature gradient is greater than M_c value of parabolic temperature gradient. Hence, inverted parabolic temperature gradient leads to a most stabilizing temperature gradient and good simulated microgravity environment for material processing in industries.

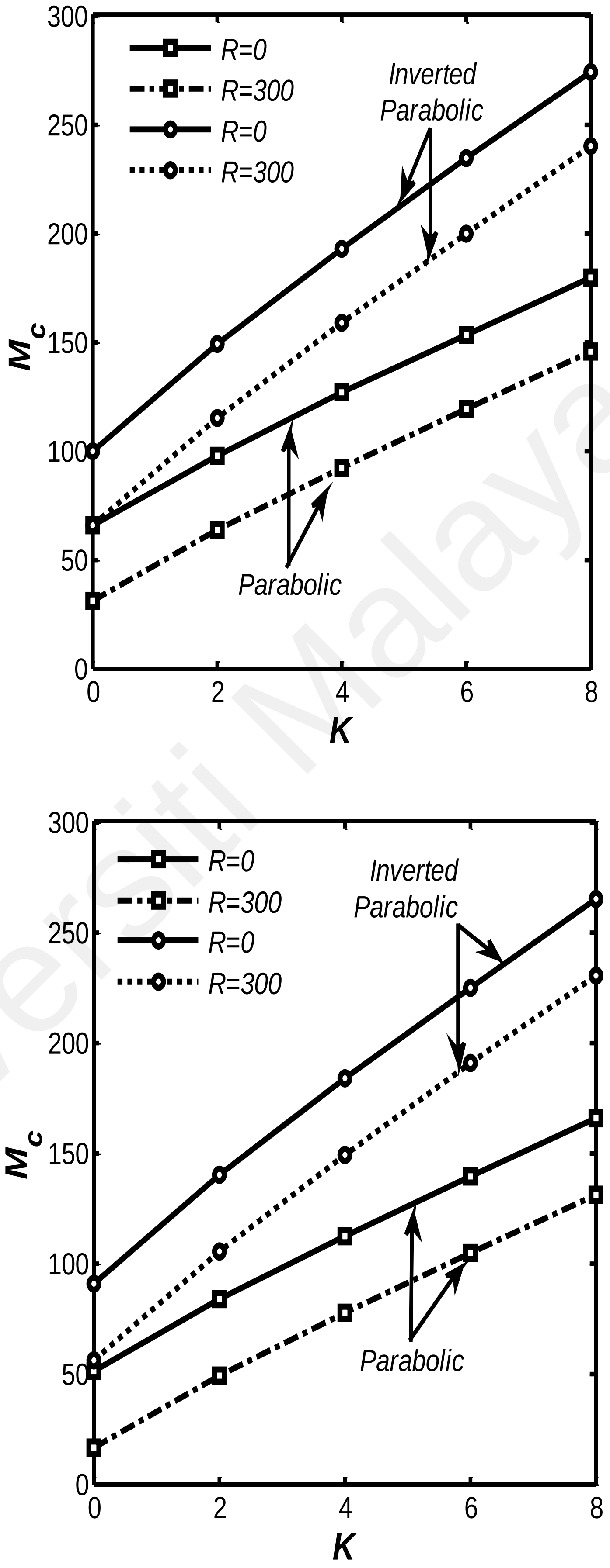

(a)

(b)

Figure 6.10: M_c as a function of K for the case of (a) N=0 and (b) N=100 for parabolic and inverted parabolic temperature profiles when R=0 and R=300

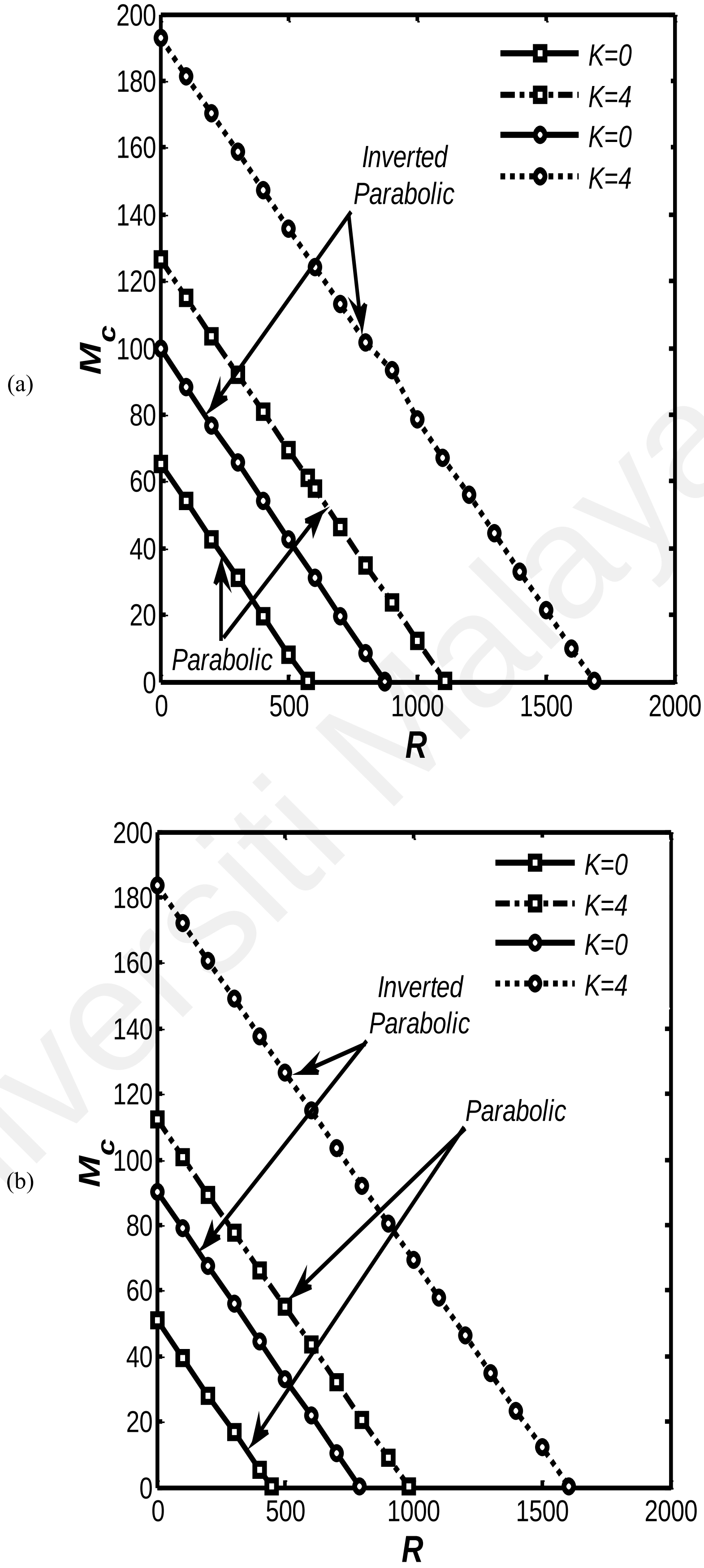

Figure 6.11: M_c as a function of R for parabolic and inverted parabolic temperature profiles when K=0 and K=4 for the case of (a) N=0 and (b) N=100

(a)

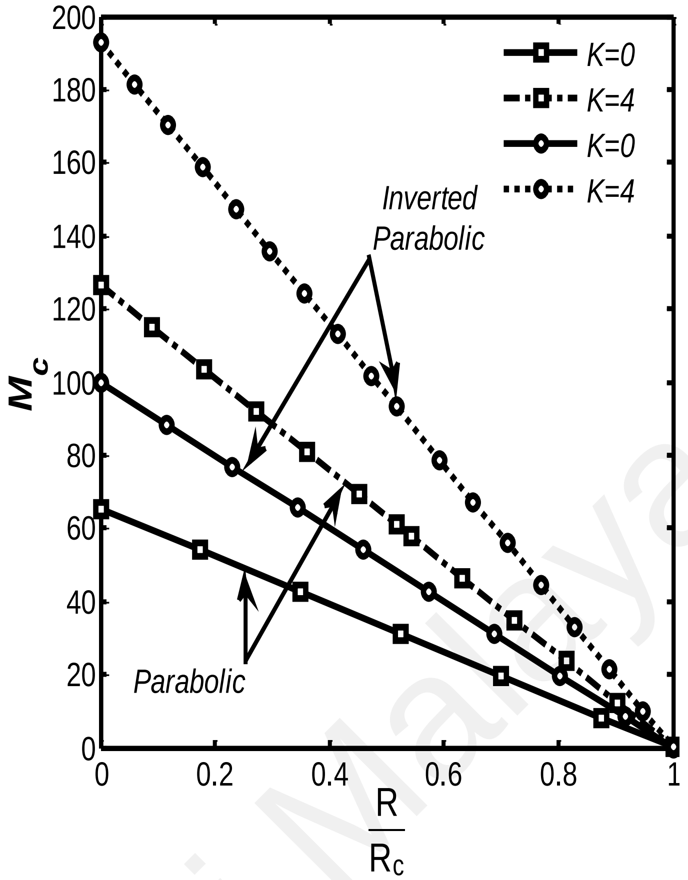

(b)

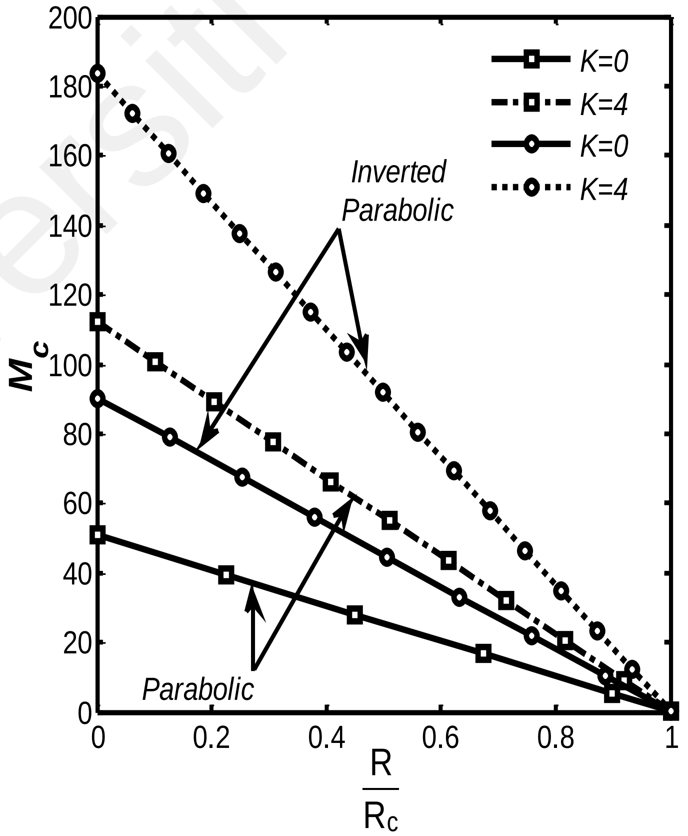

Figure 6.12: M_c as a function of $\frac{R}{R_c}$ for parabolic and inverted parabolic temperature profiles when K=0 and K=4 for the case of (a) N=0 and (b) N=100

CHAPTER 7:

CONCLUSION AND ADVANCED RESEARCH

Conclusions about the present research problems will be summarized in this chapter. In spite of that, the advanced research that will be conducted as an improvement for the previous results and to extend the method used in other fields will be suggested here.

7.1 Summary

The study on the buoyancy-driven flows is of great deal for a wide area of phenomenon prediction, physics and medical applications. The reaction towards the convective instabilities for the case of electro convection in a micropolar fluid and for the case of ferrofluids convection has been analysed in the presence of feedback control and non-uniform temperature profiles. The main components of this research are to investigate the influence of feedback control and the effect of various parameters on the onset of convective instabilities. The fluid flow studied in this research is non-Newtonian fluids which are dielectric micropolar fluid and ferrofluids. The upper non-deformable boundary with perfectly insulating is considered in this study. Meanwhile, different basic temperature gradients had been considered for the rigid and isothermal of the lower part of the boundary.

The first chapter, Chapter 1 presented some literature background on fluid flow and general introduction on convective heat transfer in fluid. Besides, there are several mechanisms of control strategy also presented in this chapter. Then, follow by the research scopes and objectives of the study.

Next, Chapter 2 presented the literature survey on the earlier studied and the related aspects to current investigation. The literature review survey from the previous study in well-known journal, past thesis, book and also conference proceeding.

The mathematical formulation and derivation of the governing equations of the model problems are described in Chapter 3. In addition, the problem solution of case for non-Newtonian fluids which is including linear stability analysis and single-term Galerkin method is discussed in details. Then, follow by the discussions on the boundary conditions for the both cases of dielectric micropolar layer and ferrofluids layer. Finally, the completion of the chapter by the concept of feedback control strategies applied to the system.

In Chapter 4, the classical analysis of linear stability is used to analyse the effects of feedback control on electroconvection in a micropolar fluid and ferrofluids. The related dimensionless variables for the governing equations and the applied of the boundary conditions also presented. Then, the critical solution for the influence of feedback control on the onset of the convection and also the effect of various parameters is obtained by using a single-term Galerkin method. In order to verify the model and also as an approaching of solving problem, the linear case is chosen to study and the validation results for both cases are presented in Chapter 5.

Then, the numerical data obtained are discussed and presented using the suitable graphical representations in Chapter 6. The influence of various parameters such as Coupling parameter, Electric number parameter, Couple stress parameter, Micropolar heat conduction parameter and Rayleigh number on the onset of Bénard–Marangoni electroconvection is discussed. In spite of that, the effect for non-linear case; parabolic and inverted parabolic temperature gradients are also investigated in this problem. Furthermore, the studied of Rayleigh–Bénard–Marangoni ferrofluids convection in the presence of feedback control is presented in this chapter. The effect of various parameters such as Rayleigh number, and magnetic Rayleigh number for suppressing or augmenting the onset of convection is analyzed in details. Besides, the solutions of eigenvalues subject to each boundary condition and the simulations data obtained will be presented as well.

Last but not least, it is available on the list of publications and papers which are written papers published in the proceedings and submitted in the ISI international journal for the two problems studied.

7.2 Conclusions

We begin our first problem of interests studied the onset about the influences of feedback control on Bénard–Marangoni electro convective instability with imposed of non-uniform basic temperature profiles. The linear case is chosen to study in order to verify the model and also as an approaching of solving problem. From this research, some conclusions are presented:

1. We recovered the results of steady marginal stability curve by Azmi and Idris (2014) for K=0, R=0 and L=100 for linear temperature profile with the critical point (2.0700, 74.31637572).
2. For the case of K = 0, that is the absence of feedback control, we also recovered the numerical analysis performed by Siddheshwar and Pranesh (1998) for the inverted parabolic temperature gradient.
3. For the present research, the results of Turnbull (1968) are recovered when $L \neq 0$, $N_1 = 0$, $f(z) = 1$ for a very limiting case.
4. The no-movement state for all wave numbers become stabilizes with the help of feedback control. As the feedback control, K, increases, M_c increases

monotonically. The presence of feedback controller can be significantly influential in suppressing the onset.

5. The presence of buoyancy force, *R* promotes the onset of convection and results to a more unstable system.
6. When the value of N_1 and N_5 increase, M_c increases. Means, the added up of suspended micron-sized particles have act as stabilizing effect to the system.
7. The Newtonian results of N_3 which act contrarily from N_1 and N_5 with act as destabilizing effect for different cases of basic temperature profiles.
8. From those three temperature gradients we had applied, the model of inverted parabolic temperature profile is shown the most stabilizing for all the considered temperature profiles.
9. $M_{c(Parabolic)} < M_{c(Linear)} < M_{c(Inverted\,Parabolic)}$. The possible results to suppress more the onset of convection in the presence of the inverted parabolic basic temperature gradient compared to linear and parabolic temperature profiles.

Further researched of the presence of feedback control *K*, on the onset of Rayleigh–Bénard–Marangoni ferrofluids convection have been observed. Other various parameters such as Rayleigh number *R*, magnetic Rayleigh number *N*, also have been analysed on the onset. Linear, parabolic and inverted parabolic temperature gradients are analysed using the analysis of linear stability. Some of the conclusions can be briefly drawn as:

1. We recovered the results published by Shivakumara et al. (2002) for *K*=0, *R*=0 and *N*=0 for linear temperature profile as in Chapter 5, parabolic and inverted parabolic temperature gradients are studied.
2. The value of M_c increased steadily, when applying the feedback control to the system. Hence, *K* is shown a stabilizing factor when added to the system. Means

that, the onset of convection can be delay in the presence of *K*. Thus, *K* can act as a good insulator and will give a good quality in the material processing and during the crystallization process.

3. Oppositely, the effect of parameter *R* or/and *N* to the system are decreasing the M_c value. Therefore, *R* and *N* can be destabilizing factor to augment the onset of Rayleigh–Bénard–Marangoni ferrofluids convection.
4. Strongly conclude that for the convective instabilities, the feedback control *K*, is a stabilizing factor to suppress the onset. The value of a_c is increasing but only on small values with increase the value of *K*.
5. Since there is no significant change in the value of a_c when there exist the value on *N* and *R*. Then, it can be proved that the parameter *N* and *R* will not affect the resulting value of a_c.
6. The inverted parabolic temperature gradient is indicated as the most stabilizing temperature gradient to suppress the onset of Rayleigh–Bénard–Marangoni ferrofluids convection. This can be shown from those two temperature profiles, the value of M_c for the inverted parabolic temperature gradient is greater than value of M_c for the parabolic temperature gradient.

7.3 Advanced Research

The study on the stability of convection is of great deal for a wide area of phenomenon prediction, biology and industries applications. We extremely hope that by using the Galerkin method, the research on the effect of feedback control with others non-uniform temperature gradients on micropolar fluid or ferrofluids can be investigated. Besides, the research on binary fluid about influences of non-uniform temperature profiles can be investigated. Research from no-motion state to motion state by using the Galerkin method can be extended by including higher number of controller gain parameter to examine either increasing number of controller gain parameter will give positive effects or negative effects on onset of convection. Further research on convective instabilities can be advanced by adding the influence of another parameter such as radiation, evaporation and heat flux.

REFERENCES

Amer-Nordin, D. (1995). *Dinamik Aliran Bendalir Suatu Penyelesaian*. Kuala Lumpur: Dewan Bahasa dan Pustaka.

Arratia, C., Mowlavi, S., & Gallaire, F. (2018). Absolute convective secondary instabilities and the role of confinement in free shear layers. *Physics of Fluids*, *3* (5), 1–24.

Awang-Kechil, S., & Hashim, I. (2008). Control of Marangoni instability in a layer of variable-viscosity fluid. *International Communications in Heat Mass Transfer*, *34*, 1368–1374.

Azmi, H. M., & Idris, R. J. (2014). Effects of controller and nonuniform temperature profile on the onset of Rayleigh–Bénard–Marangoni electroconvection in a micropolar fluid. *Journal of Applied Mathematics, 2*, 1–8.

Azmi, H. M., & Idris, R. J. (2015). Control of Marangoni convection in a rotating fluid layer with cubic temperature gradients. *International Conference on Computational Mathematics, 1*, 1–97.

Baby, R., & Pranesh, S. (2012). Effect of non-uniform temperature gradient on the onset of Rayleigh–Bénard electro convection in a micropolar fluid. *Journal of Applied Mathematics*, *3*(5), 442–450.

Bashtovoy, V. G., Berkovsky, B. N., & Vislovich, A. N. (1988). *Introduction to Thermo Mechanics of Magnetic Fluids*. Washington, DC: Hemisphere Co.

Bau, H. H. (1999). Control of Marangoni–Bénard convection. *International Journal of Heat and Mass Transfer*. *42*(7), 1327–1341.

Bénard, H. (1900). Les tourbillions cellulaires dans une nappe liquid- Méthodes optiques d'observation et d'enregistrement. *Revue Générale des Sciences*, *11*, 1261–1271, 1309–1328.

Berkovsky, B., Medvedev, V., & Krakov, M. (1993). *Magnetic Fluids, Engineering Applications*. New York: Oxford University Press.

Bewley, T., & Moin, P. (1994). Optimal control of turbulent channel flows. *American Society of Mechanical Engineers*, *1*, 1–75.

Block, M. J. (1956). Surface tension as the cause of Bénard cells and surface deformation in liquid film. *Journal of Nature*, *178*, 650–651.

Budroni, M. A., Thomas, C., & Wit, A. D. (2017). Chemical control of dissolution-driven convection in partially miscible systems: nonlinear simulations and experiments. *Applied Scientific Research*, *19*(11), 7936-7946.

Chandrasekhar, S. (1961). *Hydrodynamic and Hydromagnetic Stability*. Oxford: Oxford University Press.

Char, M. I., & Chiang, K. T. (1994). Boundary effects on the Bénard–Marangoni instability under an electric field. *Applied Scientific Research*, *52*(4), 331–354.

Choi, H., Moin, P., & Kim, J. (1994). Active turbulence control for drag reduction in wall-bounded flows. *Journal of Fluid Mechanics*, *262*, 75–110.

Currie, I. G. (1967). The effect of heating rate on the stability of stationary fluids. *Journal of Fluid Mechanics*, *29*, 337–347.

Das Gupta, M., & Gupta, A. S. (1979). Convective instability of a layer of a ferromagnetic fluid rotating about a vertical axis. *International Journal of Engineering Science*, *17*, 2–7.

Davis, S. H., & Homsy, G. M. (1980). Energy stability theory for free-surface problem: Buoyancy–thermocapillary layers. *Journal of Fluid Mechanics*, *98*(3), 527–553.

Douiebe, A., Hannaoui, M., Lebon, G., Benaboud, A., & Khmou, A. (2002). *Flow, Turbulence and Combustion*. Netherlands: Kluwer Academic Publishers.

El-Sayed, M. F. (2008). Onset of electroconvective instability of oldroydian viscoelastic liquid layer in Brinkman porous medium. *Archive of Applied Mechanics*, *78*(3), 211–224.

Eringen, A. C. (1966). Theory of micropolar fluids. *Journal of Mathematics and Mechanics*, *16*(1), 1–18.

Eringen, A. C. (1972). Theory of thermofluids. *Journal of Mathematical Analysis and Applications*, *38*, 480–496.

Eringen, A. C. (2001). *Microcontinuum Field Theories II: Fluent Media*. New York: Springer.

Finlayson, B. A. (1970). Convective instability of ferromagnetic fluids. *Journal of Fluid Mechanics*, *40*(4), 753–767.

Foster, T. D. (1965). Stability of a homogeneous fluid cooled uniformly from above. *Physics of Fluids*, *8*(7), 12–49.

Gad-el-Hak, M. (1994). Interactive control of turbulent boundary layers: A Futuristic overview. *AIAA Journal*, *32*(9), 1753–1765.

Getling, A. V. (1998). *Rayleigh–Bénard Convection: Structures and Dynamics*. Singapore: World Scientific.

Giangi, M., Stella, F., Leonardi, E., & Davis, G. D. V. (2002). A numerical study of solidification in the presence of a free surface under microgravity conditions. *Numerical Heat Transfer Applications*, *41*(6), 55–72.

Gireesha, B. J., Mahanthesh, B., Shivakumara, I. S., & Eshwarappa, K. M. (2016). Melting heat transfer in boundary layer stagnation-point flow of nanofluid toward a stretching sheet with induced magnetic field. *International Journal of Engineering Science and Technology*, *19*(1), 313–321.

Gotoh, K., & Yamada, M. (1982). Thermal convection in a horizontal layer of magnetic fluids. *Journal of Physics, Society of Japan*, *51*(9), 30–42.

Hashim, I., & Siri, Z. (2008). Stabilization of steady and oscillatory Marangoni instability in rotating fluid layer by feedback control strategy. *Numerical Heat Transfer, Part A: Applications*, *54*(6), 647–663.

Hashim, I., Mahmud, M. N., & Mustafa, Z. (2010). Effects of control on the onset of Bénard–Marangoni convection in a micropolar fluid. *International Communications in Heat and Mass Transfer*, *37*(19), 1335-1339.

Hennenberg, M., Weyssow, B., Slavtchev, S., Alexandrov, V., & Desaive, T. (2005). Rayleigh–Marangoni–Bénard instability of a ferrofluid layer in a vertical magnetic field. *Journal of Magnetism and Magnetic Materials*, *289*, 268–271.

Howle, L. E. (1997a). Linear stability analysis of controlled Rayleigh–Bénard convection using shadow graphic measurement. *Journal of Physics and Fluids*, *9*, 31–110.

Howle, L. E. (1997b). Control of Rayleigh-Bénard convection in a small aspect ratio container. *International Journal for Numerical Methods in Fluids*, *40*, 8–17.

Howle, L. E. (2000). The effect of boundary properties on controlled Rayleigh–Bénard convection. *Journal of Fluid Mechanics*, *411*, 3–9.

Idris, R., Othman, H., & Hashim, I. (2009). On effect of non-uniform basic temperature gradient on Bénard–Marangoni convection in micropolar fluid. *International Communications in Heat and Mass Transfer*, *36*(3), 255–258.

Idris, R., & Hashim, I. (2010). Effects of controller and cubic temperature profile on onset of Bénard–Marangoni convection in ferrofluid. *International Communications in Heat and Mass Transfer*, *37*(6), 624–628.

Incropera, F. P., Dewitt, D. P., Bergman, T. L., & Lavine, A. S. (2007). *Fundamentals of Heat and Mass Transfer*. New York: John Wiley and Sons (Asia) Pte Ltd.

Jacobson, S., & Reynolds, W. I. (1995). *An Experimental Investigation Towards the Active Control of Turbulent Boundary Layers*. California: Stanford University.

Kechil, S. A., & Hashim, I. (2008). Control of Marangoni instability in a layer of variable-viscosity fluid. *International Communications in Heat and Mass Transfer*, *35*(10), 1368–1374.

Koschmieder, E. L. (1993). *Bénard Cells and Taylor Vortices*. Cambridge: Cambridge University Press.

Lalas, D. P., & Carmi, S. (1971). Thermoconvective stability of ferrofluids. *Physics of Fluids*, *4*, 436–437.

Lick, W. (1965). The instability of a fluid layer with time-dependent heating. *Journal of Fluid Mechanics*, *21*, 2–65.

Loodts, V., Thomas, C., Rongy, L., & Wit, D. A. (2014). Control of convective dissolution by chemical reactions. *Physical Review Letters*, *11*, 1–13.

Lukaszewicz, G. (1999). *Micropolar Fluid: Theory and Applications.* Birkhauser: Boston.

Mahmud, M., Mansur, A., & Tap, A. O. M. (2010). *Quality Rating of Islamic Websites Features: A Single-User Evaluation*. Jakarta: IEEE Xplore Digital Library.

Medale, M., & Cerisier, P. (2002). Numerical simulation of Bénard–Marangoni convection in small aspect ratio containers. *Numerical Heat Transfer Applications*, *42*(1-2), 579–595.

Mohammed, A. K., Talabani, Z. J., & Ibraheem, R. R. (2013). Experimental study of steady state natural convection heat transfer from cylindrical heater in a vented enclosure. *Journal of Science and Engineering*, *2*(2), 87–96.

Morton, B. R. (1957). On the equilibrium of a stratified layer of fluid. *Quarterly Journal of Mechanics & Applied Mathematics*, *10*, 433–447.

Nanjundappa, C. E., Shivakumara, I. S., & Arunkumar, R. (2010). Bénard–Marangoni ferroconvection with magnetic field dependent viscosity. *Journal of Magnetism and Magnetic Materials*, *322*(15), 2256–2263.

Nanjundappa, C. E., Shivakumara, I. S., & Arunkumar, R. (2013). Onset of Marangoni–Bénard ferroconvection with temperature dependent viscosity. *Journal of Microgravity Science and Technology*, *25*(2), 103–112.

Nield, D. A. (1964). Surface tension and buoyancy effect in cellular motion. *Journal of Fluid Mechanics*, *19*(3), 341–352.

Or, A. C., Kelly, R. E., Cortelezzi, L., & Speyer, J. L. (1999). Control of long-wavelength Marangoni–Bénard convection, *Journal of Fluid Mechanics*, *387*, 321–341.

Or, A. C., & Kelly, R.E. (2001). Feedback control of weakly nonlinear Rayleigh–Bénard–Marangoni convection. *Journal of Fluid Mechanics*, *440*, 27–47.

Or, A. C., Cortelezzi, L., & Speyer, J. L. (2001). Robust feedback control of Rayleigh–Bénard convection. *Journal of Fluid Mechanics*, *437*, 1–75.

Pearson, J. R. A. (1958). On convective cells induced by surface tension. *Journal of Fluid Mechanics*, *4*, 489–500.

Pérez-Garcia, C., & Carneiro, G. (1991). Linear stability analysis of Bénard–Marangoni convection in fluids with a deformable free surface. *Physics of Fluids A: Fluid Dynamics*, *3*(2), 2–92.

Pranesh, S., & Kiran, R. V. (2010). Study of Rayleigh–Bénard magneto convection in a micropolar fluid with Maxwell–Cattaneo law. *Journal of Applied Mathematics*, *1*, 470–480.

Pranesh, S., & Baby, R. (2012). Effect of non-uniform temperature gradient on the onset of Rayleigh–Bénard electro convection in a micropolar fluid. *Journal of Applied Mathematics*, *3*, 442–450.

Qin, Y., & Kaloni, P. N. (1992). A thermal instability problem in a rotating micropolar fluid. *International Journal of Engineering Science*, *30*(9), 1117–1126.

Qin, Y., & Kaloni, P. (1994). Nonlinear stability problem of a ferromagnetic fluid with surface tension effect. *European Journal Mechanical B, Fluids*, *13*, 305–321.

Rao, R. K. V. (1974). Onset of instability in a heat conducting micropolar fluid layer. *Acta Mechanica*, *32*, 79–84.

Rayleigh, L. (1916). On convection currents in a horizontal layer of fluid, when the temperature is on the underside. *Philosophy Magazine*, *32*, 5–29.

Roberts, P. H. (1969). Electrohydrodynamic convection. *Quarterly Journal of Mechanics and Applied Mathematics*, *22*(2), 211–220.

Rosensweig, R. (1985). *Ferrohydrodynamics*. Cambridge: Cambridge University Press.

Rosmila, A. B., Kandasamy, R., & Muhaimin, I. (2012). Lie symmetry group transformation for MHD natural convection flow of nanofluid over linearly porous stretching sheet in presence of thermal stratification. *Applied Mathematics Mechanical*, *33*(5), 593–604.

Rudraiah, N., & Chandna, O. P. (1986). Effects of coriolis force and nonuniform temperature gradient on the Rayleigh–Benard convection. *Canadian Journal of Physics*, *64*(1), 90–99.

Rudraiah, N., Chandna, O. P., & Garg, M. R. (1986). Effect of non-uniform temperature gradient on magnetoconvection driven by surface tension and buoyancy. *Indian Journal of Technology*, *24*, 279–284.

Rudraiah, N., & Sekhar, G. N. (1991). Convection in magnetic fluid with internal heat generation. *ASME Transactions-Journal of Heat Transfer*, *113*(1), 1–22.

Rudraiah, N., & Siddheshwar, P. G. (2000). Effect of non-uniform basic temperature gradient on the onset of Marangoni convection in a fluid with suspended particles. *Journal of Aerospace Science and Technology*, *4*(8), 517–523.

Rudraiah, N., Shivakumara, I. S., & Nanjundappa, C. E. (2002). Effect of basic temperature gradients on Marangoni convection in ferromagnetic fluids. *Indian Journal of Pure and Applied Physics*, *40*, 95–106.

Rudraiah, N., & Gayathri, M. S. (2009). Effect of thermal modulation on the onset of electrothermoconvection in a dielectric fluid saturated porous medium. *Journal of Heat Transfer*, *131*(10), 10–109.

Sastry, V. U. K., & Ramamohan, R. V. (1983). Numerical study of thermal instability of a rotating micropolar fluid layer. *International Journal of Engineering Science*, *21*, 449–461.

Shivakumara, I. S., Rudraiah, N., & Nanjundappa, C. E. (2002). Effect of non-uniform basic temperature gradient on Rayleigh–Bénard–Marangoni convection in ferrofluids. *Journal of Magnetism and Magnetic Materials*, *248*(3), 379–395.

Shivakumara, I. S., & Nanjundappa, C. E. (2006). Effects of quadratic drag and throughflow on double diffusive convection in a porous layer. *International Communications in Heat and Mass Transfer*, *33*(3), 357–363.

Shivakumara, I. S., Reddy, R. G., Ravisha, M., & Lee, J. (2014). Effect of rotation on ferromagnetic porous convection with a thermal non-equilibrium model. *Journal of Meccanica*, *49*(5), 1139–1157.

Shivakumara, I. S., Dhananjaya, M., & Ng, C. O. (2015). Thermal convective instability in an Oldroyd-B nanofluid saturated porous layer. *International Journal of Heat and Mass Transfer*, *84*, 167–177.

Shivakumara, I. S., Ravisha, M., Ng, C. O., & Varun, V. L. (2015). Porous ferroconvection with local thermal nonequilibrium temperatures and with cattaneo effects in the solid. *Journal of Acta Mechanica*, *226*(11), 3763–3779.

Siddheshwar, P. G., & Pranesh, S. (1998). Effect of a non-uniform basic temperature gradient on Rayleigh–Bénard convection in micropolar fluid. *International Journal of Engineering Science*, *36*(11), 1183–1196.

Singer, J., & Bau, H. H. (1991). Active control of convection. *Physics of Fluids A*, *3*(12), 2859–2865.

Siri, Z., & Hashim, I. (2008). Control of oscillatory Marangoni convection in a rotating fluid layer. *International Communication in Heat and Mass Transfer*, *35*(9), 1130–1133.

Siri, Z., Mustafa, Z., & Hashim, I. (2009). Effects of rotation and feedback control on Bénard–Marangoni convection. *International Journal of Heat and Mass* Transfer, *52*(25), 5770–5775.

Siri, Z., & Hashim, I. (2009a). Feedback control of thermocapillary convection in a rotating fluid layer with free-slip bottom. *Journal of Sains Malaysiana*, *38*(1), 119-124.

Siri, Z., & Hashim, I. (2009b). Control of oscillatory of Bénard–Marangoni convection in rotating fluid layer. *International Conference on Signal Processing Systems*, *1*, 938–941.

Straughan, B. (1991). Stability problems in electrohydrodynamics, ferrohydrodynamics, and thermoelectric magnetohydrodynamics. *Journal of Fluid Mechanics*, *274*, 163–192.

Takashima, M. (1970). The effect of rotation on thermal instability in a viscoelastic fluid layer. *Physics Letters A*, *31*(7), 379–388.

Takashima, M. (1970). Nature of the neutral state in convective instability induced by surface tension and buoyancy. *Journal of the Physical Society of Japan*, *28*(3), 8–10.

Takashima, M., & Namikawa, T. (1971). Surface-tension-driven convection under the simultaneous action of a magnetic field and rotation. *Physics Letters A*, *37*(1), 55–57.

Tang, J., & Bau, H.H. (1998). Numerical investigation of the stabilization of the no-motion state of the fluid layer heated from below and cooled from above. *Physics of Fluids*, *10*, 1597–1610.

Venkatasubramanian, S., & Kaloni, P. N. (1994). Effects of rotation on the thermoconvective instability of a horizontal layer of ferrofluids. *International Journal of Engineering Science*, *32*(2), 2–37.

Walzer, W. (1976). Convective instability of a micropolar fluid layer. *Gerlands Beiträge zur Geophysik*, *85*, 137–143.

Weilepp, J., & Brand, H. (1996). Competition between the Benard–Marangoni and the Rosensweig instability in magnetic fluids. *Journal de Physique II France*, *6*, 419–441.

White, F. M. (2008). *Fluid Mechanics: McGraw-Hill*. New York: University of Rhode Island.

Yuen, P. K., & Bau, H. H. (1996). Rendering subcritical hopf bifurcation supercritical. *Journal of Fluid Mechanics*, *317*, 91–109.

Yuen, P. K., & Bau, H. H. (1998). Controlling chaotic convection using neural nets– theory and experiments. *Neural Networks*, *11*, 557–569.

Yuen, P., K., & Bau, H. H. (1999). Optimal and adaptive control of chaotic convection– theory and experiments. *Physics of Fluids*, *11*(6), 1435–1448.